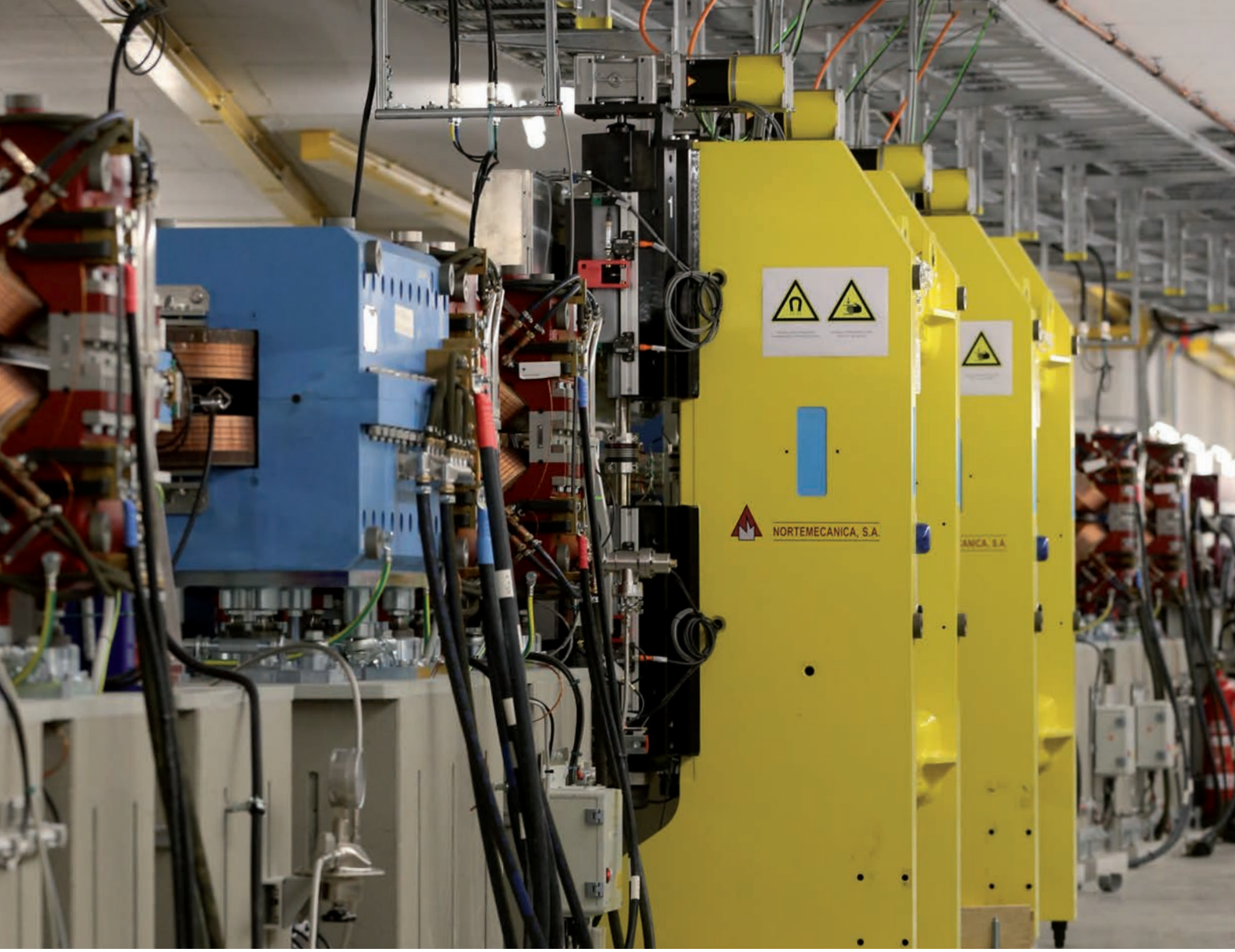

ACCELERATORS 2015.

Highlights and Annual Report

Accelerators | Photon Science | Particle Physics

Deutsches Elektronen-Synchrotron
A Research Centre of the Helmholtz Association

Cover

One of the highlights of 2015 was the successful recommissioning of PETRA III and the delivery of light to two of the new beamlines in the extension section North in autumn. The photograph shows part of the new magnetic lattice and the two new undulators in the section North.

ACCELERATORS 2015.

Highlights and Annual Report

Contents.

The year 2015 at DESY.

Chairman's foreword

2015 – the UNESCO "International Year of Light" – was a highly dynamic year for DESY, and many areas of the research centre were buzzing with activity. Ongoing projects, extensive construction work for new facilities and significant planning work towards new projects kept us busy. At the same time, DESY engaged in new national and international research collaborations and developed a region of excellence concept for both the Hamburg and the Zeuthen campus.

The construction of the European XFEL X-ray free-electron laser – currently DESY's largest project – is in full swing. More than two thirds of the required 100 superconducting accelerator modules have already been installed in the tunnel (Fig. 1). Our plan is to inject the first electron beam into the linear accelerator before the end of 2016.

The PETRA III synchrotron radiation source was recommissioned in 2015 after a long shutdown to expand the facility. The outer facades of the two PETRA III extension halls were completed, and the technical equipment is now being put into place inside the halls.

The extension of the FLASH soft X-ray free-electron laser facility progressed similarly well. The new FLASH2 experimental hall, named "Kai Siegbahn" in a symbolic ceremony (Fig. 2), was completed in 2015, and commissioning of the experimental setups started. Next door, in the "Albert Einstein" experimental hall, experiments at the FLASH1 beamline are operating routinely.

With those upgrades coming to a close, considerations regarding the next major project have gathered momentum. In the second half of 2015, an accelerator design study towards an upgrade of PETRA III to an ultralow-emittance "diffraction-limited" storage ring was started, with the ambitious objective to develop a practical concept for such a new PETRA IV storage ring.

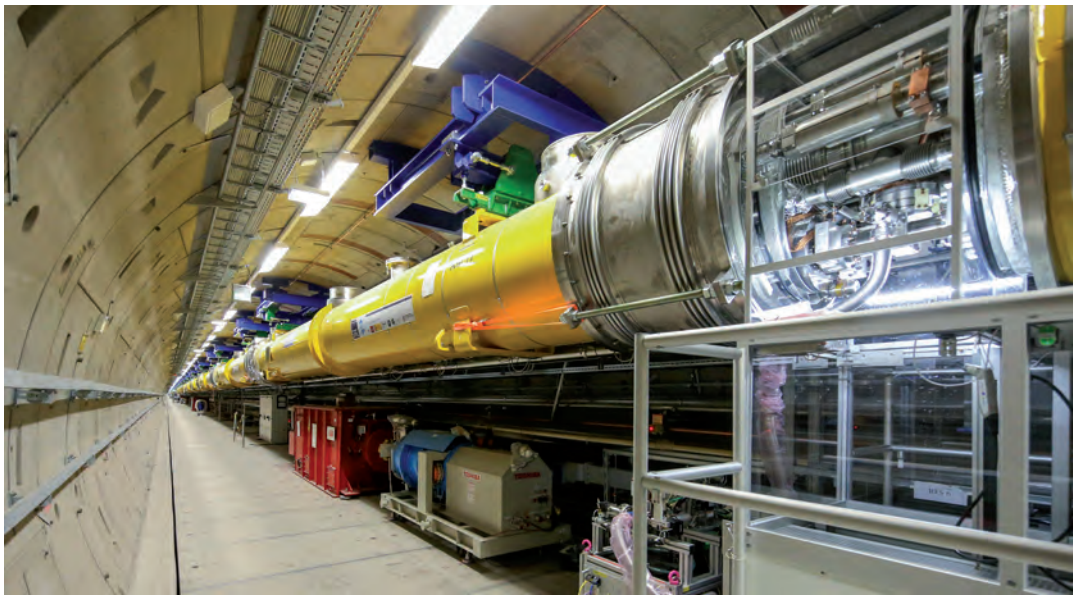

Figure 1

Accelerator tunnel of the European XFEL (April 2015)

Figure 2

In a symbolic ceremony, the two FLASH experimental halls were named after the Nobel laureates Albert Einstein and Kai Siegbahn by Beatrix Vierkorn-Rudolph of the German Federal Ministry of Education and Research (BMBF), the Swedish Secretary of State Anders Lönn, DESY Director Helmut Dosch, Hamburg's Mayor Olaf Scholz and Hans Siegbahn, son of Kai Siegbahn (from left to right).

Figure 3

Mikhail Yurkov and Evgeny Schneidmiller with the Director of DESY's Accelerator Division, Reinhard Brinkmann, and DESY Director Helmut Dosch (first row, from right to left)

There were several occasions for celebrations in the past year at DESY, such as the topping-out ceremony for the new Centre for Structural Systems Biology (CSSB), which will become home for many new colleagues in 2017, or the naming ceremony for the two FLASH experimental halls mentioned above. We also got to celebrate awards for scientific excellence, and I am very happy that in August 2015, DESY scientists Mikhail Yurkov and Evgeny Schneidmiller received the 2015 Free-Electron Laser Prize for their outstanding contributions to the field (Fig. 3).

I am aware that our many and diverse activities and projects are a challenge for all staff members at DESY – a challenge that, I am proud to say, we handle admirably. I cannot extend a big enough "thank you" to fully express the appreciation I have for the excellent work and continued commitment of our staff members and external collaborators. I am very much looking forward to their results in 2016!

Helmut Dosch
Chairman of the DESY Board of Directors

Accelerators at DESY.

Introduction

Regarding DESY's accelerator construction, operation and research activities, the year 2015 was again a very busy and successful year.

The PETRA III synchrotron radiation source was recommissioned after a long shutdown to implement the photon beamline extension project in the northern and eastern sections of the storage ring. Photon beam delivery to the users restarted as planned in April. The pre-accelerators had been put back into operation earlier so that the high-energy test beams at the DESY II synchrotron had become available to users from the particle physics community already in January. The operation of PETRA III went well from the start and, except for an expected slight increase in beam emittance due to the lattice modifications and the necessity for vacuum conditioning, did not show significantly different behaviour from the one before the extension project. The facility achieved its availability goal of 95% by the end of the 2015 user run period. Trips of the radio frequency (RF) system in the high bunch charge "timing mode" of operation were reduced by optimising the tuning of the cavities. Still, more issues will have to be addressed in the future to further reduce the downtime to well below the original goal of 5%.

The considerations for a major upgrade of PETRA towards an ultralow-emittance "diffraction-limited" storage ring picked up momentum in 2015, and an accelerator design study heading in this direction was launched in the second half of the year. The ambitious goal is to work out, within the next few years, a practical concept for such a new PETRA IV storage ring with an emittance of 20 pm, a factor of 50 below the present PETRA III emittance. This study is still at a very early stage and it is much too early for conclusions, but it is already clear that the large circumference of PETRA is a very valuable asset for being able to achieve such an unprecedented performance in a hard X-ray synchrotron radiation storage ring.

The FLASH soft X-ray free-electron laser (FEL) was in operation throughout most of the year and delivered self-amplified spontaneous emission (SASE) FEL beams to users at the FLASH1 photon beamline with good performance and high reliability. The downtime averaged over the user run periods amounted to only about 4%. Frequent changes in the beam parameters regarding photon wavelength, bunch charge, number of bunches per linear accelerator pulse, etc. are a typical feature of routine operation at FLASH. These changes require additional tuning time (as part of the scheduled user time), but they also demonstrate the high flexibility of the facility for a wide range of scientific user requirements. The new FLASH2 beamline will make wavelength changes much faster and thus operation more efficient thanks to tunable undulator gaps. This was demonstrated in 2015 very successfully during FLASH2 studies. Simultaneous operation of the two FLASH undulator beamlines has become more and more routine so that the perspectives for parallel user operation in the two FLASH experimental halls starting in 2016 are very good. Among the accelerator studies carried out in 2015, the sFLASH experiment, performed in cooperation with the University of Hamburg, was one of the highlights. A very clear signal of seeded photon beam at 38 nm was achieved using the high-gain harmonic generation (HGHG) method.

In a symbolic ceremony in May 2015, the two experimental halls of FLASH were named after the Nobel laureates Albert Einstein and Kai Siegbahn. The celebrations were also a good opportunity to recall 10 years of successful user operation at FLASH, which started operating for photon science users as a truly pioneering facility in summer 2005. Yet another excellent reason for celebration was the awarding of the prestigious FEL Prize to the DESY scientists Mikhail Yurkov and Evgeny Schneidmiller at the International Free Electron Laser Conference in August 2015 for their outstanding contributions to the field.

At the PITZ photoinjector test facility at DESY in Zeuthen, studies of an electron source (RF gun) setup with two RF windows continued and showed very low breakdown event rates at the windows. It is yet too early to conclude that the two-window solution will be the necessary modification for FLASH and the forthcoming European XFEL X-ray laser to guarantee reliable operation. PITZ also demonstrated that good beam quality can be achieved with somewhat reduced RF power (and accelerating gradient) and a relatively simple concept of photocathode laser pulse shaping.

In the European XFEL accelerator construction project, production of the superconducting accelerator modules, the key components of the linear accelerator (linac) complex, proceeded at an average rate for 2015 of one module assembled at CEA in Saclay, France, and delivered to DESY per week. This led to two thirds of the 100 linac modules being available at DESY and about 50 of them installed in the tunnel by the end of 2015. The module tests at the Accelerator Module Test Facility (AMTF) were even further accelerated, and by autumn 2015, there were no more modules waiting for the cooldown, conditioning and RF test procedure so that newly delivered modules could go on the test stand without

Figure 1

Reinhard Brinkmann, Director of the Accelerator Division at DESY

delay. Installation of all components in both the superconducting linac and the warm beamline sections is ongoing with utmost effort and urgency in order to maintain the ambitious goal of starting beam commissioning of the European XFEL linac in autumn 2016. Regarding the injector, beam commissioning started in 2015 as planned. After cooldown of the 1.3 GHz accelerator module and the 3.9 GHz higher-harmonic module, acceleration of the electron beam to 127 MeV and transport up to the end of the approximately 40-m-long injector beamline was demonstrated for the first time on 18 December. This provided an excellent starting point for further studies and optimisations of the injector before the beam is needed in the main linac later in 2016.

With the official start of the third Helmholtz programme-oriented funding (POF III) period in 2015, the new Accelerator Research and Development (ARD) topic held its kick-off meeting in February as part of the "Matter and Technologies" research programme, which comprises six Helmholtz centres and two institutes. The many presentations of recent ARD achievements showed that the previous ARD implementation phase already led to new, fruitful cooperations and joint projects and plans. One prominent example is the ATHENA proposal for a distributed accelerator R&D facility focusing on laser plasma acceleration, which was submitted to the Helmholtz Association in June. If funded, ATHENA will give a strong additional boost to the SINBAD R&D infrastructure, which DESY started building in the former DORIS accelerator housing. First laser plasma acceleration is getting closer at DESY with progress on the 200 TW laser, which has already been commissioned, and the LUX beamline, which is being built as a joint project with the University of Hamburg. Laser acceleration with THz pulses in tiny accelerating structures was demonstrated for the first time in 2015 as part of the AXSIS project, a joint activity of DESY, the Center for Free-Electron Laser Studies (CFEL), the University of Hamburg and Arizona State University. DESY and the University of Hamburg are also taking part in the "accelerator on a chip" R&D activity, which received a funding approval by the Moore Foundation in 2015. Furthermore, the EuPRAXIA design study towards a multi-GeV plasma accelerator, coordinated at DESY, was approved by the EU in 2015. In the area of superconducting RF technology, accelerating gradients of 15–19 MV/m were achieved in 2015 in a superconducting accelerator module test in continuous-wave or high duty cycle mode. Further remarkable progress was also achieved in femtosecond instrumentation and synchronisation systems.

Enjoy reading more about our exciting accelerator activities on the following pages!

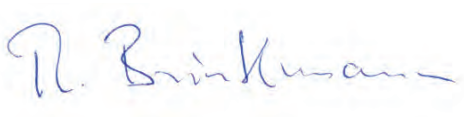

Reinhard Brinkmann
Director of the Accelerator Division

News and events.

News and events.

A busy year 2015

January

FLASH becomes first optically synchronised free-electron laser

Scientists at DESY developed and implemented an optical synchronisation system for DESY's FLASH soft X-ray free-electron laser (FEL), achieving facility-wide synchronisation with femtosecond precision. The performance of the system is expected to ultimately be at least ten times better than what has been achieved anywhere so far using electronic techniques. At this level of control, ultrafast experiments can be performed systematically with the highest temporal resolution.

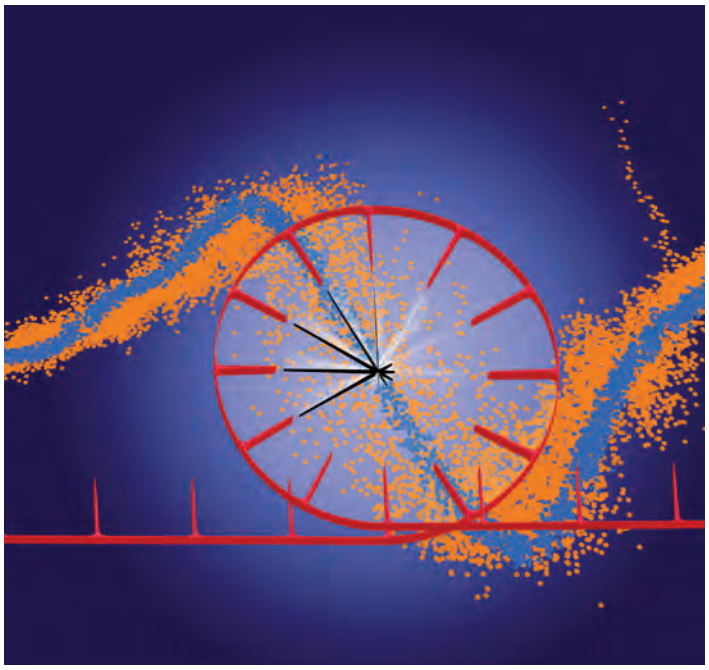

Artistic illustration of the precise clock signal for facility-wide synchronisation at FLASH. The orange curve is acquired using conventional synchronisation, while all-optical synchronisation is active for the blue curve. The narrower the line, the more precise the synchronisation.

X-ray FELs generate ultrashort and intense laser-like radiation pulses that can be used to reveal the dynamics of the microcosm, such as chemical reactions or the properties of biomolecules. For these investigations, however, the timing of the pulses and all the components of the facility must be synchronised with the highest possible precision. So far, accelerator facilities and X-ray FELs have primarily been synchronised using electronic radio frequency clock signals. The best synchronisation achieved in this way is limited to about 100 fs – a restriction that prevents the use of FELs at their full potential for certain applications and inhibits their future development. In this key demonstration at FLASH, the optical synchronisation system locked all independent accelerator subsystems and external experiment lasers with a precision of 28 fs – a mere fraction of the X-ray FEL pulse duration of 90 fs.

For the optical synchronisation, a train of near-infrared femtosecond pulses is transmitted on an optical fibre network to remote stations at the accelerator. To assess the performance of the system, the relative arrival time between the synchronised optical laser pulses and the X-ray pulses is measured.

The optical synchronisation generally improves the characteristics of the X-ray FEL pulses, including arrival time stability, photon energy, intensity and pulse duration. From the experimentalists' perspective, however, delivering X-ray pulses with stable properties at exactly the right time is only half of the challenge. The other half rests in the ability to simultaneously deliver an independent optical laser pulse, which is required to initiate ultrafast processes including chemical reactions in molecules and phase transitions in materials. The evolution of these complex dynamics can then be observed using an X-ray FEL pulse. To achieve the maximum time resolution in these studies, the optical laser pulse should ideally be delivered with a timing precision that is a fraction of the X-ray FEL pulse duration. The optical synchronisation system demonstrated at FLASH does just that.

Crucially, the team found that the quality of the optical synchronisation is limited primarily by the X-ray FEL pulse duration, meaning that the precision should be even better with shorter X-ray pulses. This level of control will not only allow ultrafast experiments with highest temporal resolution, but also open up new possibilities for FEL development. An optical synchronisation system based on this prototype will be implemented in the European XFEL X-ray laser, which is currently under construction from DESY in Hamburg to the neighbouring town of Schenefeld.

April

Breakthrough in sFLASH seeding experiment

A team of researchers from DESY, the University of Hamburg and the Technical University of Dortmund in Germany demonstrated seeding by high-gain harmonic generation (HGHG) at the sFLASH test setup in April – an important milestone towards incorporating seeding in user experiments at DESY's FLASH soft X-ray laser facility.

sFLASH undulators in the FLASH tunnel

Free-electron lasers (FELs) produce very brief, high-intensity pulses of X-rays. These are generated by bunches of accelerated electrons travelling through an undulator at close to the speed of light. In a process called self-amplified spontaneous emission (SASE), light of a certain wavelength is amplified by several orders of magnitude to produce an X-ray laser pulse. However, due to the nature of the SASE process, the properties of the individual pulses vary slightly. To make the process more reproducible and further improve the time and energy resolution of FEL experiments, scientists are looking for ways of triggering, or "seeding", the radiation generation process by introducing a carefully defined pulse of laser radiation. The seeding experiment sFLASH uses its own undulators in the FLASH accelerator tunnel for this purpose, as well as a special measuring station at which the properties of the radiation pulses can be determined.

The team demonstrated seeding at sFLASH through HGHG by superimposing laser light with a wavelength of 266 nm onto the FLASH electron beam. During the trajectory of the beam through the undulator, a periodic microstructure builds up within the electron bunches, leading to a selective amplification of the FEL radiation. This is not only the case at the incoming laser wavelength, but also at its higher harmonics. At 38.1 nm, the seventh harmonic, the team managed to produce high-intensity FEL pulses with an energy of over 10 µJ. The result shows that the HGHG principle can be used to augment the unique properties of the electron beam at FLASH in order to generate fully coherent radiation pulses in the extreme ultraviolet range.

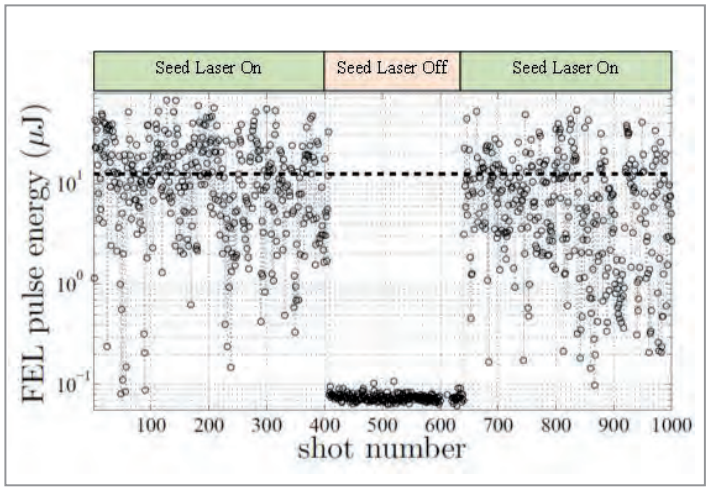

In HGHG mode, the radiation pulses inside the 10-m-long sFLASH undulator have mean energies of over 10 µJ, whereas the "normal" SASE intensity observed when the laser beam is switched off is a factor of about 1000 lower.

April

PETRA III resumes operation

Following a year-long shutdown to expand the facility, user operation at DESY's high-brilliance synchrotron radiation source PETRA III resumed on 27 April.

Around 2000 researchers from all around the world use the X-ray radiation generated by PETRA III every year to study new drug substances, new materials or chemical processes. The facility is regularly overbooked, however, and only a fraction of experiment requests can be granted. In the future, two new experimental halls will allow more researchers to access the brilliant X-ray radiation. While user operation resumed in April at the 14 existing measuring stations in the "Max von Laue" experimental hall, the two new halls will gradually be equipped with up to 11 further stations. The focus of the experiments there will be on studies of the properties of new materials.

"Max von Laue" experimental hall at PETRA III

For the construction of the two new halls, the tunnel of the PETRA III storage ring had to be torn down completely in two about 80-m-long sections. In these sections, the storage ring was rebuilt with new components after the foundations for the new halls were finished. Research operation in the new experimental halls is scheduled to begin in 2016.

May

DESY creates new research opportunities at FLASH

After a comprehensive technological upgrade and expansion, DESY's soft X-ray free-electron laser (FEL) facility FLASH opens up new vistas into the nanocosm, providing the international scientific community with novel experimental opportunities and groundbreaking technologies. At a symbolic ceremony on 20 May, Olaf Scholz, First Mayor of Hamburg, and Anders Lönn, State Secretary to Sweden's Minister for Higher Education and Research, named the two FLASH experimental halls after the Nobel Prize laureates Albert Einstein and Kai Siegbahn.

In a symbolic ceremony, the two FLASH experimental halls were named after Nobel laureates Albert Einstein and Kai Siegbahn by Beatrix Vierkorn-Rudolph of the German Federal Ministry of Education and Research (BMBF), the Swedish Secretary of State Anders Lönn, DESY Director Helmut Dosch, Hamburg's Mayor Olaf Scholz and Hans Siegbahn, son of Kai Siegbahn (from left to right).

In the future, scientists will be able to peer into the nanocosm using FLASH at up to 12 different experimental stations – twice as many as before – to record films of chemical reactions, for instance, examine the dynamics of new types of data storage devices or observe biomolecules at work. FLASH is used annually by some 200 scientists from all over the world, but this corresponds to only a fraction of the research proposals submitted. In the past three years, DESY has therefore extended the facility at a cost of 33 million euros, adding a second FEL beamline and a second experimental hall. In doing this, DESY is not just increasing the number of experimental stations available; the quality of the X-ray flashes has also been improved thanks to new technological developments, and the facility is more flexible. In contrast to the original beamline, FLASH1, the wavelength of the X-rays at the new beamline, FLASH2, can be varied during operation. The X-rays delivered by FLASH2 will further be used for experiments in the field of plasma acceleration, enabling novel activities in accelerator research.

The two experimental halls were named after Einstein and Siegbahn to underline the special relationship between the two eminent physicists and the research carried out at FLASH. Albert Einstein's explanation of the photoelectric effect by postulating that light behaves like particles is what enables scientists to take a chemical fingerprint of samples. Fifty years later, the Swedish physicist Kai Siegbahn developed photoelectron spectroscopy, a method that allows the chemical composition of samples to be unravelled. This method, which has become an indispensible tool for materials scientists, is being developed further at FLASH as a way of studying ultrafast processes. In addition, the choice of names emphasises the close German–Swedish collaboration in research, which was taken to a new level with the creation of the Röntgen Ångström Cluster in 2009 – a collaboration in the fields of materials science and structural biology.

FLASH at DESY is a pioneering facility: In 2005, it became the world's first FEL in the X-ray range. Since then, other such facilities have been under construction or are already in operation around the world. One of them is the European XFEL X-ray laser, which uses the technology developed at FLASH and is currently being built. It will go into operation in 2017. The FLASH extension, which was launched in May 2015, breaks new ground too: It is the first FEL in the world to work with two laser lines.

The FLASH facility with the two experimental halls in the foreground

July

SLAC and DESY join forces at bilateral strategy meeting

The US research centre SLAC and DESY will work closer together in the future. That was the outcome of a meeting of senior managers of both labs who convened on 16–17 July at SLAC in California to discuss a joint strategy for more collaboration.

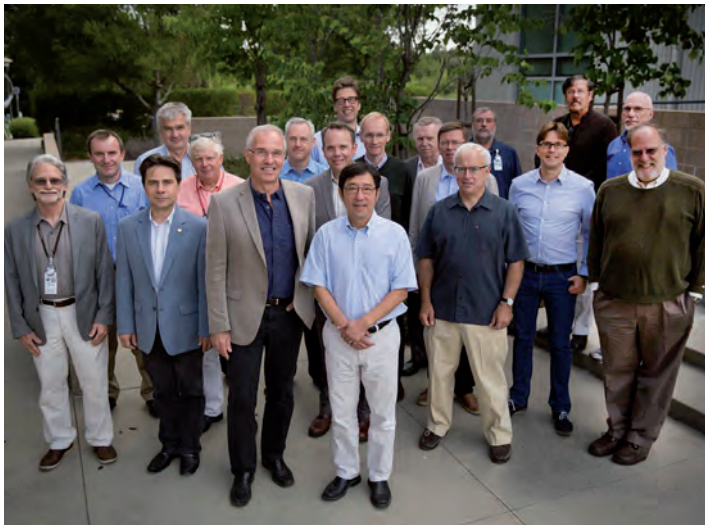

First DESY–SLAC strategy meeting at SLAC in July 2015

SLAC and DESY representatives reviewed their labs' current research activities and future plans, exposing a variety of commonalities and also differences between the research centres. This led to discussions that identified areas where the labs could best collaborate with each other. The meeting's attendees found plenty of common ground. They compiled a comprehensive list of common interests, including advancements in X-ray laser technology, particle physics detectors, future compact accelerators and computing methods to handle ever-increasing amounts of data produced in X-ray, particle physics and cosmology experiments.

SLAC and DESY share a rich history of collaboration and competition. Founded only a few years apart some 50 years ago, both centres were conceived as accelerator labs for particle physics experiments. Over the years, X-rays – an initially unwanted by-product of particle accelerators – have become an increasingly important tool for science in both locations. Today, SLAC and DESY are multipurpose labs with similarly broad research programmes, including accelerator research, particle physics, cosmology, X-ray science, bioscience, chemistry and materials science.

The meeting was the first of its kind, kicking off future regular collaboration meetings of the two labs. SLAC and DESY will now form bilateral working groups to flesh out detailed proposals for more collaboration in the identified areas.

August

Free-Electron Laser Prize for DESY pioneers

The 2015 Free-Electron Laser (FEL) Prize was awarded to the two DESY researchers Mikhail Yurkov and Evgeny Schneidmiller at the Free-Electron Laser Conference in South Korea in August for their pioneering work in developing and improving FELs. The award recognises outstanding contributions to the study and development of this key future-oriented technology.

X-ray FEL technology was pioneered at DESY's FLASH facility, giving birth to an entire generation of X-ray lasers all over the world. These include the European XFEL X-ray laser, which is currently under construction and will eventually reach from the DESY campus in Hamburg to the nearby town of Schenefeld in the German federal state of Schleswig-Holstein.

Mikhail Yurkov and Evgeny Schneidmiller with the Director of DESY's Accelerator Division, Reinhard Brinkmann, and DESY Director Helmut Dosch (first row, from right to left)

Right from the start, Yurkov and Schneidmiller were instrumental in designing the FEL at DESY's TESLA Test Facility, which gave rise to FLASH in 2005. They also made key contributions towards improving the performance of FLASH. At the European XFEL, they are strongly involved in calculating and optimising the FEL processes, with Mikhail Yurkov leading the work package on FEL concepts.

This is the second time the award goes to Hamburg: In 2006, the FEL Prize was awarded to Jörg Roßbach of the University of Hamburg and Evgeny Saldin of DESY.

October

Prototype demonstrates feasibility of THz accelerators

An interdisciplinary team including scientists from DESY's Center for Free-Electron Laser Science (CFEL) built the first prototype of a miniature particle accelerator that uses terahertz (THz) radiation instead of radio frequency structures. A single accelerator module is no more than 1.5 cm long and 1 mm thick. The THz technology holds the promise of miniaturising the entire setup by at least a factor of 100, enabling numerous applications – for future linear accelerators for use in particle physics, as a means of building compact X-ray lasers and electron sources for use in materials research and for medical applications using X-rays and electron beams.

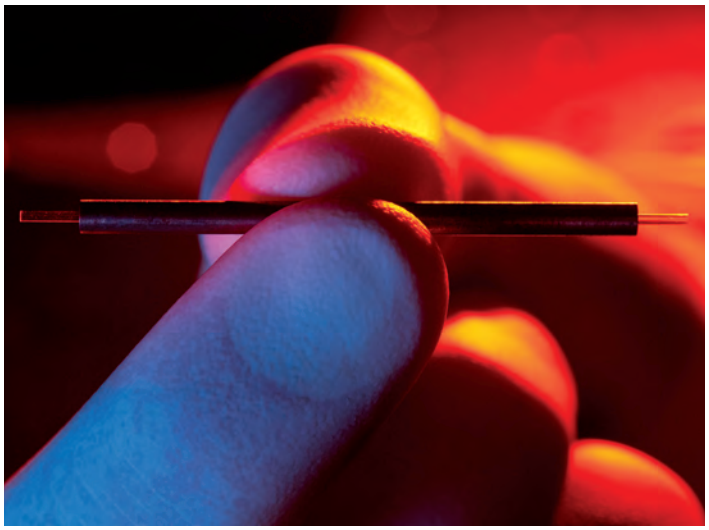

THz accelerator modules easily fit into two fingers.

In the electromagnetic spectrum, THz radiation lies between infrared radiation and microwaves. Particle accelerators usually rely on radio frequency waves; DESY's particle accelerator PETRA III, for example, uses a frequency of around 500 MHz. The wavelength of the THz radiation used in this experiment is around 1000 times shorter, which has the advantage that everything else can be 1000 times smaller too.

For their prototype, the team used a special microstructured accelerator module, specifically tailored to be used with THz radiation. The physicists fired fast electrons from an electron gun into the miniature accelerator module, where the

particles were further accelerated by the THz radiation fed into the module. This first prototype of a THz accelerator increased the energy of the particles by 7 keV, thereby demonstrating that the principle works in practice.

Theory indicates that THz accelerators should be able to achieve an accelerating gradient of up to 1 GeV/m. This is more than 10 times what can be achieved with the best conventional accelerator modules available today. Plasma acceleration technology, which is also at an experimental stage right now, promises to produce even higher accelerations, however it also requires significantly more powerful lasers than those needed for THz accelerators.

Over the coming years, the CFEL team in Hamburg plans to build a compact, experimental X-ray free-electron laser (FEL) on a laboratory scale using THz technology – a project supported by a Synergy Grant of the European Research Council. The experimental X-ray FEL is expected to be less than 1 m long and produce much shorter X-ray pulses, lasting less than a femtosecond, than current X-ray FELs. Because the pulses are so short, they will reach a comparable peak brightness to those produced by larger facilities, even if there is significant less light in each pulse. With these very short pulses, the scientists hope to gain new insights into extremely rapid chemical processes, such as those involved in photosynthesis. Developing a detailed understanding of photosynthesis would open up the possibility of implementing this efficient process artificially and thus tapping into increasingly efficient solar energy conversion and new pathways for CO_2 reduction.

Photosynthesis is just one example of many possible catalytic processes scientists would like to investigate using the new THz X-ray FEL. Beyond this, the compact device could also be used to seed pulses in large-scale facilities to enhance the optical quality of the radiation. In addition, certain medical imaging techniques could benefit from the enhanced characteristics of the novel X-ray source.

November

Towards a particle accelerator on a microchip

The Gordon and Betty Moore Foundation awarded 13.5 million US dollars (12.6 million euros) to promote the development of a particle accelerator on a microchip. DESY and the University of Hamburg are among the partners involved in this international project, headed by Robert Byer of Stanford University (USA) and Peter Hommelhoff of the University of Erlangen-Nürnberg (Germany). Within five years, they hope to produce a working prototype of an “accelerator-on-a-chip”.

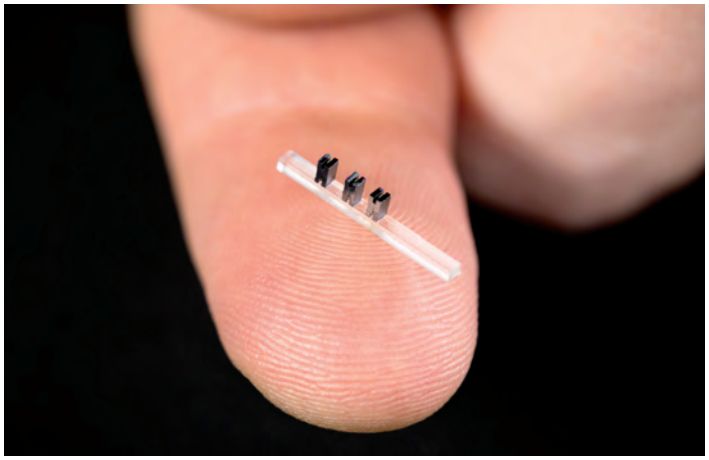

Three accelerators-on-a-chip made of silicon are mounted on a clear base.

The aim of the project is to develop a new type of small, inexpensive particle accelerator for a wide range of different uses. Apart from exploiting the accelerated electrons themselves, the devices could be used to produce high-intensity X-rays. The prototype to be developed could set the stage for a new generation of table-top accelerators, with unanticipated discoveries in biology and materials science and potential applications in security scanning, medical therapy and X-ray imaging.

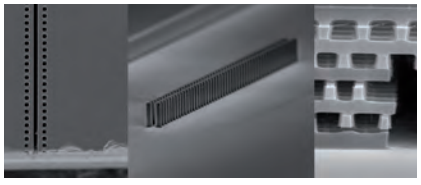

Some of the accelerator-on-a-chip designs being explored by the international collaboration.

The project is based on advances in nanophotonics, the art of creating and using nanostructures to generate and manipulate different kinds of light. A laser using visible or infrared light is used to accelerate the electrically charged particles, rather than the radio frequency (RF) waves currently used. The wavelength of this laser radiation is some 10 000 to 100 000 times shorter than that of the RF waves, meaning that steeper accelerating gradients can be achieved than those using RF technology. As a consequence, the typical transverse dimensions of an accelerator cell, for example,

would shrink from 10 cm to 1 µm. At the moment, the material of choice for the miniature accelerator modules is silicon, which has the advantage that the scientists can draw on the highly advanced production technologies already available for silicon microchips.

DESY will bring its vast know-how in laser technology to the project, which has already paid off in a collaboration involving the University of Erlangen-Nürnberg. There, Hommelhoff's group showed that, for slow electrons, a microstructured accelerator module is able to achieve higher accelerating gradients than RF technology. Byer's group in California had independently demonstrated the same effect for relativistic electrons.

However, it is still a long way from an experimental setup in a lab to a working prototype. Individual components will have to be developed from scratch. Among other things, DESY is working on a high-precision electron source to feed the particles into the accelerator modules, a powerful laser for accelerating them and an undulator for creating X-rays. In addition, the interaction between the miniature components is not yet a routine matter, especially not when it comes to joining up several accelerator modules.

Members of the international collaboration to build a working prototype of an accelerator-on-a-chip gathered at the Moore Foundation in October for a kick-off meeting.

The SINBAD (Short Innovative Bunches and Accelerators at DESY) accelerator lab that is currently being set up at DESY will provide an ideal testing environment for the miniature accelerator modules. SINBAD will allow the scientists to feed high-quality electron beams into the modules, test the quality of the radiation and work out an efficient way of coupling the laser.

November

EU funds design study for European plasma accelerator

The European Union supports the development of a novel laser-driven plasma particle accelerator with three million euros from the Horizon 2020 programme. The EU project EuPRAXIA (European Plasma Research Accelerator with eXcellence In Applications) will produce a design study for a European plasma research accelerator focusing on applications of the new technology.

Laser-driven plasma acceleration, which relies on electrically charged plasmas generated by strong lasers instead of the radio frequency waves used in conventional accelerators, has demonstrated accelerating fields 1000 times stronger than those provided by current accelerator technology. As such, the novel technology promises to significantly shrink the costs and size of particle accelerators.

Image of a plasma cell

The EuPRAXIA consortium includes 16 laboratories and universities from five EU member states, as well as 18 associated partners from eight further countries, involving leading institutes in the EU, Japan, China and the USA. By the end of 2019, the consortium will produce a conceptual design report for the worldwide first 5 GeV plasma-based accelerator with industrial beam quality and dedicated user areas. EuPRAXIA is the required intermediate step between proof-of-principle experiments and versatile ultracompact accelerators for industry, medicine or science.

The study will design accelerator components, laser systems and feedback technology for improving the quality of plasma-accelerated electron beams. Two user areas will be developed for a novel free-electron laser, high-energy physics and other applications. An implementation model will be proposed, including a comparative study of possible sites in Europe, a cost estimate and a model for distributed construction but installation at one central site. As a new large-scale research infrastructure, EuPRAXIA would place Europe in the 2020s at the forefront of the development of novel accelerators, driven by the world's most powerful lasers from European industry.

December

First electrons accelerated in the European XFEL

A crucial component of the European XFEL X-ray free-electron laser, which is currently being built from DESY in Hamburg to the neighbouring town of Schenefeld, took up operation in December: The injector – the first part of the superconducting linear accelerator that will drive the X-ray laser – accelerated its first electrons to nearly the speed of light. This is the first beam ever accelerated at the European XFEL and represents a major advancement toward the completion of the facility.

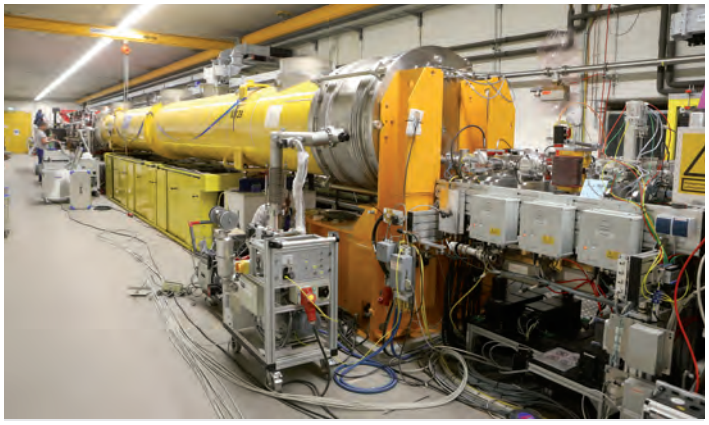

Injector area of the European XFEL. The yellow tube is the first superconducting accelerator module.

The European XFEL X-ray laser is an international research facility in northern Germany that will produce ultrabright X-ray laser flashes for unprecedented studies of the nanocosmos. It consists of a 2-km-long superconducting linear electron accelerator, followed by a series of highly precise undulators in which the extremely brilliant X-ray laser pulses are produced.

The injector, which is located on the DESY campus in Hamburg and has been under construction since 2013, produced a series of tightly packed electron bunches that passed through the 45-m-long injector beamline. The electrons made the full trip from start to end of the injector in 0.15 ms, achieving near light speed. The injector shapes the highly charged electron bunches and gives them their initial energy. This energy will then be gradually increased across the main linear accelerator, which is still being assembled.

DESY, which is European XFEL's main shareholder and close partner, is responsible for the construction and operation of the electron injector and the rest of the linear accelerator. Components for the injector were produced across Europe by the 17 institutes of the European XFEL Accelerator Consortium, which is led by DESY. Contributions include work done by DESY as well as in-kind contributions from institutes in France, Italy, Poland, Russia, Spain, Sweden and Switzerland.

The design of the injector is strongly based on the one at DESY's FLASH facility, the prototype facility for the European

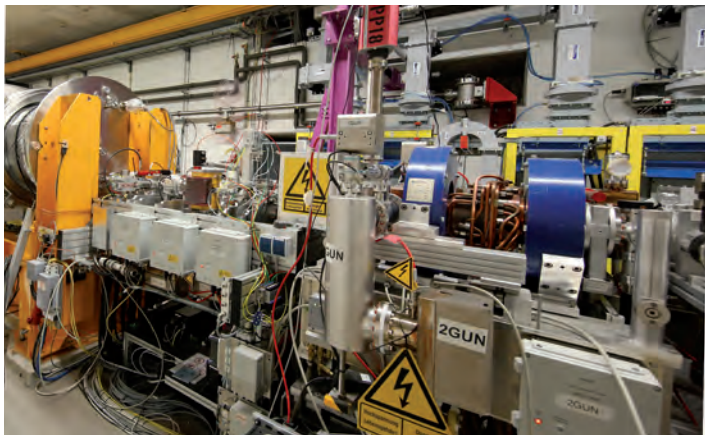

The electron gun releases the electrons and accelerates them shaped in bunches.

XFEL that began operation as a user facility in 2005. Several billion electrons are released from an electrode of caesium telluride upon impact of an intense ultraviolet laser flash. The electrons form a bunch, which is accelerated by radio frequency waves and kept together by intense magnetic fields. The bunch is accelerated, first through a normal-conducting cavity made of copper, then through a pair of superconducting accelerator cryomodules. The two latter devices are chilled to -271°C by liquid helium to allow for highly efficient beam acceleration. These modules give the electron beam the required characteristics needed for producing the X-ray flashes that will be used to investigate matter at the atomic scale.

The injector will continue to go through rigorous testing while the rest of the linear accelerator is installed. The next major milestone will be to accelerate electrons along the full accelerator length to the European XFEL's Osdorfer Born site, approximately 2.1 km away from the start of the injector. This is expected in late 2016, with user operation to follow in 2017.

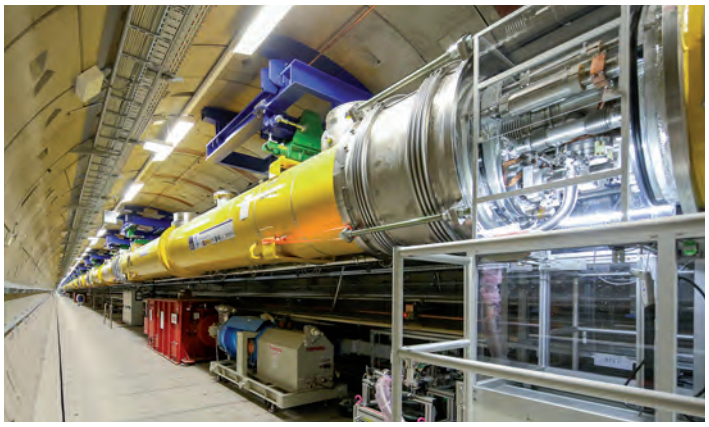

View into the main accelerator tunnel of the European XFEL, where 100 superconducting accelerator modules are being installed.

Accelerator operation and construction.

PETRA III.

Back in operation after major extension

A one-year-long shutdown to extend DESY's PETRA III synchrotron radiation source ended in February 2015. The recommissioning of the accelerator with beam started on schedule, exactly one year after the end of user operation in February 2014. On 27 April 2015, with external users restarting experiments at the 14 already existing beamlines in the Max von Laue experimental hall, PETRA III was back in operation as a synchrotron radiation facility. Two of the new beamlines in the extension section North became operational in autumn 2015.

Recommissioning of PETRA III

During the one-year-long shutdown, DESY implemented the PETRA III extension project, which will eventually accommodate 10 additional beamlines in two new halls in the northern (PXN) and eastern (PXE) sections of the storage ring. The corresponding tunnel sections were completely reconstructed, and the magnet lattice was redesigned. One of the main goals during the extension work was to minimise the idle time for the 14 already existing beamlines in the main experimental hall, called Max von Laue hall, and to re-establish good conditions for user runs for these beamlines before the new beamlines would become operational step by step. The recommissioning of PETRA III with beam started on schedule in February 2015.

First turn steering began on 6 February. Ten days later, after some non-conformities had been identified and successfully cured, it was possible to accumulate a beam of about 1 mA in the storage ring. The transverse and longitudinal multibunch feedback systems quickly became operational, and after 18 February, it was possible to store higher beam currents, which was also important for conditioning the vacuum system. At the end of February, the new optics was carefully corrected, based on orbit response measurements with all correctors. The emittance diagnostic beamline became quickly available, and the measured horizontal emittance was found to be in very good agreement with the design value of 1.2 nm for the PETRA III extension optics. The orbit feedback was extended to guarantee the required pointing stability of the particle beam. The commissioning of the modified system with a new central control unit was finished just in time in mid-March. The tuning to achieve good conditions for the existing 14 beamlines in the Max von Laue hall started in parallel to the final commissioning steps.

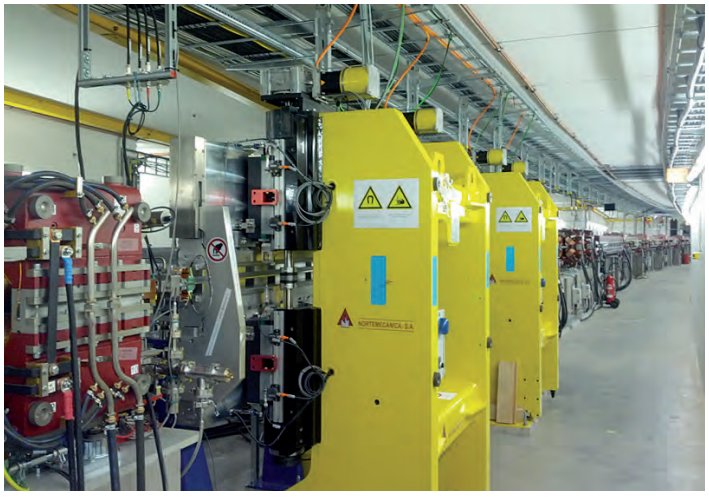

Figure 1

View into the accelerator tunnel in the extension section North (PXN) after installation of the two new undulators PU64 and PU65

The user run with internal users started as scheduled on 28 March with 60 equally spaced bunches and a total current of 80 mA, which could be increased to the design current of 100 mA in the course of the 2015 run period. Starting on 27 April, external users began to carry out experiments at the 14 existing beamlines, which put PETRA III back in operation as a synchrotron radiation facility. Two of the new beamlines in the extension section North became operational in autumn.

User operation

User operation in 2015 started on 28 March and ended on 12 November. During this period, 3815 h were scheduled for internal and external users. The full user period was divided into six run periods, interrupted by service weeks for the necessary maintenance. The service weeks were also used to install two new undulators (PU64 and PU65) in the extension section North (Fig. 1). Every Wednesday, user operation was interrupted by regular weekly maintenance, machine

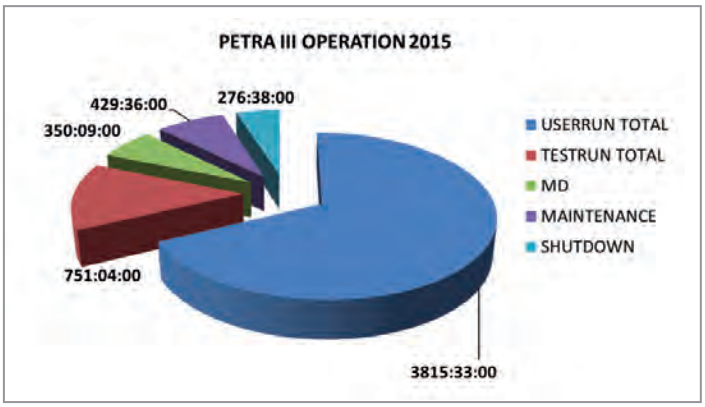

Figure 2

Distribution of different machine states during the run period 2015

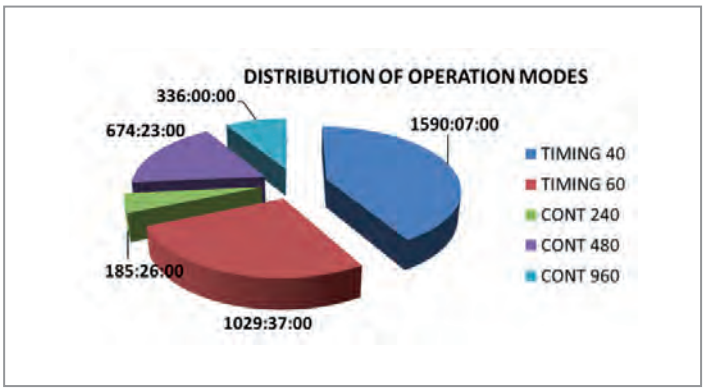

Figure 3

Distribution of different operation modes in 2015

development activities and test runs for about 24 h. The distribution of the different machine states in 2015 is shown in Fig. 2.

During user runs, the storage ring was operated in two distinct modes, characterised by their bunch spacing. In the “continuous mode”, 100 mA were filled in 240, 480 or 960 evenly distributed bunches corresponding to 32 ns, 16 ns and 8 ns bunch spacing, respectively. Operation with 960 bunches was initially affected by ion cloud effects, resulting in a degenerated beam quality in the vertical plane. However, the vacuum conditions in the two new extensions sections improved during the run periods, and the ion cloud effects became less significant for the beam quality.

The “timing mode” allows users to perform time-resolved experiments and is thus characterised by a considerably larger bunch spacing. Two filling schemes are used in this mode, initially 80 mA and then 100 mA in 60 bunches and 90 mA to 100 mA in 40 bunches, corresponding to 128 ns and 192 ns bunch spacing, respectively. Due to the high demand for time-resolved measurements, PETRA III was mainly operated in timing mode. The detailed distribution of the operation modes in 2015 is shown in Fig. 3.

During machine development time, several efforts were made to improve the bunch purity and remove satellite bunches using the multibunch feedback system.

High reliability is one of the key requirements for a synchrotron radiation facility. The key performance indicators are availability and mean time between failures (MTBF). In 2015, the weekly availability exceeded the targeted 95% over several periods of the year. At the end of the user run, the average availability just reached the target availability of 95%. This is a remarkable achievement considering that PETRA III restarted in 2015 after a one-year-long shutdown with a six-week-long recommissioning period for the new extension sections. The reliability of the radio frequency system was improved compared to the previous run periods in 2013 and 2014 by using a different tuning procedure. Nevertheless, the MTBF was 31 h, which is not on a par with that of other world-leading facilities and leaves room for the improvement of several technical components.

First light from new undulators

After a short maintenance and shutdown period from 24 August to 4 September 2015, the two new undulators PU64 and PU65 in the extension section North were operational. On 8 September, first light was observed on the photon screens located in front of the beam shutters in the front-end sections of the new beamlines (Fig. 4).

This success was partly compromised by the observation that the fringe field of the deflecting dipole between the two undulators affected the orbit of the beam more than expected. Nevertheless, the commissioning process of the new beamlines continued after a feed-forward correction procedure was established to adjust the orbit. Further actions will be taken to improve the fringe field of the dipole magnet.

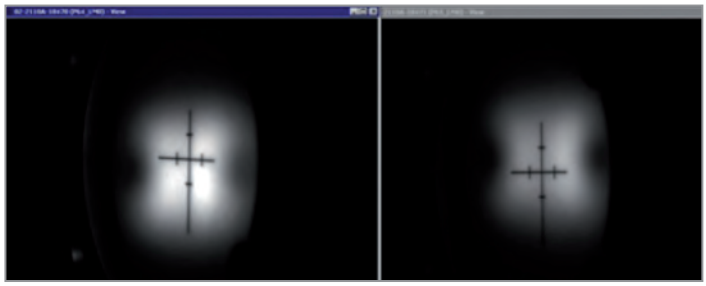

Figure 4

First light from the new undulators PU64 and Pu65 on 8 September 2015

Contact: Rainer Wanzenberg, rainer.wanzenberg@desy.de
Michael Bieler, michael.bieler@desy.de

FLASH.

15 years of free-electron laser operation at DESY

2015 was an anniversary year for DESY's FLASH free-electron laser (FEL) facility, marking 15 years since its worldwide first lasing in the vacuum-ultraviolet (VUV), 10 years of self-amplified spontaneous emission (SASE) operation for users, five years of lasing in the water window and one year of simultaneous operation of two FEL beamlines. All these were world records and world-first achievements. But 2015 was also a very successful year by itself – featuring not only highly stable operation for user experiments, but also the parallel operation of the new and old beamline, FLASH2 and FLASH1, the generation of seeded radiation at 38 nm wavelength, the first-ever simultaneous production of three SASE wavelengths with one linear accelerator and the stable long-term operation of FLASH2 with high beam power.

Highlights

FLASH is the world's first soft X-ray FEL facility (Fig. 1). It was the first to produce SASE radiation in the VUV range at 109 nm, in February 2000 – that is, 15 years ago. Since summer 2005, FLASH has been operated as a user facility, pioneering research into ultrafast processes in atoms, molecules and new materials. Numerous upgrades made it possible to achieve SASE lasing in the water window between 2.34 and 4.4 nm in September 2010. For one year now, FLASH has been operated with two beamlines in parallel as a tandem. On 20 May 2015, in a symbolic naming ceremony, the two FLASH experimental halls received their new names, "Albert Einstein" and "Kai Siegbahn".

In early 2015, the sFLASH seeding team succeeded in generating the seventh harmonic of the 267 nm seed laser wavelength. The 38 nm radiation pulses had an energy of up to 75 µJ with a bandwidth of 0.2 nm. This is an important milestone towards establishing seeding for user experiments at the FLASH2 beamline. The team also succeeded in using the same electron bunch twice: for SASE lasing in the sFLASH undulators at 38 nm and in the FLASH1 undulators at 13.6 nm – while FLASH2 was lasing with a second bunch at 20 nm. Thus, for the first time, one linear accelerator drove the SASE process in three beamlines in parallel, producing three photon wavelengths simultaneously. This is a major step forward towards true parallel operation of sFLASH and FLASH1.

The commissioning of the new FLASH2 beamline made great progress. Parallel operation with FLASH1 has now been established as a standard – a precondition for FLASH2 user runs to start in 2016. First attempts have been made at tapering the FLASH2 undulators, pushing the SASE single photon pulse energy to 600 µJ at a wavelength of 15 nm, a new world record.

FLASH operation

In 2015, FLASH was available for beam for 7322 h (83.6% of the year) with scheduled shutdown times of 1035 h for maintenance and other work. Downtime due to technical failures was 403 h. Besides the usual shutdown at the end of the year

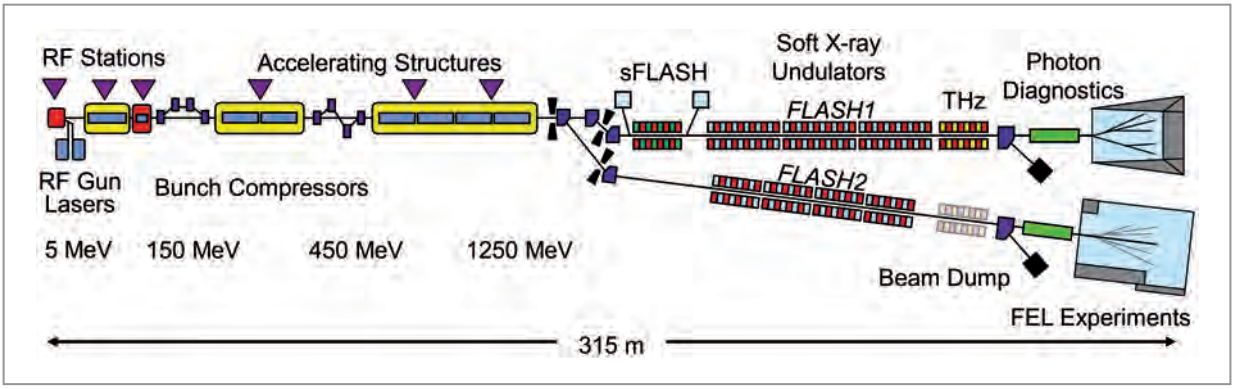

Figure 1
Sketch of the FLASH facility with the accelerating section and the two beamlines, FLASH1 and FLASH2 (not to scale)

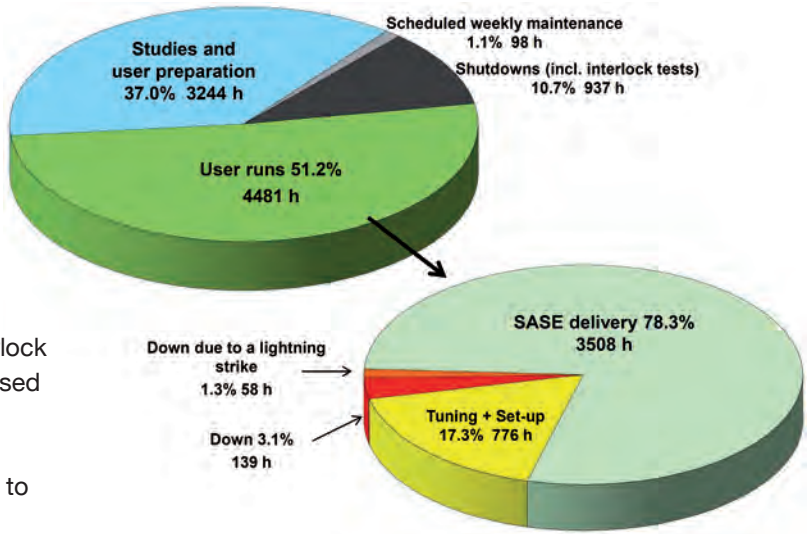

Figure 2

Beamtime distribution in 2015 (downtime included) and breakdown of user beamtime in terms of SASE delivery to user experiments and setup/tuning time

and one week for the annual tests of the personnel interlock system, a three-week shutdown in May and June was used to complete the radiation shielding of FLASH2. Another 1000 t of sand were placed on top of the facility, giving FLASH2 the permission to run with a beam power of up to 100 kW. The interlock system based on beam loss measurements, which prevents accidental damage of the undulator magnets by beam losses, was finalised and successfully tested.

A long-term test was set up with more than 4000 electron bunches per second directed into the FLASH2 beamline with open undulators to measure long-term beam losses. The result was very positive, so that SASE operation with many thousands of bunches per second is now also possible in FLASH2.

The fifth FLASH user run period, which started in February 2014, ended in May 2015; the sixth user period started in June and was concluded at the end of 2015. With 4481 h in 2015, FLASH thus again provided more beamtime to users than in any previous year (Fig. 2). Another 3244 h were used for machine studies, improvements and developments of the photon beamlines and preparation of user runs.

In 2015, machine studies included 400 h of beamtime for general accelerator R&D. This programme will continue with 750 h of beamtime per year, giving researchers the possibility to use FLASH for accelerator-related science independently of the FEL user programme. An example is the preparation of the FLASHForward beam-driven plasma acceleration experiment, which is being set up in a new third beamline, FLASH3.

Regarding user runs in 2015 (Fig. 2), the tuning and setup time could be slightly reduced, from 21% to 17.3%, so that SASE radiation was actually delivered to the experiments for 78.3% of the beamtime – a higher quota than in 2014. At 3.1%, the downtime due to failures of machine components was remarkably low. An unfortunate lightning strike hit the DESY site in June, imposing another 1.3% of downtime.

Stabilisation

The implementation of the new low-level radio frequency (RF) control system for the superconducting accelerator modules led to a remarkable rms stability in RF amplitude ($dA/A < 0.01\%$) and phase ($d\varphi < 0.01°$), further improving the stability of the SASE energy, wavelength and photon pulse arrival time.

A series of slow feedbacks on beam energy, arrival time, compression ratio, charge and other parameters are now routinely used to stabilise the performance over many hours.

At this point, the stability of the electron source needs to be improved as well. A considerable effort has been made to stabilise RF gun operation. The RF gun and the RF window installed in early 2014 are now working without breakdowns – yet still with a reduced RF pulse length of 550 µs. A fast interlock scheme has been implemented to reduce damage in case of breakdowns.

The water system is now regulating the gun temperature to better than 0.02°C, the resolution limit of the system. A second feedback loop has been implemented based on the measurement of the reflected power acting on the RF pulse length. The cascaded scheme – basic water regulation, usual low-level RF feedback system on RF amplitude and phase, plus the new pulse-length-based feedback – improved the RF amplitude stability to $dA/A < 0.005\%$ and, more importantly, the phase stability by a factor of three to $d\varphi = 0.009°$.

Further work is ongoing to upgrade the arrival time and beam position monitors for better resolution and low-charge operation down to 20 pC. This will make it possible to use the slow feedbacks in arrival time and orbit down to the very small charges required for ultrashort-pulse generation.

In addition, efforts are ongoing to better understand beam optics and to work on the reproducibility of magnet settings. New reference files are being produced that include FLASH2, supporting operators in quicker setting up beam.

Contact: Siegfried Schreiber, siegfried.schreiber@desy.de

PITZ.

New developments at photoinjector test facility

In 2015, operation of the PITZ photoinjector test facility at DESY in Zeuthen focused on studying stability and reliability issues of radio frequency electron sources (RF guns) for the European XFEL X-ray free-electron laser. In parallel, a number of new developments were put into operation throughout the year.

Reliability studies for the European XFEL

Gun 4.2: a setup for improved reliability

Gun 4.2 was put into operation at PITZ in September 2014. The main feature of this setup is that it is equipped with two Thales windows to feed the RF to the gun, which has the advantage that the power load on each window is reduced by a factor of two compared to setups with a single window. A two-window solution was already successfully used at PITZ in 2010 with DESY-type RF windows at RF pulse lengths up to 300 µs.

At the end of December 2014, tests for studying the long-term stability of the gun setup with two Thales windows started. After the standard conditioning period, the two RF windows could be operated reliably and no problems from the windows were observed anymore. A two-window setup thus indeed helps to avoid the destruction of the sensitive and expensive RF windows that was previously observed at PITZ, FLASH and the European XFEL.

However, problems appeared in the gun itself. Since the new cathode RF spring design (contact stripe) did not seem to be the reason, appearing to work reliably, the problems could be associated with the long life cycle of the gun, which was already used at PITZ and FLASH from 2008 to 2012. Therefore, it was decided to reduce the peak power in the gun from 6.5 to 5 MW (corresponding to a cathode gradient of 53 MV/m as foreseen for the start-up of the European XFEL) in order to gain some long-term operation experience with long RF pulses (650 µs) at this RF power level.

In spring 2015, beam quality measurements at PITZ successfully demonstrated the requirements for the start-up conditions of the European XFEL (53 MV/m, ~11 ps long Gaussian laser pulses, 500 pC bunch charge). In summer and autumn, further measurements relevant for FEL user facilities were performed, e.g. work on the RF regulation with the same modulator system as used at the European XFEL and emittance measurements as a function of cathode aging.

Future plans

In November 2015, Gun 4.2 was dismounted from PITZ in order to test another gun setup (Gun 4.6) with two DESY-type RF windows, which are significantly cheaper than the Thales windows. In addition, the T-combiner in the waveguide system was slightly modified, changing the position of the RF windows in such a way that the power load due to reflections from the gun is significantly reduced. Furthermore, Gun 4.6 has a modified design of the cathode area, based on an improvement of the old watchband design of the contact spring. Finally, the new gun is an unused cavity, which should show no such limitations of the RF performance as were observed with Gun 4.2. It is therefore expected that, with Gun 4.6, beam quality and reliability can be demonstrated for the full operation parameters of the European XFEL.

Test of new developments at PITZ

Time-resolved beam characterisation with a TDS

In 2015, the commissioning of an S-band travelling-wave transverse deflecting RF structure (TDS) for high-resolution

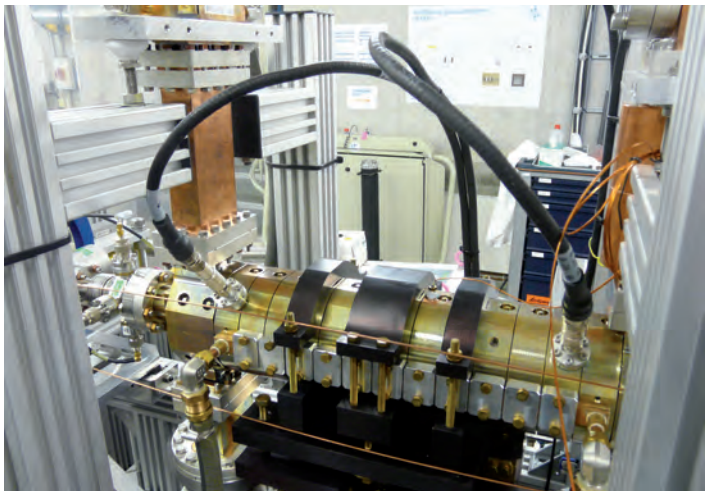

Figure 1

Transverse deflecting cavity at the PITZ beamline

time-resolved electron beam characterisation started at PITZ (Fig. 1). The system was designed and manufactured by the Institute for Nuclear Research (INR RAS) in Moscow, Russia, as a prototype for the TDS in the injector part of the European XFEL.

The TDS shears the bunch transversely, mapping the longitudinal coordinate onto a transverse axis on an observation screen downstream, thus enabling bunch length measurements. The full longitudinal phase space can be obtained when deflecting the sheared beam into a dispersive section. Furthermore, the TDS system can be used to measure the slice emittance along the bunch.

Beam measurements done so far comprised bunch length measurements for different bunch charges, laser spot sizes and phases in the gun and the booster cavity. Comparisons with simulations suggest a slightly shorter laser pulse length than originally assumed. Full commissioning of the system with high-resolution longitudinal phase space characterisation and slice emittance measurements will take place in 2016.

First plasma acceleration experiments

In the first months of 2015, preparatory work for plasma self-modulation experiments took place in the lab and at the PITZ accelerator. An 8-µm-thick Kapton foil was identified as exit window for safe operation of the plasma cell in the beamline environment. Machine setup studies, beam focusing into the plasma channel and beam propagation studies in the plasma cell region were conducted using a specially inserted screen station at the plasma cell position in the PITZ beamline. In summer 2015, the plasma cell was finally installed for two measurement periods (Fig. 2), and first experiments towards the demonstration of self-modulation of long electron beams were performed.

All functionalities of the plasma cell were shown successfully, including the generation of plasma (Fig. 3), which was a world premiere as it was the first time that plasma was generated in a cross-shaped heat pipe oven. However, as the necessary plasma density could not be generated, it was not possible to measure the energy modulation of the electron beam passing through the plasma. The problems are now understood, and an upgraded plasma cell is currently being built for the next experimental run period in 2016.

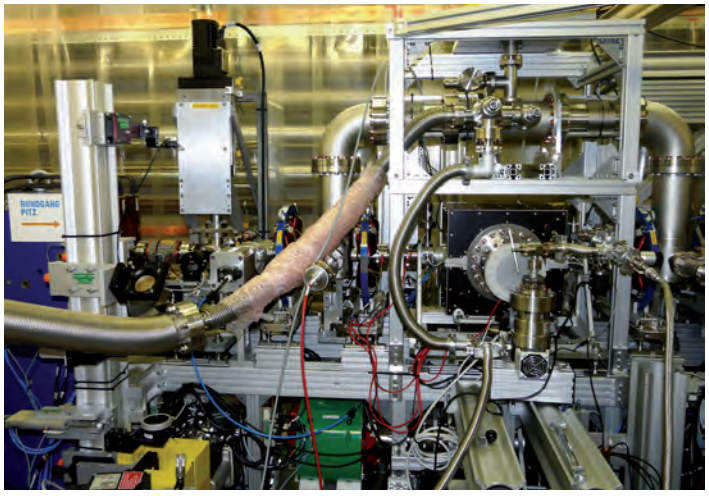

Figure 2

Plasma cell inserted into the PITZ beamline

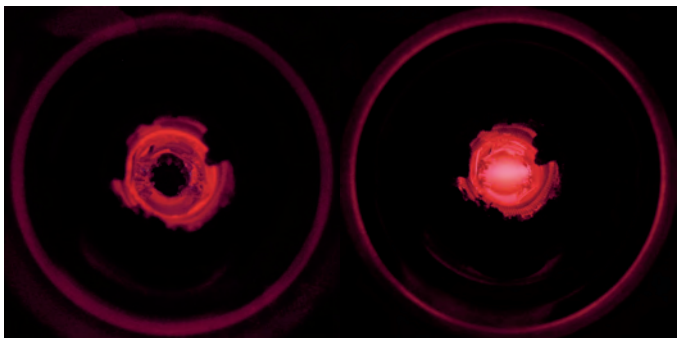

Figure 3

Lithium plasma generated by laser ionisation. Left: ionisation laser off (heat glowing). Right: ionisation laser on (plasma). This type of experiment was done for the first time in a cross-shaped heat pipe oven.

Commissioning of 3D ellipsoidal laser system

To develop a photoinjector system able of producing ultimate beam quality for FEL operation, a new photocathode laser system capable of generating quasi-ellipsoidal laser pulses was installed at PITZ at the end of 2014. This system, which was developed at the Institute of Applied Physics in Nizhny Novgorod, Russia, was commissioned in 2015. By coupling the new laser system to the existing primary photocathode laser beamline, first photoelectrons were produced.

Several improvements of the system were implemented throughout 2015. An infrared auto-correlator was installed for temporal characterisation of the ultrashort probe pulses and the unshaped, chirped photocathode pulses. Two cross-correlators were put into operation for the characterisation of the shaped infrared and ultraviolet pulses. These online devices are critical for feedback corrections of the beam shaping system. In addition, the water cooling system was replaced with a new solution utilising a heat exchanger for reliable and accurate thermal regulation of some of the laser subsystems, which should significantly improve the stability of the system.

On-table studies and experiments of beam shaping, system reliability and stability as well as frequency conversion optimisation have begun. Work on the synchronisation of the laser with the RF system is ongoing and will be finished in a few months. First electron beam characterisation measurements are expected in 2016.

Contact: Anne Oppelt, anne.oppelt@desy.de

European XFEL.

Accelerator construction and injector commissioning

The accelerator complex of the European XFEL X-ray free-electron laser is being constructed by an international Accelerator Consortium of 17 European research institutes under the leadership of DESY. It consists of the injector, the main linear accelerator with altogether 100 superconducting accelerator modules and a number of warm (that is, not cryogenically cooled) beamlines used to transport the electron beam either between successive accelerator sections or to the undulators. In 2015, the injector was complemented by its two accelerator sections. Commissioning of the injector started in the fourth quarter of the year. The installation of the main accelerator sections is proceeding at a high pace. Full accelerator commissioning will start in 2016.

Building the accelerator

Tunnel installation of the accelerator components is carried out by a large team coordinated by DESY. The installation work is proceeding at a quick pace, and remarkable progress is visible in all accelerator sections. Figure 1 shows the cold (that is, cryogenically cooled) linear accelerator section L3.

The accelerator modules are assembled at IRFU of CEA in Saclay, France, in a strong collaborative effort. All components need to be delivered at a sufficient rate and quality so the assembly team can concentrate on the procedures and especially on the throughput of the different workstations. Meanwhile, all 800 superconducting cavities – an in-kind contribution of DESY and INFN in Milano, Italy – have been delivered. A team from IFJ-PAN in Poland successfully tested the cavities and demonstrated their high performance. The high-power radio frequency couplers are still among the most challenging components needed for the accelerator modules, requiring care and excellent quality control in all production steps. The in-kind contributor, LAL in France, continued to supervise the coupler vendors. During most of 2015, couplers were regularly delivered from LAL to IRFU after successful conditioning. However, a buffer to cushion irregularity in the delivery rate could not yet be established.

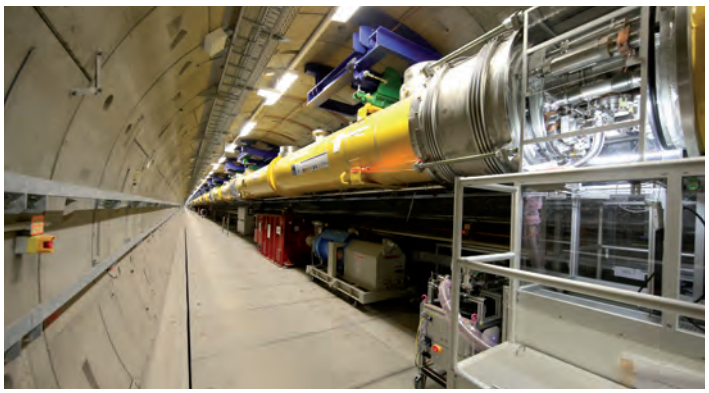

Figure 1

Accelerator modules installed in the linear accelerator section L3. Only some of the 59 modules that were put in place by the end of 2015 are visible. The continuous string of modules at the end of 2015 exceeded 400 m.

All other components of the accelerator modules were available for module integration. The superconducting quadrupole packages were built in a collaboration between CIEMAT in Spain, IRFU and DESY, with magnet tests performed by IFJ-PAN. The frequency tuners were provided by DESY in collaboration with INFN. IRFU took care of assembly material like magnetic shielding. The cryostats, with the cold mass and the outer vessel, were produced under supervision of DESY together with INFN. Cold vacuum components are provided by BINP in Russia.

All accelerator modules of the European XFEL are tested at the Accelerator Module Test Facility (AMTF) at DESY. In spring 2015, a dedicated effort of IFJ-PAN and DESY helped to drastically shorten the testing time, ensuring that newly arriving modules could be installed in one of the test benches almost immediately after their delivery to DESY. By the end of 2015, nearly 75 modules had been tested. For most of them, the average usable accelerating gradient was found to clearly exceed the European XFEL specification. An average of 27.4 MV/m was reached, which is 16% above the design value and ensures a wide margin for the final electron energy. The last 14 measured modules even showed an average gradient of 29.3 MV/m. The variation of the maximum usable accelerating gradients of the individual cavities and modules was within acceptable limits. Right after the cold module test in the AMTF at DESY, an individually tailored waveguide distribution system is assembled for each module, with the help of a team from Sofia University in Bulgaria.

Beamline magnets, vacuum chambers and a variety of beam diagnostic elements, such as cold beam position monitors

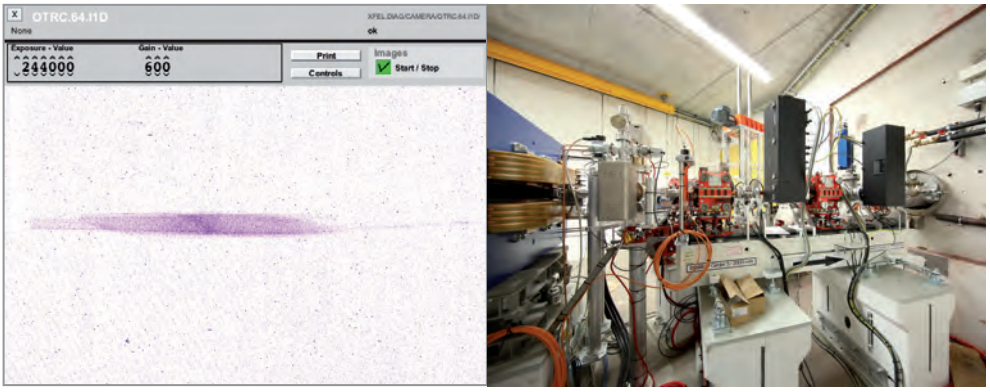

Figure 2

Left: First image of the electron beam on a scintillating screen in front of the injector beam dump. Right: The dump area in the injector tunnel. The camera that took the electron beam image is inside the black box on the right.

(BPMs), warm BPMs, current transformers, dark-current monitors, scintillator-based screen stations and wire scanners, were delivered by consortium partners. For the bunch compressor sections, pre-assembled girders are used, and chicane vacuum systems from BINP complement the installation. After finishing the cryogenic transfer line, which is located above the electron beamline, installation in these sections now continues. Beam distribution systems downstream of the cold linear accelerator are currently being put in place. In 2015, the focus was on the construction and installation of the steel suspension system for about 400 m of electron beamline. In the undulator areas SASE1 and SASE3, all beam transport magnets were installed, and the SASE1 electron vacuum system was completed.

First electron beam accelerated in injector

The injector is the first section of the accelerator. It is about 40 m long and located on the seventh underground floor of the injector building on the DESY-Bahrenfeld site. Here, the electrons are extracted from a photoelectric cathode exposed to an ultraviolet laser. After acceleration to relativistic energies in a normal-conducting 1.6 cell cavity, the electrons enter the first two superconducting accelerator modules: a standard 1.3 GHz module similar to the other 100 modules that are being installed in the accelerator tunnel and a 3.9 GHz higher-harmonic module used to manipulate the longitudinal beam shape. At a beam energy of about 130 MeV, the electron bunches pass through the laser heater, where the longitudinal bunch properties are altered again. The beam properties can afterwards be measured with various devices in an extensive diagnostic section.

All the members of the Accelerator Consortium contributed to the construction of the injector, which was completed with the insertion of the 3.9 GHz module in November 2015. After the final approval of the personnel safety measures by the authorities, commissioning started. For the first time, the complete cryogenic installation in the injector was cooled down to 2 K, and the modules were ready to be operated with radio frequency. Thanks to the careful preparation of all the subsystems and a thorough technical commissioning, it was possible, within five hours on 18 December, to accelerate and steer the electron beam all the way to the injector beam dump (Fig. 2).

In early 2016, a comprehensive beam commissioning will follow, with the aim to investigate the complete electron beam parameter space that is required to serve the various user needs. In addition, an R&D programme has been launched to improve the reliability of some crucial injector components that showed early fatigue during high-power operation. DESY and European XFEL have also decided to prepare a second photocathode laser system to eliminate this single point of failure and improve the overall availability of the accelerator during commissioning and operation.

Full accelerator commissioning to start in 2016

In 2016, installation of all the sections of the accelerator complex will be finished. Depending on the availability of the required subcomponents, the last module (XM100) should be at DESY before the end of the second quarter. AMTF tests and tunnel installation will follow immediately. In order to concentrate on the final module installation, the tunnel installation team aims to finish all the beam transport sections before the summer.

The beam-based commissioning of all the injector systems that began in 2015 will continue in 2016. About 12 months are foreseen to reach all the injector commissioning goals and be well prepared for the full accelerator commissioning, which should start in the second half of 2016, marking the transition from construction to operation phase. DESY will be responsible for the operation of the accelerator and has begun to prepare for this new and exciting task.

European XFEL technology sets benchmark

The successful implementation of superconducting accelerator technology at DESY's FLASH facility, and now in much larger scale at the European XFEL, led to the decision to realise the upgrade of the LCLS X-ray laser at SLAC in the USA as a superconducting continuous-wave facility – a choice of technology that underlines the world-leading position of the European XFEL project. Essentially all the basic technology used for FLASH and the European XFEL is going to be reproduced for the LCLS upgrade, and corresponding collaborations between SLAC and DESY have been established.

Contact: Hans Weise, hans.weise@desy.de
Winfried Decking, winfried.decking@desy.de

REGAE.

First steps into the attosecond world

Simulations and analytical studies show that with a new compression concept, the bunch length accessible with REGAE – the Relativistic Electron Gun for Atomic Exploration facility at DESY – could be further decreased into the attosecond range. The practical application of this new parameter range requires significant advances in the longitudinal beam diagnostics and further improvements in the stability of the facility.

To reach the challenging beam parameters required for experiments at REGAE, which include time-resolved electron diffraction experiments and a plasma experiment, the facility has to operate in a very unusual and widely unexplored parameter range. While for the injection of the electron beam into a plasma channel the beam has to be focused down to a radius of a few micrometres, electron diffraction requires a minimal divergence of the beam at the location of the target. In both cases, a small transverse beam emittance (the product of rms beam size and uncorrelated rms divergence) is essential, since it results in a small beam divergence at not too large beam size as well as in a manageable divergence at small beam size as required for the plasma experiment. Space charge forces set rigorous limits to the achievable emittance, so that the generation of transverse emittances on the order of some 10 nm (normalised) becomes only possible at low bunch charges of 10–100 fC.

An alternative to generating the low charge from a tiny spot right at the cathode is to produce a larger charge and pass the beam through a collimator at higher energy. While the charge is reduced, the emittance can be improved significantly, because tails of the distribution that have suffered from non-linear space charge forces are cut off. The measurements presented in Fig. 1 show the emittance versus the radius of a collimator used for this operation mode. These record emittances are about a factor of 2 smaller than comparable values achieved without collimator for the same charge.

While this procedure promises significant operational simplifications and somewhat improved transverse beam parameters, it also has disadvantages as the longitudinal phase space degrades due to the larger charge at the cathode. The application of this operation mode remains hence limited to experiments for which the bunch length is less important, while for the majority of experiments the standard procedure is still required.

Both the time-resolved diffraction experiments and the plasma experiment need short electron bunches in the range of about 10 fs. In pump–probe type diffraction experiments, a reaction of the material under investigation is initiated by irradiating the target with laser light (pump). When the electron beam (probe) hits the target with a defined delay, the temporal evolution of the reaction can be deduced. Combining measurements with varying delay allows a movie of the reaction under investigation to be compiled. The ultimate temporal resolution of such an atomic movie is given by the length of the electron bunch.

When electrons are accelerated in a sinusoidal (plasma) field, their energy gain depends on their position inside the field. Even when the electron bunch is placed at the crest of the

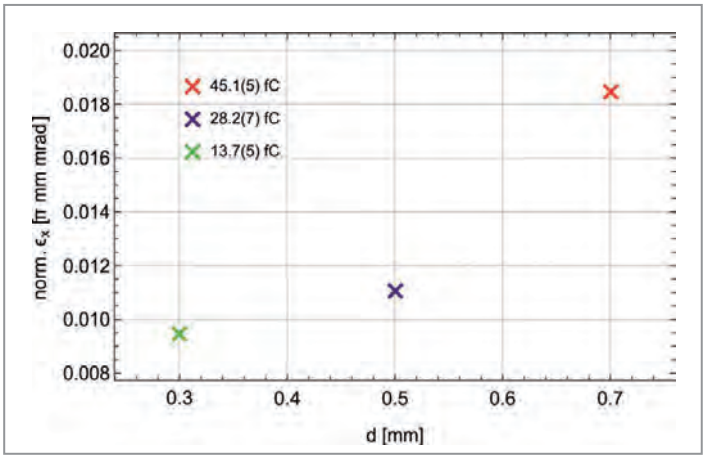

Figure 1

Normalised emittance and charge versus collimator radius

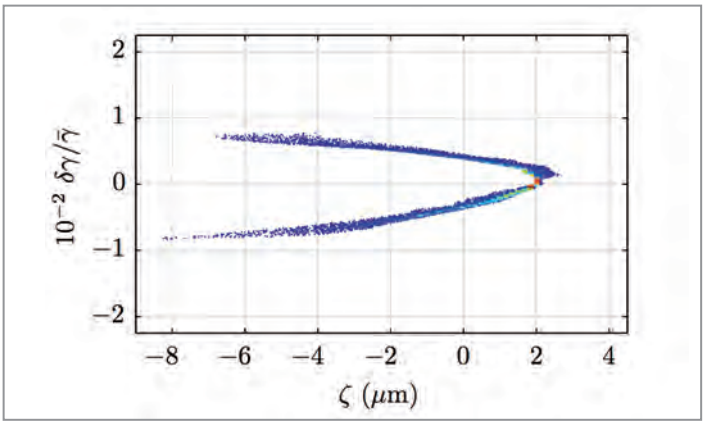

Figure 2

Longitudinal phase space at the focus position with the characteristic curvature resulting from acceleration in a sinusoidal field

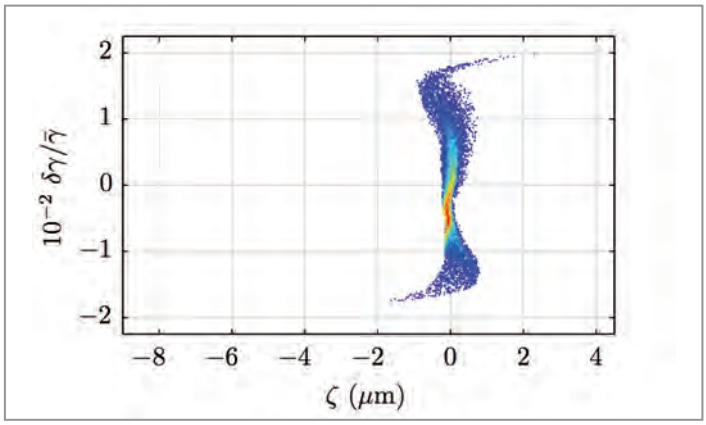

Figure 3

When the non-linear correlations are removed, the rms bunch length can reach values of nearly 800 as (240 nm).

wave, particles in the front or the back will get a somewhat smaller energy gain than a particle in the centre of the bunch. The energy spread is thus directly related to the bunch length relative to the wavelength of the accelerating field. New acceleration techniques like plasma acceleration work with significantly shorter wavelengths than conventional accelerators and thus require much shorter electron bunches.

At REGAE, electron bunches are created at the photocathode as relatively long packages, which are compressed longitudinally after acceleration to energies of a few MeV. Compared to the generation of short bunches directly at the photocathode, the compression at higher energies allows for shorter bunches with better transverse quality, due to diminished space charge effects. For the compression, a simple longitudinal focusing is employed, i.e. the bunch is passed off-crest through a buncher cavity, so that a linearly correlated energy spread is imprinted onto the charge distribution. Thus, particles in the tail travel faster than particles in the front of the bunch, and the bunch length decreases in a drift region following the buncher cavity.

This apparently simple process reveals a complex beam dynamics in its details. The achievable bunch length is limited by non-linear correlations in the longitudinal phase space resulting from space charge effects, the curvature of the accelerating fields and the drift dynamics itself, which is not strictly linear due to the non-linear relation between energy and velocity.

A compensation of the non-linearities is possible, for example by means of an additional radio frequency (RF) structure operating at a higher frequency than the accelerating cavities. With such a structure in place and re-optimised emission parameters, a bunch length down to 700 as (attoseconds) would be achievable at REGAE. However, the optimisation of the RF parameters of gun, buncher and higher-harmonics cavity is complex, and another cavity (plus power source) would require a significant investment.

Detailed studies have now revealed a new concept for compensating the non-linearities. By shifting the emission from the photocathode to an unusual phase, far off-crest, it is possible to impress an energy spread onto the electron distribution that leads to a longitudinal expansion of the bunch in the drift region between gun and buncher. When the electron packet reaches the buncher, it is structured as if it had been emitted by a gun operating at a lower frequency, so that then the buncher itself works like a higher-harmonic cavity. A complete analytical description of the beam dynamics allows optimal parameter combinations to be found in which the buncher compensates non-linearities up to the third order and introduces the linearly correlated energy spread required to compress the bunch down to 800 as. Figures 2 and 3 compare the longitudinal phase space at the position of the longitudinal focus without and with correction of the non-linear correlations.

Even shorter bunches could be generated by re-adjusting the distance between gun and buncher and between buncher and target. It has to be noted, however, that neither the temporal stability nor the longitudinal diagnostics is yet available to make use of attosecond bunches in experiments. While the studies demonstrate the feasibility in principle, significant development work still needs to be carried out in the forthcoming years before attosecond beams will become useful for practical applications at REGAE.

Contact: Klaus Flöttmann, klaus.floettmann@desy.de

Highlights · New technology · Developments.

FLASH2.

Commissioning of the second undulator line for user operation at FLASH

Starting in 2011, DESY's FLASH free-electron laser (FEL) facility was extended with a second undulator beamline called FLASH2. The new beamline contains 12 variable-gap undulators, which allow the wavelength to be varied in a wide range independently of the first beamline, FLASH1. Commissioning of FLASH2 was very successful: In the past two years, parallel operation of the FLASH1 and FLASH2 beamlines was established and lasing at wavelengths between 4 and 60 nm in FLASH2 was demonstrated. In 2015, a new record FEL single-pulse energy of 600 µJ was achieved in the new beamline. User operation at FLASH2 will start in 2016.

Starting in autumn 2011, FLASH was upgraded with a second undulator beamline and a second experimental hall. From 2016 on, the facility will thus be able to accommodate twice as many experiments as before. The multi-beamline approach is made possible by the superconducting TESLA accelerator technology employed at FLASH, which allows two undulator beamlines to be fed in parallel.

The new FLASH2 beamline branches off the main beamline behind the last accelerator module. Figure 1 shows a picture of the new beamline, which includes 12 new undulators with variable gap as well as photon diagnostics. In 2014, FLASH2 was put into operation for commissioning. First XUV and soft X-ray photon pulses were generated in summer 2014. In 2015, the simultaneous operation of both FLASH beamlines was established as standard operation.

At FLASH, electron bunch trains of up to 800 µs can be generated at a repetition rate of 10 Hz. Each bunch train can be split into two parts. The bunch pattern can be chosen freely, so the FLASH2 starting time is flexible as well. In addition, the repetition rate of FLASH2 can be switched to 1 Hz independently of the standard 10 Hz operation of the main accelerator. An important feature is that both beamlines can be operated with thousands of electron bunches at the same time. This simultaneous operation with high bunch rate poses a major challenge for the machine and undulator protection system, which has been successfully met. As an example, Fig. 2 shows the operation of FLASH2 with a bunch train of 420 bunches at a repetition rate of 10 Hz, i.e. with 4200 bunches per second.

The main beam parameters, such as intra-pulse repetition rate, bunch charge and bunch duration, can be adjusted independently to the different needs of experiments at FLASH1 and FLASH2. This is possible because the two beamlines are served by different lasers and because the RF phase and amplitude of all accelerator modules can be varied

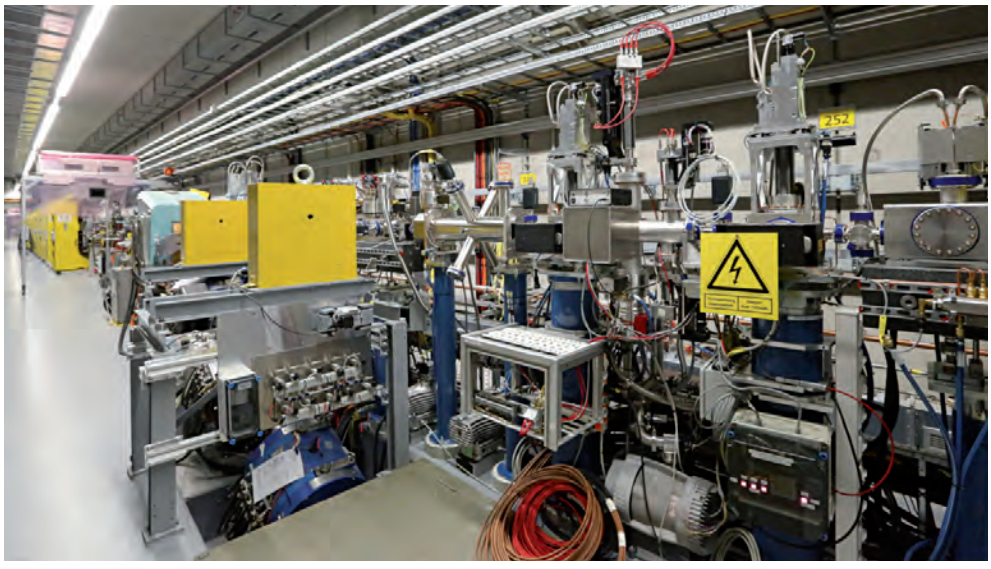

Figure 1
FLASH2 undulator beamline with variable-gap undulators (yellow supports in the background). The beam dump can be seen in the front on the left, and part of the diagnostic instruments used to measure the properties of the XUV and soft X-ray pulses are visible on the right. The beam travels from left to right.

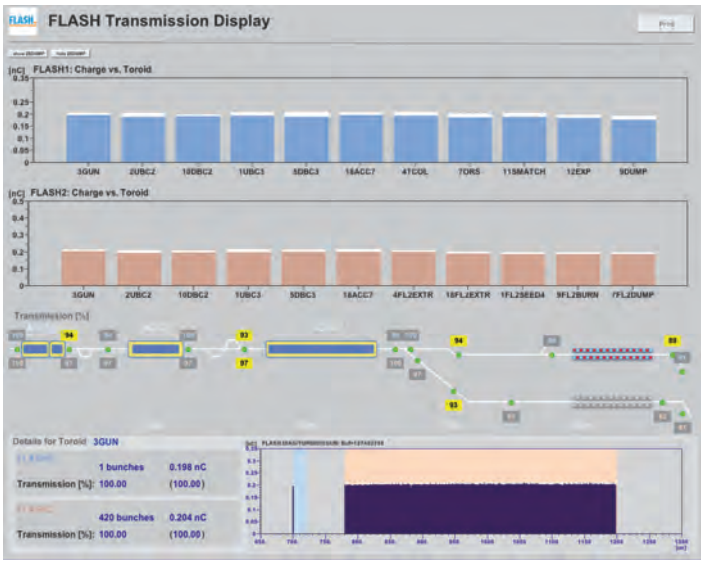

Figure 2

Simultaneous operation of FLASH1 and FLASH2 with the FLASH2 beamline being operated with an electron bunch train of 420 bunches (i.e. 4200 bunches per second – lower plot, pink background)

independently in a wide range between the FLASH1 and FLASH2 part of the RF pulse. The usual FLASH1 feedback system was extended to also regulate the compression and charge of the FLASH2 electron beam.

Because of the fixed-gap undulators in FLASH1, the electron beam energy delivered by the accelerator is determined by the wavelength required for the FLASH1 experiments. Thanks to the variable-gap undulators in FLASH2, the wavelength for FLASH2 can nonetheless be varied in a wide range. A campaign was started to explore the FLASH2 wavelength range for a given electron beam energy. It was shown that the complete wavelength range from 4 to 60 nm can be covered. Figure 3 shows the obtained wavelengths with an FEL single-pulse energy above 50 µJ.

In 2015, a new world record was achieved at FLASH2: At an electron beam energy of 1.1 GeV and a wavelength of 15 nm, an average FEL pulse energy of 600 µJ was reached (Fig. 4). In addition, first approaches were made to taper the FLASH2 undulators, which will allow the FEL pulse energy to be further increased.

New diagnostics for electrons and photons to control the electron beam and optimise the properties of the photon radiation were commissioned and tested. The new bunch diagnostics is also sensitive to small bunch charges down to 20 pC. The use of such small bunch charges is of rising interest, as is the generation of ultrashort radiation pulses of a few femtoseconds in duration.

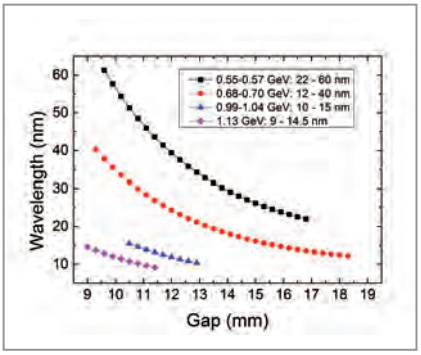

Figure 3

Wavelengths achieved at FLASH2 as a function of the corresponding gap width of the variable-gap undulators. Each curve is for a different electron beam energy. Only wavelengths with an FEL single-pulse energy of more than 50 µJ are shown.

Contact: Juliane Rönsch-Schulenburg, juliane.roensch@desy.de

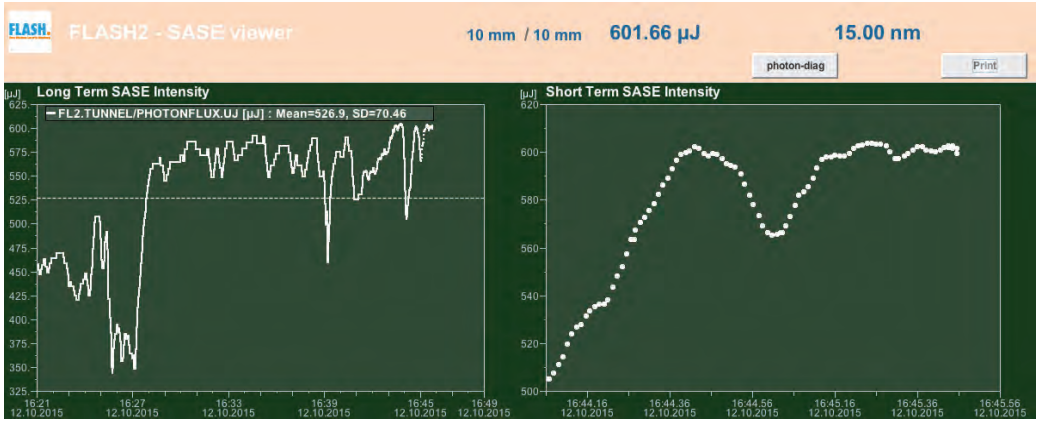

Figure 4

A record 600 µJ FEL pulse energy was reached at FLASH2 at a wavelength of 15 nm and an electron bunch energy of 1.1 GeV.

LLRF at FLASH – status and experience.

Successful operation using the MTCA.4 standard

The low-level RF (LLRF) system for the FLASH free-electron laser (FEL) facility at DESY was completely upgraded to a novel technology standard based on the MTCA.4 platform. After 2.5 years of operation of the superconducting radio frequency (RF) stations and one year of operation of the normal-conducting RF gun, the system has demonstrated its reliability and performance improvements. Nonetheless, developments are ongoing to further enhance the performance and functionality of the system, focusing on software and firmware improvements as well as on automation routines. In addition, further steps are being taken to improve the system reproducibility and long-term stability. Prototype hardware components are being replaced step by step with improved components developed for the European XFEL X-ray laser. The direct transfer of methods and component developments between FLASH and the European XFEL is one of the major advantages of having this new common technology standard.

LLRF control system

The LLRF system at FLASH controls the acceleration voltage and phase with respect to the electron beam to a desired operational set point. To fulfil this requirement, very precise measurements of these parameters are required as well as high-performance data processing for the digital feedback loop. Precision computations are performed using latest field programmable gate array (FPGA) techniques on a sub-micro-second time scale. Within the LLRF system, more than 60 RF signals are processed in parallel to control up to 16 cavities in the vector sum for a single RF transmitting station. A schematic view of the data processing is presented in Fig. 1.

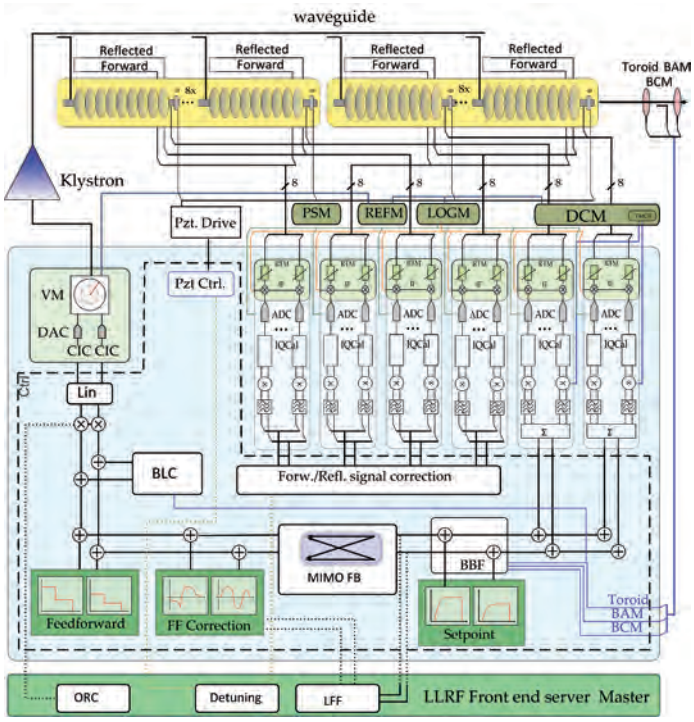

Figure 1

Schematic view of the LLRF control system layout. Data processing steps are performed on FPGA level.

The LLRF system output is a driving RF waveform to a high-power multibeam klystron, which feeds power to the 16 cavities through a waveguide system. The transmitted, forward and reflected RF signals are monitored and processed within the LLRF system. This takes place in two stages, firstly within the digitiser board where the RF signals are digitised and pre-processed (calibration and filtering), before secondly the data is concentrated on a main processing board. Here, the cavity vector sum is used as input for the complex intra-pulse multiple-input and multiple-output (MIMO) feedback controller. This signal is then added to a feed-forward drive signal before the data is sent to a digital-to-analogue converter to control the driving RF output signal. Special algorithms for linearisation of the klystron input–output transfer function, compensation of beam loading and self-adapting drive optimisation are included in the controller.

During operation of the system, the required amplitude and phase regulation of 0.01% and 0.01°, respectively, are being routinely demonstrated. Furthermore, measurements of beam arrival time prove that the system stability has been improved compared to the previously installed LLRF system. The demonstration of successful operation has been particularly important for the European XFEL, since the installation, commissioning and performance indicate that the LLRF system is mature enough to be used on a larger scale.

For about one year, the normal-conducting RF gun has also been controlled by an MTCA.4 LLRF system. The main difference is that the controller is implemented on the digitiser board, reducing the latency of the feedback loop. The

firmware layout was derived from the superconducting control framework, and basic routines and algorithms could easily be migrated. By using a new concept of RF-based resonance control of the gun cavity, the performance of the system was greatly improved compared to the former VME-based LLRF system.

Compensation of long-term drifts

Excellent reproducibility of the amplitude and phase of the accelerating fields is key to minimising switching times between different FEL users. The LLRF system can be one of the main contributors to long-term drifts that influence the RF field properties with respect to the electron beam. Those drifts are caused by environmental changes in temperature and humidity, which affect the electronic RF field detection circuits. While the ambient temperature of the electronics is regulated to a level of 0.2°C (rms), humidity changes are uncontrolled and vary by up to 20% in relative humidity (RH) within days. The impact of humidity on the field detection was measured, yielding a coefficient of 0.06°/% RH for 1.3 GHz systems.

To actively compensate for this effect, a new drift calibration module was developed and installed in the accelerating RF station ACC23. The device constantly compares the facility RF reference to the measured signals for each single RF channel. Deviations are automatically detected and used to calibrate the field detection chain. Beam-based measurements were used to demonstrate the proper functionality of the drift calibration module, as shown in Fig. 2.

The figure shows the arrival time change as a function of an induced temperature jump. In the uncompensated case, the arrival time changes significantly and resumes its initial value once the temperature is set back. When repeating this measurement with active compensation, the arrival time remains constant. The long-term change in both signals is induced by other effects in the machine. Environmental changes of the humidity are compensated in the same way as temperature changes, but it is not feasible to deliberately induce such changes in a controlled way.

Improvement of system components

Beside long-term drift compensation, improvements were achieved in the field detection itself. A new digitiser board with very low noise performance was developed and installed. For comparison, the readouts of the old and new board are plotted in Fig. 3. Compared to the black curve (old), the red curve (new) does not show any spurious RF signals in the range of a few hundred kHz. Also clearly visible is the contribution of the fundamental 7π/9 mode, while a notch filter is applied to suppress the 8π/9 mode. In addition, the improvement enables a more accurate measurement of the electron beam loading effect, a more precise calibration of signals and finally a more effective suppression of potential field disturbances. In addition to the preprocessing digitiser module, the main controller card was also upgraded, allowing

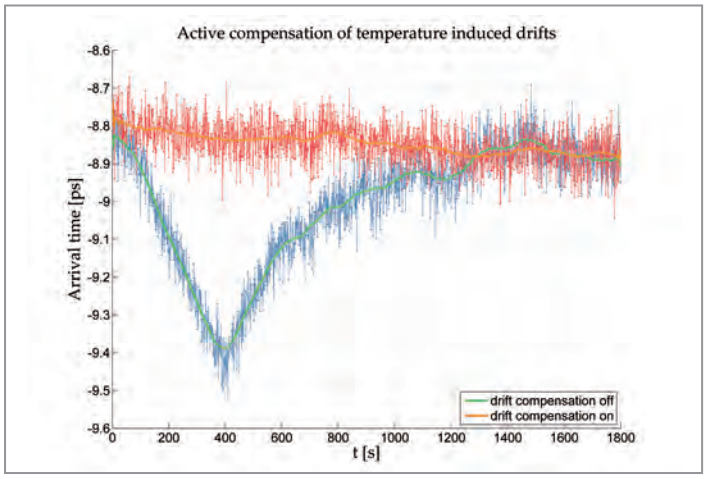

Figure 2

Measurement of the arrival time change as a function of an induced temperature jump in a compensated and uncompensated case. The temperature change is 2°C starting at $t = 0$ and set back at $t = 400$ s to its original set point.

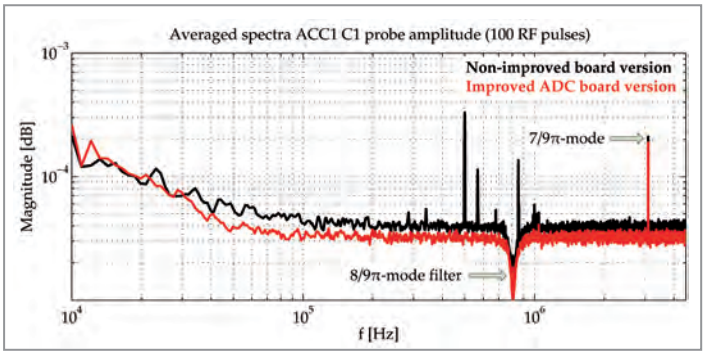

Figure 3

Comparison of a single cavity probe amplitude spectrum for the improved and initial version of the preprocessing analogue-to-digital converter (ADC) board. The spectrum for the improved version is nearly spur-free.

for high processing power, large data transfer and an increased number of I/Os. The new Kintex7 FPGA-based controller module provides for future upgrades of the feedback controller design.

Conclusion and future plans

After two years of successful operation of the MTCA.4 LLRF system at FLASH, the focus shifted to selective upgrades of specific components. The given field stability requirements of $dA/A < 0.01\%$ and $d\varphi < 0.01°$ were fulfilled and demonstrated by beam-based measurements. Since 2015, the normal-conducting RF gun has also been equipped and operated with the MTCA.4 LLRF system.

Beside software and automation upgrades, components have been installed to improve the long-term stability and reproducibility of the system. One of the upgrade goals is to unify the LLRF systems of FLASH and the European XFEL to reduce the maintenance time and development effort.

Contact: Christian Schmidt, christian.schmidt@desy.de

MTCA.4 laser pulse controller for FLASH.

Operating a multi-beamline FEL with multiple injector lasers

The FLASH facility at DESY is a multi-beamline free-electron laser (FEL) with a common superconducting linear accelerator driving two – and in the near future three – undulator beamlines. The electron bunches are produced in a normal-conducting radio frequency (RF) gun with a laser-driven photocathode. The use of superconducting technology allows FLASH to accelerate hundreds of electron bunches within one RF pulse, and the train of these bunches is separated by a fast kicker–septum system into the two undulator beamlines. To fulfil the parameter ranges of the user experiments, the tuning possibilities for both bunch trains have to be the same. To make this possible, two main and one optional third injector laser system are used, allowing the laser settings to be varied independently for both bunch trains. A laser controller, implemented using the MTCA.4 technology, has been newly developed to make the multi-user operation mode possible.

Overview and connected systems

Producing different bunch patterns for two, and in the near future three, undulator beamlines is a basic requirement for multi-user operation at FLASH. To fulfil the parameter ranges of the user experiments, the bunch patterns needed for the undulator beamlines are produced by various injector lasers. This allows FLASH to produce multiple subtrains of electron bunches within the RF pulse (also called macropulse), and each train can have different electron beam parameters (Fig. 1). At FLASH, the injector lasers are controlled by a laser pulse controller electronics based on the MTCA.4 technology, and all the controllers are linked to each other.

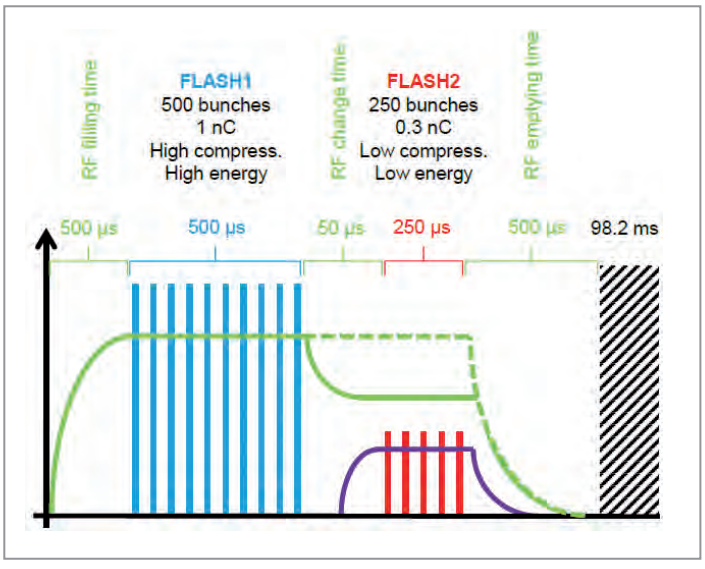

Figure 1

Example of bunch patterns for the two FLASH beamlines, FLASH1 and FLASH2, with different settings of the injector lasers. The blue train is produced by one laser and the red train by another. The purple curve represents the magnet pulse of the kicker that separates the two bunch trains. Courtesy: S. Ackermann

The multi-beamline operation places high demands not only on the laser system but also on the timing and machine protection systems. These systems are strongly linked to each other, and the interaction between them is a basic requirement for this operation mode.

The timing system delivers the information about the desired bunch pattern for each laser system to the pulse controller at a repetition rate of 10 Hz. It defines the time structure of each electron bunch within the RF pulse, the intended undulator beamline of the bunch (FLASH1, FLASH2 and later also FLASH3) and the injector laser responsible for the bunch (LASER1, 2 or 3). In addition, the timing system delivers trigger and clock signals to the laser controller.

The machine protection system (MPS) collects the alarm data of all subsystems in FLASH and limits the number of bunches per macropulse or blocks the beam when necessary. If a beamline alarm occurs, the MPS sends a limitation signal to the timing system, causing the bunch pattern of the next macropulse to be corrected. This mechanism is called slow protection. However, it might be necessary to stop the beam immediately within the macropulse. In this case, the MPS sends inhibit signals directly to the laser controller using the so-called fast alarm lanes. The fast protection is an important system to prevent the undulators or the beam pipe from damage, for example if beam losses occur within pulse trains. The response time of the fast protection is a few nanoseconds.

FLASH has two systems to measure beam losses: beam loss detectors (BLMs) located at suitable positions along the beamline and a system based on toroids (TPS) to measure bunch charge differences along the beamline within a particular section (one toroid at the beginning and another at the end of the beamline section). These sections are the accelerator up

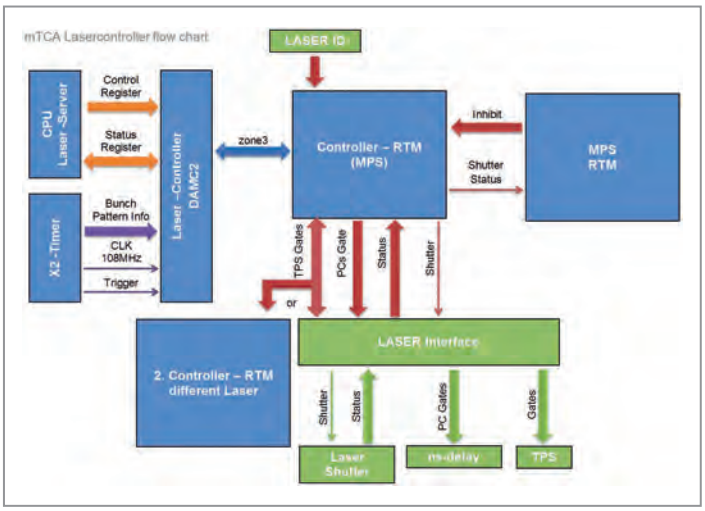

Figure 2

Overview of the communication paths between the laser controller and the connected systems. Blue: MTCA.4 AMCs and RTMs. Green: Laser hardware and interface including the dongle (LASER ID). Red: RS422 communication between MPS, laser and interface. Orange: PCIe bus (communication between CPU and FPGA). Purple: M-LVDS bus (communication between timer and laser FPGA)

to the bifurcation between the beamlines, the FLASH1 beamline and the FLASH2 beamline. A TPS module controlling a given section receives a trigger signal from the laser controller if the connected laser is producing bunches for that beamline section. The TPS thus verifies the validation of beam for the particular section. The laser controller sends this beamline trigger to the TPS based on the incoming bunch pattern information of the timing system.

Hard- and software of the laser controller

The laser pulse controller is responsible for controlling the pulse structure of the injector laser according to the desired bunch pattern and the fast alarm signals. The laser controller selects the desired sequence of laser pulses out of the existing laser burst by gating a fast Pockels cell in the laser beam path. Furthermore, a laser shutter can be controlled that allows for blocking the laser beam completely. In addition, the controller creates triggers for the different TPS modules if a beam is produced for the particular beamline. Figure 2 provides an overview of the communication paths between the controller and the connected systems.

The controller was developed using the DAMC2 advanced mezzanine card (AMC). This board is based on the MTCA.4 standard and provides a field programmable gate array (FPGA) into which the controller logic is implemented. All lasers have an MTCA.4 system available (including a chassis, management controller, CPU AMC, X2-timer AMC, analogue-to-digital converter (ADC) AMC and the DAMC2 controller board). The FPGA gets the bunch pattern information and a timing-synchronised clock from the timing module via the crate M-LVDS backplane bus. A DOOCS server is running on the CPU AMC to display the FPGA status and set the shutter control register. The communication between CPU and FPGA is based on the PCIe bus on the crate backplane. An MPS rear transition module (RTM) is used for the communication with the specific laser hardware and the MPS. The RTM has seven output channels and 45 input channels (galvanically isolated RS422 I/Os). Four inputs are used for the MPS fast alarm lanes.

If the FPGA detects an alarm at the RTM input, it compares the beamline inhibit with the beamline destination of the bunch pattern. If an alarm is set for the respective laser, the controller blocks the output signals (Pockels cell gate and/or shutter signal). The laser controller ensures that an alarm for the FLASH1 laser does not affect the beam of the FLASH2 laser and vice versa.

Since the MPS-RTM only supports the RS422 signal standard, an additional printed circuit board – the laser interface – was developed to convert the RS422 signals into different signal standards needed for the laser hardware. The laser shutter, ns-delay (trigger for the Pockels cell driver) and the TPS are connected to this device. Several outputs were doubled to generate monitoring signals. The interconnection of the complete system is shown in Fig. 3.

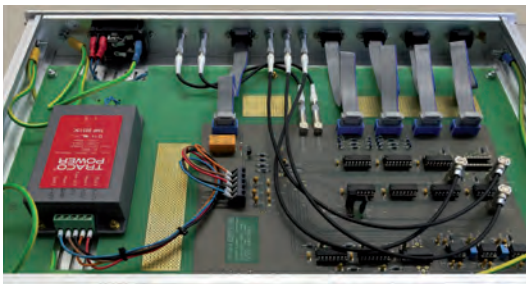

Figure 3

Laser interface converting the RS422 signals of the MPS-RTM board into the laser interface signal standards

All the injector lasers run with identical hardware and software to keep maintenance as simple as possible, but all of them have different requirements to ensure safe operation. To fulfil these safety requirements, an ID dongle has been established. The dongle is connected to the laser controller RTM, and the FPGA reads the ID number and sets the internal safety control registers to the particular value depending on the ID on the input channel. The maximum pulse repetition rate and the maximum number of pulses per macropulse are limited by the FPGA logic, and these limits depend on the laser and the accelerator operation mode. In 2015, the injector laser of the European XFEL X-ray laser was set up with an identical system except for the ID dongle, which configures the laser controller for European XFEL or FLASH machine operation mode.

Another main feature of the controller is the generation of TPS triggers depending on the destination beamline information of the bunch pattern. It is possible to change the laser-to-beamline assignment without changing any configuration of the laser or TPS system. The timing of the trigger signals can be adjusted remotely.

Contact: Christian Grün, christian.gruen@desy.de
Torsten Schulz, torsten.schulz@desy.de

RF gun stabilisation.

Cascaded control scheme for best performance

Controlling the radio frequency (RF) gun at DESY's FLASH free-electron laser facility to optimum performance requires sophisticated controller design, advanced disturbance rejection and comprehensive exception handling. The normal-conducting standing-wave RF gun is operated in a pulsed mode with a repetition rate of 10 Hz. The system identification, which is essential to achieve high-performance control, is based on a grey-box model, with *a priori* knowledge about the physical behaviour. The feedback regulation concept is separated into two basic controller parts. An RF controller design, based on the identified RF model, is followed by system identification and regulation of the RF pulse length to overcome the limitation of the underlying temperature regulation. The combination of both into a cascaded control scheme finally leads to the desired RF field performance.

Introduction

The key element of the FLASH electron source is a normal-conducting RF gun operated with an RF frequency of 1.3 GHz. It is a 1.5-cell water-cooled copper cavity with a longitudinal coaxial high-power RF coupler (Fig. 1). The RF gun is operated with RF pulses with a length of currently 550 µs at a repetition rate of 10 Hz and a peak power of 5 MW. The electron bunches are generated at a photocathode at the backplane by impinging laser pulses. The maximum field at the cathode is 54 MV/m. The electrons leave the RF gun with a momentum of 5.7 MeV/c.

For proper and stable operation of the accelerator, the RF field in the gun needs to be controlled in amplitude and phase with a high precision. The electrons are produced in bunches of a few ps duration and with a charge of up to 1 nC. During one RF pulse, several hundred bunches can be accelerated. The bunch distance is usually 1 µs; other bunch distances are possible as well. The specification for amplitude and phase stability is based on the requirements of the superconducting accelerator following the gun.

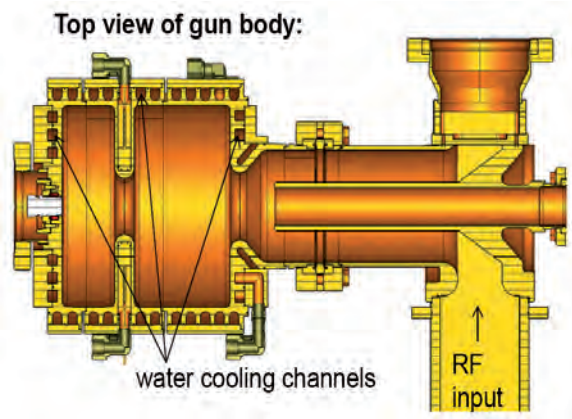

Figure 1

Sketch of the 1.5-cell RF gun with coaxial RF input coupler and water cooling channels

The goal is to achieve an amplitude stability of better than $dA/A < 0.01\%$ and a phase stability approaching $d\varphi < 10$ mdeg. FLASH is a free-electron laser operating in the self-amplified spontaneous emission (SASE) regime to produce high-brilliance XUV and soft X-ray pulses. The stability in energy, wavelength, pulse duration and arrival time of the radiation pulses strongly depend on the stability of the electron source. For example, an RF phase deviation of only 80 mdeg already results in an arrival time deviation of 70 fs at the first acceleration module, leading to a deviation in pulse compression.

The average RF power in the gun is more than 25 kW, of which a large amount is dissipated in the copper walls. A water cooling system (Fig. 2) removes this heat and stabilises the gun body temperature to better than 0.02 K rms.

Water and RF regulation

The temperature of the incoming water T_{in} is controlled to keep the iris temperature T_{iris} close to its set point. A pump with control signal α_p regulates the water flow in the circuit. The water leaves the RF gun with temperature T_{out}. A heater with control signal α_h keeps the water temperature constant. A water tank is installed between the heater and mixing valves damping possible water temperature oscillations. The tank acts as a low-pass filter from a control perspective. To compensate the RF load, the heated water is mixed with cold water of temperature T_{cw} using the control signal α_{cw}, while α_{out} keeps the amount of water within the circuit constant. Currently, the water regulation system is controlled to ±1 bit error, corresponding to 0.02 K, limited by the analogue-to-digital converter (ADC) used by the proportional–integral (PI) controller implemented in a programmable logic controller (PLC).

Since January 2015, the gun low-level RF (LLRF) system and signal detection have been adapted to the MTCA.4 standard.

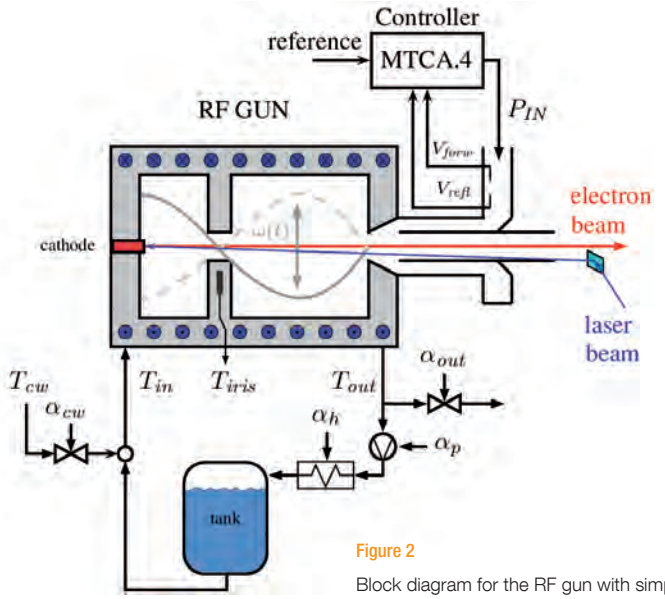

Figure 2

Block diagram for the RF gun with simplified subsystems. Lower part: water regulation concept. Upper part: LLRF controller.

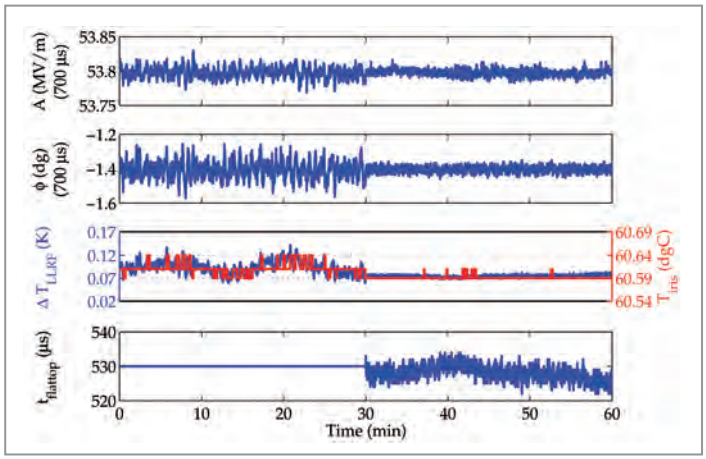

Figure 3

From top to bottom: RF amplitude and phase (down-sampled 100 kHz signal) at the first bunch position (700 µs), computed temperature based on LLRF signals together with T_{iris} readout and flat-top length. The first 30 min show the achieved performance with activated RF field feedback, while the last 30 min demonstrate the improvement achieved by additionally applying the newly developed pulse width modulation feedback (PWMFB).

The new system opens up new possibilities, such as a higher detection precision of the RF field and a low-latency feedback loop compared to the previous VME-based system. From the measurement of the forward and reflected RF signals (see Fig. 2), the vector sum is built in order to determine the amplitude and phase of the field in the cavity, the so-called virtual probe.

Thorough understanding of system behaviour is essential to develop tools for reliable system operation. System behaviour can be divided into two parts: basic functionality determined by observation and using mathematical models. The latter can be based on one or more physical equations describing the entire system behaviour. Another way is an identification procedure approximating the system behaviour. Such a system identification can be based on physical equations to cope with subsystem imperfections. In the case of the RF gun, parameter modelling is needed for precise regulation. By doing so, the RF field controller and additional functionalities such as learning feed-forward can be optimised based on this model.

The basic temperature of the RF gun is controlled by the water regulation system described above, which intrinsically has a large latency. To improve the stability, a much faster scheme is required. A newly developed feedback scheme – the pulse width modulation feedback (PWMFB) – is based on modulating the RF pulse width and thus the power dissipated in the gun body. The induced temperature change is approximately 50 times faster than what the water regulation system can achieve.

Using the difference between the phases of the virtual probe and the forward wave, the detuning angle and resonance frequency of the RF gun are computed. Precise temperature information of the gun body is computed using the linear relation of -21 kHz/K between detuning frequency and temperature mismatch.

Summary and future plans

The transition to the MTCA.4-based LLRF control system greatly increases the performance of the RF field regulation, by a factor of 7 in amplitude and a factor of 2.5 in phase. The evaluated performance is summarised in Table 1, for deactivated and activated PWMFB. The data were taken at a signal sampling rate of 9 MHz and down-sampled to 100 kHz. The down-sampling is compatible with twice the RF gun open-loop bandwidth and reduces additional effects such as distortions caused by sensor noise, which should theoretically not be present in the RF field as this is above half the cavity bandwidth. The listed values display the standard deviation (rms) within a time frame of 30 min for deactivated and activated PWMFB (Fig. 3). The LLRF-based temperature computation shows an RF gun temperature improvement from 14 mK to 2.5 mK (rms).

ADC frequency	PWMFB	$\sigma(A)$ [%]	$\sigma(\varphi)$ [mdeg]
100 kHz	Off	0.0069 (0.015)	25.5 (50.0)
	On	0.0052 (0.008)	9.0 (16.1)

Table 1: Measured performance of the LLRF feedback system, without and with pulse width modulation feedback (PWMFB) in terms of standard deviations (rms) of the RF amplitude A and phase φ. Given is the mean rms value during the flat top; the number in brackets refers to the corresponding first bunch position (700 µs).

With 0.0052% and 9 mdeg, the amplitude stability and the phase stability meet the performance goal of $dA/A < 0.01\%$ and $d\varphi < 10$ mdeg, respectively. It is planned to extend the RF field feedback loop with a Smith predictor to overcome the latency that limits the current maximum feedback gain. Increasing the RF field feedback gain will further improve the amplitude and phase stability at the beginning of the flat top.

Contact: Sven Pfeiffer, sven.pfeiffer@desy.de

High-gain harmonic generation.

Seeding at FLASH

The temporal and spectral properties of highly intense radiation pulses of free-electron lasers (FELs) such as FLASH at DESY can be improved by giving the electron beam a defined density modulation prior to the FEL radiator. To generate this defined density modulation, the electron beam is manipulated with external laser fields. This process, called seeding, enables the generation of fully coherent FEL radiation pulses. The experimental seeding setup at FLASH allows for studying different seeding techniques and offers the unique opportunity of being operated simultaneously with the two unseeded FEL beamlines FLASH1 and FLASH2.

Seeding of FELs

High spectral brightness in combination with a high degree of coherence as provided by FELs is one of the key features that scientists at such radiation sources are interested in. These properties are achieved by properly initiating the FEL amplification process. To do so, a periodic microstructure is created in the electron bunch (so-called microbunches) by manipulating the ultra-relativistic electron beam with external laser fields in combination with special magnet arrangements.

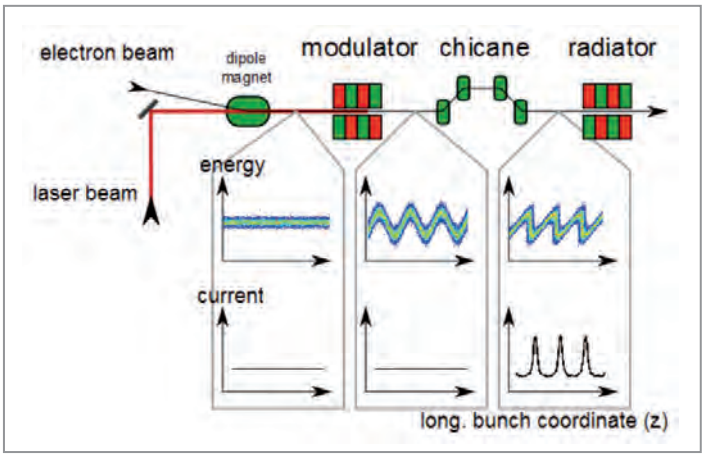

Figure 1

Schematic of the HGHG seeding principle. Starting with a flat energy distribution along the electron bunch, the interaction of the electrons with the laser inside the modulator leads to a sinusoidal energy modulation. At the exit of the magnetic chicane, the electrons are longitudinally redistributed, resulting in a modulated current profile. These electron bunches then pass the second undulator (radiator) where the FEL process takes place.

Figure 1 shows the high-gain harmonic generation (HGHG) operation mode, which has proven to reliably generate fully coherent FEL pulses in the soft X-ray wavelength range. At the FLASH1 beamline, an experimental setup dedicated to seeding development was installed in 2010 and used for feasibility studies of seeding with short-wavelength laser radiation. Since 2014, the installations have been serving as an R&D platform for seeding techniques such as HGHG and other more advanced schemes that will pave the way to fully coherent FEL radiation at even shorter wavelengths. The research team, made up of members of DESY's Accelerator Research and Development (ARD) programme, the University of Hamburg and TU Dortmund University in Germany, recently demonstrated the operation of HGHG at FLASH down to 38 nm.

HGHG seeding at 38 nm

After the commissioning of the new seed laser injection beamline in 2014 and the successful manipulation of the electron beam microstructure, the FLASH1 seeding setup was used to generate intense seeded FEL radiation at 38 nm, the seventh harmonic of the 267 nm seed laser wavelength (Fig. 2).

A maximum pulse energy of 75 µJ was observed, while the average pulse energy was 12.5 µJ. For unseeded pulses, the energy dropped to 2.6 nJ. With a relatively low electron beam peak current of 0.6 kA, the resulting FEL gain length was determined to be 0.9 m. The relative spectral width of the seeded FEL pulses was measured to be 0.5% on average.

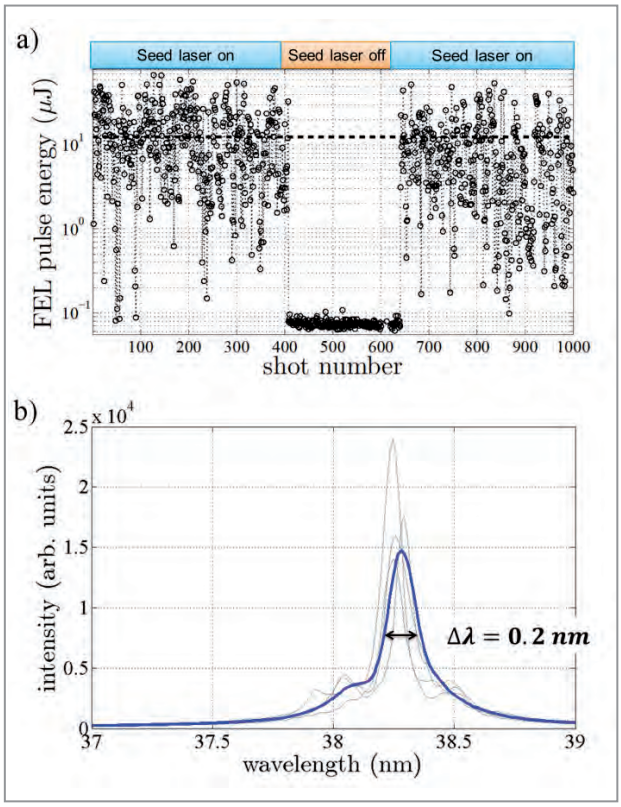

Figure 2

a) FEL pulse energy for 1000 consecutive shots. At shot number 400, the seed laser beam was blocked for 250 shots. Consequently, no HGHG amplification took place.
b) Example of seeded spectra for HGHG operation. The blue curve shows an average over 1000 shots. The grey lines are single-shot spectra around the mean pulse energy.

This experimental result is an important milestone for the R&D programme on seeding at FLASH. The next step, namely the temporal characterisation of the seeded FEL pulses, will reveal the coherence properties, opening up a new class of experiments for the scientific community.

The operational experience gained with the experimental seeding setup provides important information for the design of a seeding upgrade of the FLASH user facility.

Simultaneous operation of three FELs

The setup of the FEL seeding experiment sFLASH is installed upstream of the FLASH1 undulator beamline. Consequently, the electron bunches used to generate FEL radiation in the seeding undulator also travel through the 30-m-long FLASH1 main undulator, where they can generate highly intense FEL radiation again. On top of that, the FEL of the FLASH2 beamline has been operated in parallel thanks to the multibunch pattern of the accelerator.

Because the radiation from each FEL (sFLASH, FLASH1 and FLASH2) can be extracted in separate photon beamlines, this mode of operation allows in principle for serving three experimental stations simultaneously. In addition, the wavelengths of the three FELs can be tuned independently within the wavelength range of the variable-gap undulators at sFLASH and FLASH2. This result demonstrates the FEL multiplexing capabilities from a single accelerator as foreseen for the European XFEL project.

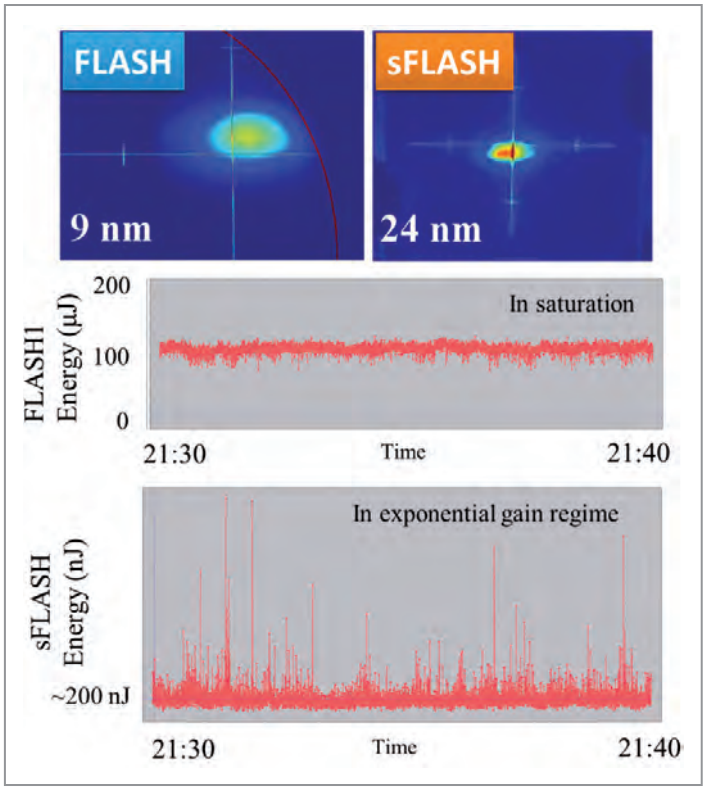

Figure 3

Result of the simultaneous operation of the seeding undulator sFLASH tuned at 24 nm wavelength and the FLASH1 main undulator operated at 9 nm wavelength. The upper panels show the FEL beam profiles. The lower plots show the pulse energies for both FELs in the same time interval.

Contact: Jörn Bödewadt, joern.boedewadt@desy.de

Compensation of steerer crosstalk between FLASH1 and FLASH2.

Decoupling the extraction area with orbit three-bump scheme

FLASH2, the new beamline at DESY's FLASH free-electron laser facility, branches off the FLASH1 beamline after the last accelerator module. In the region where the FLASH2 beam is extracted from the FLASH1 beamline, both beamlines are close to each other; the angle between them is only 6.5°. It has been observed that the steering dipoles in the extraction area have an influence on both beamlines. Thus, steering the orbit in one beamline perturbs the orbit in the other beamline. This perturbation can significantly degrade the self-amplified spontaneous emission (SASE) energy in the other beamline.
We solved this problem using a combination of local orbit bumps, whereby the crosstalk from one steerer is corrected using additional steerers in the other beamline. This concept was successfully tested at FLASH.

Crosstalk between FLASH1 and FLASH2

The new FLASH2 beamline was commissioned in 2014. During the commissioning, it was discovered that the steering dipoles (steerers) in FLASH2 influence the beam in FLASH1 and vice versa. This effect is caused by the transverse stray field of the steerers. Since they are mounted close to the other beamline (Fig. 1), a significant part of the stray field extends to this other beamline, deflecting the electron beam in an unwanted manner. Additionally, since the stray field outside of the steerer gap is not purely horizontal or vertical, the beam is deflected horizontally and vertically at the same time. This leads to a distorted orbit after the extraction area.

The orbit distortion causes a significant decrease of the SASE energy in the other beamline, because the overlap between the light wave and the electron bunch is not maintained. In the worst case, the orbit offset becomes large enough for part of the beam to be lost in collimators or at the vacuum beampipe walls. Since the steerers in the extraction area are needed to control the beam, not using them is not a choice. Therefore, other solutions had to be found.

Implementing a shielding using μ-metal, which is a common practice to ameliorate the effect of stray fields, is not feasible in the current design. The first steerer does not leave enough

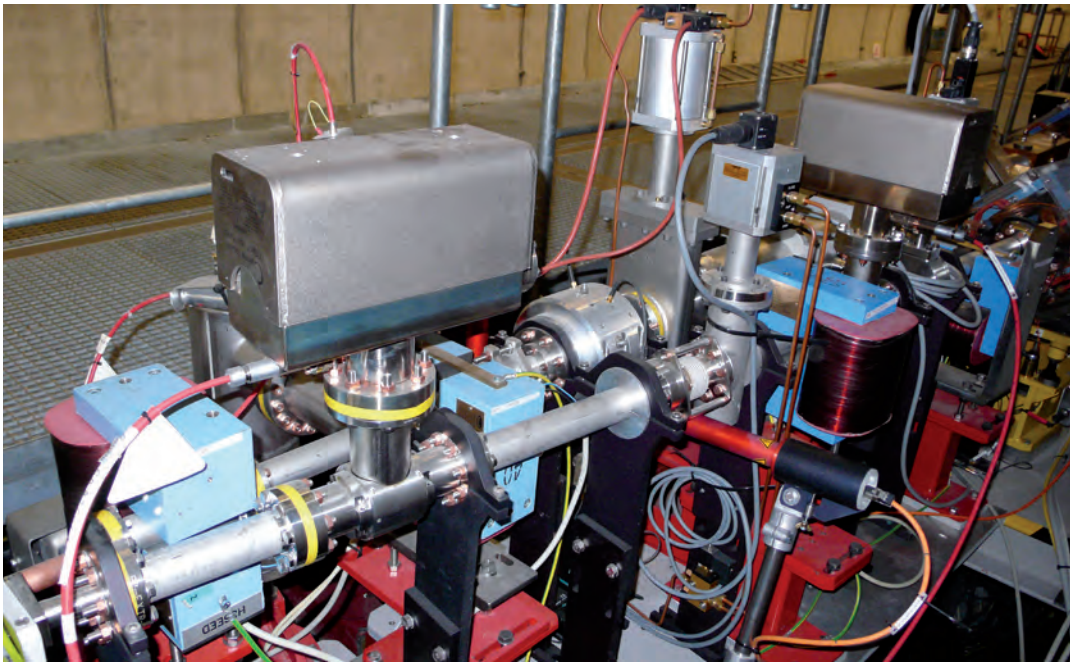

Figure 1
FLASH extraction area. The FLASH1 beamline is to the left of the FLASH2 beamline. The light-blue magnets are the steerers.

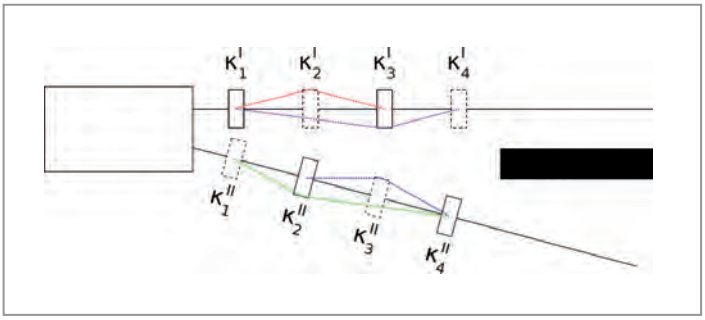

Figure 2

Visualisation of the recursively coupled short three-bump scheme (in one plane). The solid lines represent real steerers, the dashed lines are the stray fields of the crosstalking steerers.

space to fit anything between the beamline and the steerer, and there are several other magnets and components that prevent easy installation of a shielding.

Reducing the magnetic field inside the return yoke of the steerers could also be achieved by redesigning the magnets; however, this would require a completely new layout and new magnets. Therefore, we came up with another solution, which uses only the hardware currently installed in the FLASH tunnel.

The local orbit three-bump concept is generally used to create a local orbit offset in an accelerator, which should not influence the behaviour of the rest of the machine. A kick produced at a first steering coil is corrected using two additional steerers downstream or also upstream. A kick of α is created at the first steering coil, which is bent back by -2α at the second one. At the third steering coil, the orbit is straightened by introducing another kick of α on the beam. After this three-bump combination, the orbit thus returns to the design orbit. In this way, we created a closed bump with a local orbit offset, which is not affecting the orbit in the rest of the machine.

At FLASH, we chose to confine the kicks due to crosstalk from the steerers of the other (perturbing) beamline to local bumps with the steerers installed in the perturbed beamline. The kick from the “virtual” steerer is corrected using additional “real” steerers in both planes to compensate the orbit offset locally.

There are different types of three-bump schemes suitable for FLASH, for example the long three-bump scheme, where the orbit is corrected using non-crosstalking steerers downstream of the extraction area, or the interleaved short three-bump scheme, where the orbit is corrected using the next two, possibly crosstalking, steerers downstream.

Compensation of steerer crosstalk using orbit three-bump combination

The most elegant solution is the so-called recursively coupled short three-bump scheme, which is shown in Fig. 2. Only three additional steerers are used to correct the crosstalk, and the correction takes place as locally as possible.

The perturbation from the first steerer – located in beamline one – is corrected using two steerers in beamline two, which can be either downstream or upstream. Since these two steerers can have an influence on beamline one as well, their crosstalk is corrected again in beamline one, using the first steerer and a second one also possibly influencing beamline two. This crosstalk is then corrected again using the two steerers in beamline two and so on. In other words: every perturbation in each beamline is corrected using the same two steerers, which react back on the other beamline.

This recursion can be solved analytically by rewriting it in terms of a power series for matrices, which turns out to be the well-known geometric series. Therefore, the kick strengths of the correcting steerers can be determined analytically, and this elegant method to compensate the crosstalk can be applied at FLASH.

Test versions of these crosstalk compensation schemes have been successfully tested at FLASH. A more robust server solution will be developed in the near future.

Contact: Mathias Vogt, mathias.vogt@desy.de,
Florian Müller, florian.mueller@desy.de

RF gun window.

Simulation, measurements and results

In the last years, the radio frequency (RF) power applied to the RF gun for DESY's FLASH free-electron laser, the European XFEL X-ray laser and at DESY's PITZ photoinjector test facility was increased in order to achieve the European XFEL specifications of 6.5 MW pulse power, 650 µs pulse length and 10 Hz repetition rate. However, this operation mode causes stress to the gun cavity, the gun coupler and the RF window, which transmits the power. Vacuum leaks and breakdowns occurred in some windows. For a better understanding, we investigated the electrical fields in the window and in the gun. One result is that the field distribution depends on both the reflection behaviour of the gun and the window position relative to the gun cavity. Based on this result, a new position of the RF window relative to the RF gun was proposed in order to lower the stress on the window.

Introduction

The RF power is supplied by a klystron and transmitted by a waveguide distribution to the window and by the gun coupler to the gun cavity where the electrons are accelerated. The window separates the air-filled part (waveguide distribution) from the vacuum part (gun coupler and cavity) of this high-power system (Fig. 1, top).

Simulation

At the beginning of the pulse, the complete input power is reflected by the gun cavity and a standing wave builds up, which can be simulated in the time domain using CST Microwave Studio (Fig. 1, top graph). Within several microseconds, the peak values of the electrical field strength decrease, because the gun cavity takes most of the power and less power is reflected. During the flat top of the RF pulse, the reflection factor does not approach zero and a standing wave remains. In this steady state, the reflection factor and phase depend on the tuning of the gun cavity. The reflection behaviour in the steady state is simulated in the frequency domain, and the scattering parameters (S-parameters) are obtained.

Measurements

To verify the simulation results, we first measured the S-parameters of the FLASH gun. The measurement confirms the simulation results, but the reflection in resonance is 1.6%, which is 10 times higher than simulated. It is most likely that the matching of the quality (Q) factors between gun cavity and coupler in the simulation model is better than in reality.

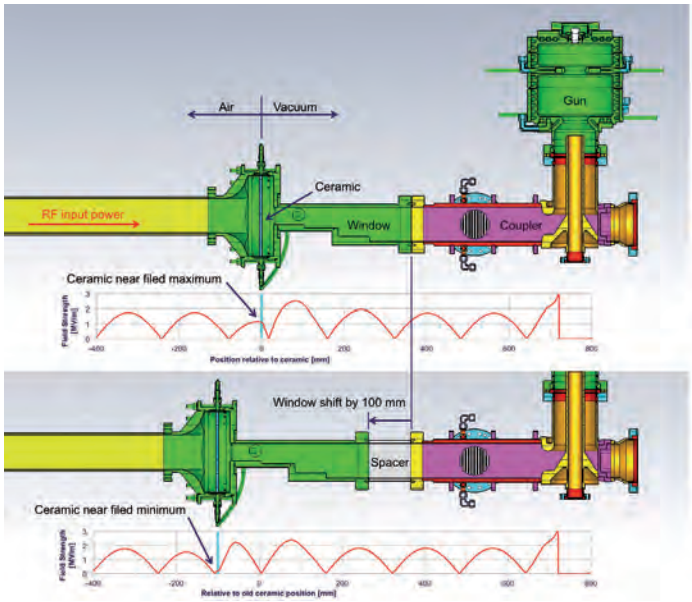

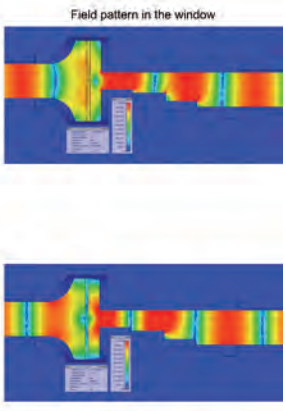

Figure 1

Change of window position at the European XFEL gun. Field strength monitored at the centre of the waveguides. Situation at the beginning of the pulse. Top: Old window position → field strength of the standing wave close to its maximum. Bottom: New window position → field strength close to its minimum.

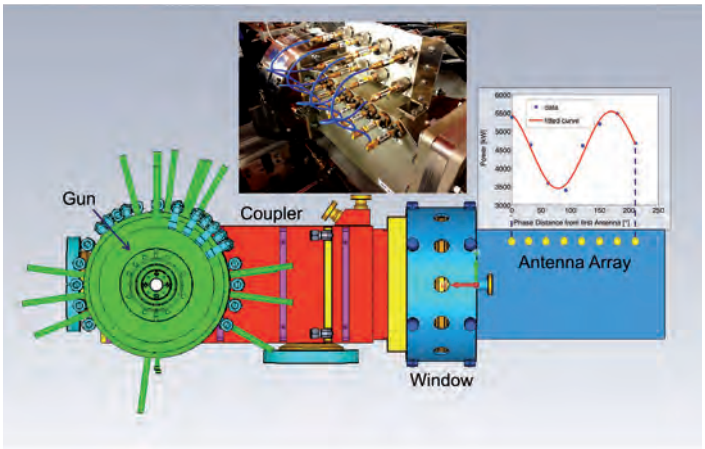

Figure 2

Measurement of the standing wave at FLASH using a different window type. Picture: Model and measurement principle. Photo: Real window and antenna array at FLASH.

Because the S-parameter measurement provides information only about the steady state, an additional standing-wave measurement was done to observe the change in reflection factor and phase during the RF pulse.

The measurement setup is shown in Fig. 2. By means of an antenna array in a waveguide located right before the window, the electrical field was measured at eight points every 111 ns. The measurement values were squared and a sine wave was fitted to this result. From the gained sine wave, the standing-wave ratio and hence reflection factor were derived. Furthermore, the position of the standing wave and thus the reflection factor were calculated. Measurements were done in normal operation mode at FLASH (4.5 MW / 500 µs / 10 Hz).

The results show that the reflection factor is close to 100% at the beginning of the pulse, then decreases within 20 µs to 1.1% and rises again within 500 µs to 2%. The variation of the reflection factor from 1.1% to 2% is caused by heating of the gun cavity induced by the RF power during the pulse, which slightly detunes the resonance of the gun cavity. This effect is reinforced when more pulse power and longer pulses are applied to the gun. At PITZ, an increase of the reflection factor up to 10% was observed.

But not only the reflection factor changes, so does the reflection phase. Observations at the FLASH gun show that the reflection phase at the beginning of the pulse is equal to the reflection phase in perfect resonance. After several microseconds, the reflection phase decreases by ~10°, returns to the starting value and then increases further by ~30°. For the standing wave in Fig. 1 (top), this means that the standing wave appears at the beginning of the pulse, then moves 5 mm towards the gun and later 20 mm in the opposite direction. During this movement, the amplitude of the standing wave decreases significantly at first and then increases again. During European XFEL operation with a pulse power of 6.5 MW and a pulse length of 650 µs, the gun cavity will be heated more and thus the standing-wave shift will be bigger.

Impact on the window

From the simulation and measurement results, information on the field distribution in the RF window was gained. The field pattern in the window is shown in Fig. 1 (top right; red: high fields; green: low fields). It can be seen that the ceramic of the window is exposed to particularly high field strengths of the standing wave (Fig. 1, top graph). This causes two problems: Breakdowns can build up along the ceramic surface; and the electrical fields heat up the ceramic, which stresses the brazed joint between the ceramic and the surrounding metal. This might cause vacuum leaks in the long term. A better position for the RF window should be one where the window ceramic is exposed to lower electrical field strengths.

New window position

Simulations show that the field strength can be lowered significantly in the ceramic if the window is shifted by 100 mm (Fig. 1, bottom). While in the original setup the ceramic is close to the field strength maximum (Fig. 1, top), it is now located close to the minimum. On average, it can be assumed that only 5% of the input power is reflected by the gun, but nonetheless this means a reduction of the field strength in the ceramic by roughly 30% overall.

Based on this result, the decision was taken to shift the window at the European XFEL gun into this position by means of a 100-mm-long vacuum waveguide (spacer) (Fig. 3). The conditioning of this setup was unproblematic, but experience from normal operation is still limited as there were only some weeks of operation time in 2015. The evaluation of the long-term performance will therefore continue in 2016.

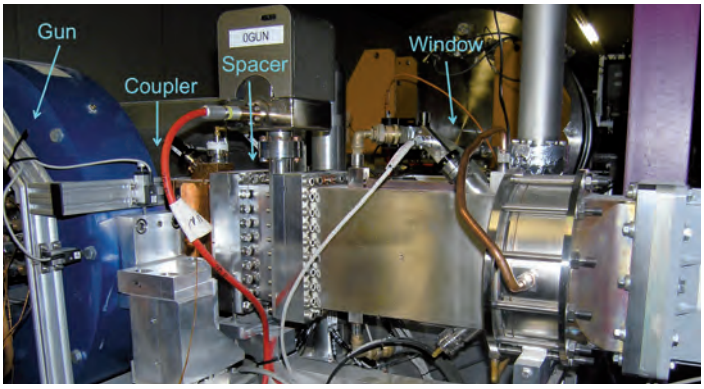

Figure 3

Realisation of the new window position at the European XFEL gun

Contact: Michael Bousonville, michael.bousonville@desy.de, Stefan Choroba, stefan.choroba@desy.de

Plasma glow.

Spectroscopic measurement of plasma accelerator targets

In plasma wakefield acceleration, a key to more stable beams is the increased control and exact knowledge of the plasma parameters. Control of the longitudinal plasma density profile is achieved through advanced target design and sophisticated gas control systems. Measuring the plasma density may be challenging, however, in particular at the low densities of 10^{17} cm^{-3} or less required for upcoming facilities such as FLASHForward at DESY's FLASH free-electron laser facility.
To solve these issues, we have investigated a method for measuring electron densities that is new in its application to plasma accelerator target characterisation. In this technique, the light emitted by a capillary discharge waveguide is used to determine the longitudinal electron density profile inside the plasma by analysing the line width and central wavelength of the emitted spectral lines. This is possible with a spatial resolution down to a few micrometres and a temporal resolution of a few nanoseconds for electron densities down to 10^{16} cm^{-3}, thereby overcoming limitations of state-of-the-art detection techniques such as laser interferometry and Raman scattering.

Relativistic particle acceleration in plasmas

Acceleration of charged particles based on charge separation induced in plasmas has gained a lot of attention over the past decade and made remarkable progress in the past few years. Plasma accelerators use high-intensity laser pulses or high-current-density particle beams to ionise a gaseous target material and locally push the freed plasma electrons outward while the ions remain confined due to inertia. The induced charge separation, which propagates with the generating beam, can give rise to field gradients above 10 GV/m, allowing the acceleration of electrons to GeV energies on a centimetre scale – that is, on distances some two to three orders of magnitude shorter than is possible with radio frequency accelerators. In the future, plasma wakefield acceleration will be explored at DESY at the FLASHForward beamline at FLASH (beam-driven acceleration) and within LUX – a Laser Plasma Driven Light Source (laser-driven acceleration), a collaboration between DESY and the University of Hamburg at the Center for Free-Electron Laser Science (CFEL).

Know your plasma

The exact density distribution of the plasma inside the target has a direct influence on multiple features of the acceleration process and must be known in order to produce and control high-quality beams. While the shape of the transverse density profile is important for guiding a drive-laser pulse, the longitudinal density profile influences the beam capturing, the electron injection, the propagation of the electrons inside the target and the release of the electrons into the vacuum.

Established techniques to determine the longitudinal density profile are vibrational and rotational Raman spectroscopy, which yield the gas density, and plasma interferometry. Unfortunately, no experiment so far has shown applicability of these methods to wakefield accelerator targets below a density of 10^{17} cm^{-3}. However, with multi-petawatt lasers and next-generation beam-driven plasma accelerators just around the corner, the characterisation of these low electron densities becomes crucial as they constitute more

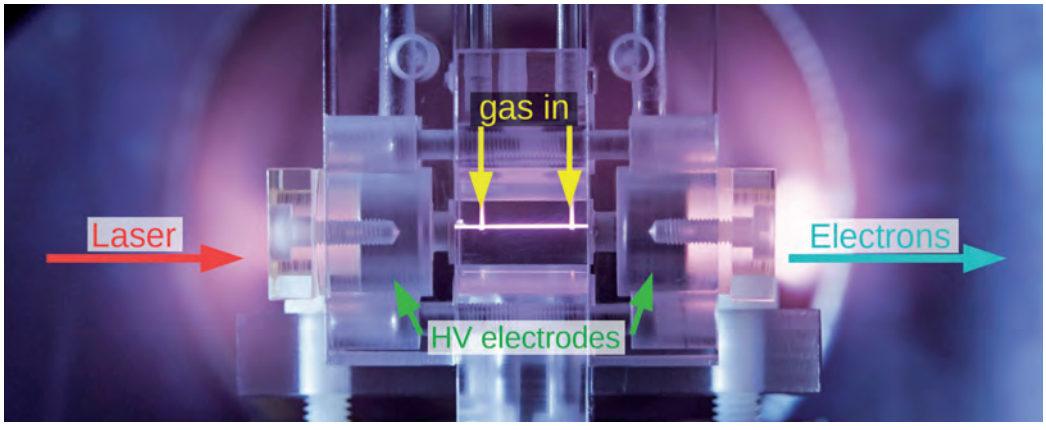

Figure 1

Picture of the plasma target. The capillary is filled with gas through the two inlets on top, and the plasma is ignited by a high-voltage (HV) discharge. For acceleration, a laser is coupled in from the left. The accelerated plasma electrons exit on the right.

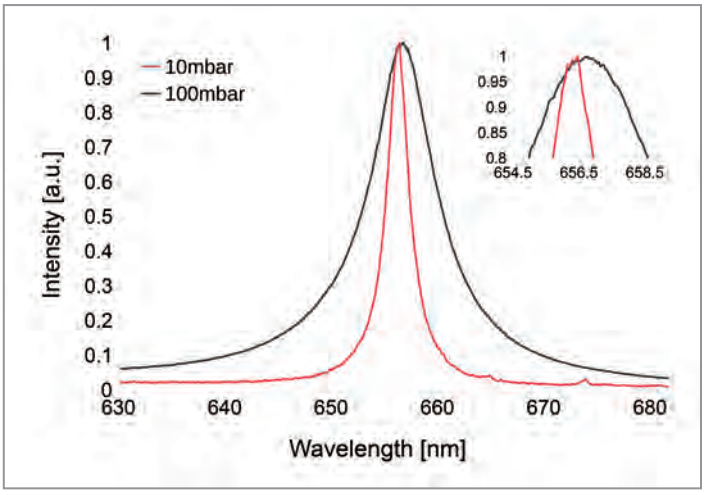

Figure 2

Normalised line profile of the Hα line for gas pressures of 10 mbar and 100 mbar applied to the capillary. The increase in line width and the shift of the central wavelength are clearly visible.

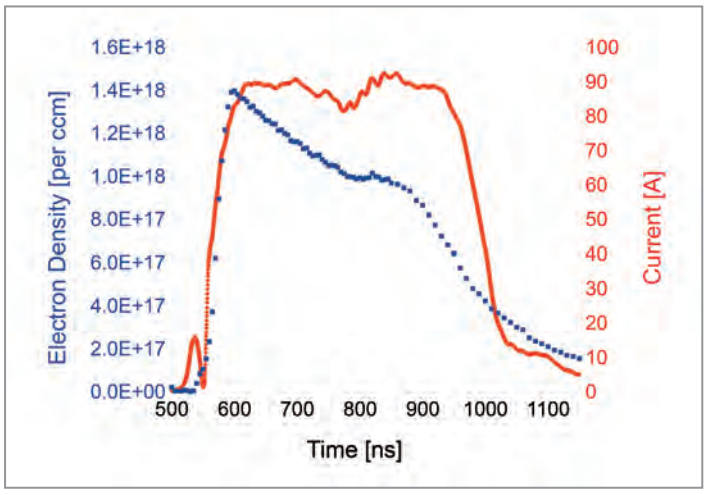

Figure 3

Temporal evolution of the electron density (blue) with the discharge current (red) in a capillary of 200 µm diameter and 15 mm length with 75 mbar of H_2 applied. Over the 400 ns of the discharge, the electron density quickly rises to a maximum and then slowly decreases over time.

favourable operation conditions. Thus, alternative methods are required.

We have investigated a non-intrusive approach in which the light emitted by the plasma is observed and spectrally analysed. The obtained spectra show distinct lines, which are a fingerprint of the gas species forming the plasma, over a continuous background, which is produced by the recombination of electrons with ions. The width and central wavelength position of these spectral lines is affected by the local plasma distribution.

This effect, called Stark broadening and shift, is of particular interest as it is directly linked to the microfields within the plasma and hence to the local electron density. In our setup, the plasma is formed by a high-voltage discharge applied with two electrodes at the entrance and exit of a capillary (Fig. 1). The light emitted by the plasma is then imaged onto the entrance slit of an imaging spectrometer such that the spectrum can be captured by an intensified CCD camera, allowing for temporal resolution on the nanosecond level. The emission feature resulting from the hydrogen Balmer-α transition yields a spectral contribution at 656 nm (Hα line), which is particularly interesting here since it is of sufficient intensity to be detectable with high signal-to-noise ratio, clearly separated from other lines and theoretically well understood.

The intensity-normalised line profiles in Fig. 2 for pressures of 10 mbar and 100 mbar applied to the target illustrate the influence of the electron density on the spectral line width and central wavelength of the Hα line. At low pressures, the full width at half maximum (FWHM) is considerably smaller than at higher pressures, in this case ~2.5 nm at 10 mbar compared to ~7.8 nm at 100 mbar. The shift in central wavelength is on the sub-nm level and hence less obvious than the broadening but well detectable. It offers the possibility for cross-calibration of the electron density obtained via line broadening.

This technique was used to measure the temporal evolution of the electron density during a 400 ns discharge at 20 kV with 75 mbar of pressure applied to a target capillary of 200 µm diameter and 15 mm length, as shown in Fig. 3. The temporal resolution achieved here is 5 ns. At the beginning of the discharge, the electron density quickly rises to its maximum and then slowly decreases until the end of the discharge. This is most likely due to the plasma being blown out of the capillary by the discharge. This measurement clearly shows that, in order to make use of a specific electron density, the acceleration process has to be timed accurately with respect to the discharge ignition.

Controlling the plasma parameters in such a way that stable electron beams are produced is a major activity in the quest to make plasma wakefields a key component of particle accelerators. This spectroscopy technique promises to enable the characterisation of advanced plasma target designs with high sensitivity.

Contact: Lars Goldberg, lars.goldberg@desy.de,
Lucas Schaper, lucas.schaper@desy.de

Assembly of the European XFEL main linear accelerator.

Planning and controlling the installation process

The installation of the main linear accelerator of the European XFEL X-ray free-electron laser involves a total of 14 work packages. Defining a proper sequence of installation steps and translating this sequence into action in the tunnel is not trivial, but decisive for the installation rate. Methods developed for the assembly and installation process by the RF System work package group were adopted for the cold accelerator sections in August 2015 in order to support the European XFEL linear accelerator project management, which is the responsibility of DESY.

Components

The main linear accelerator of the European XFEL consists of a large number of different components required to accelerate electrons up to 17.5 GeV. A total of 100 accelerator modules, each comprising eight superconducting cavities, will be installed. Radio frequency (RF) power will be provided by klystrons and fed to the modules via a branched waveguide distribution.

The installation of the components is divided into sections. Each installation section (one so-called cryostring) is 144 m long and contains 12 accelerator modules, which will be fed by three klystrons. To control one cryostring, 13 electronic racks are needed, which are located below the modules together with the klystrons. All these components are interconnected by cables. Furthermore, electrical power and cooling water are needed.

The assembly of the cold accelerator sections involves the following work packages:

WP 01	– RF System	WP 32	– Survey & Alignment
WP 02	– LLRF System	WP 33	– Tunnel Installation
WP 03	– Accelerator Modules	WP 34	– Utilities
WP 05	– Power Couplers	WP 36	– General Safety
WP 08	– Cold Vacuum	MDI	– Cabling
WP 13	– Cryogenics	IT	– Fibre Optics and Ethernet
WP 28	– Accelerator Control System		

Because of the large number of contributing groups, planning and controlling the installation process is a complex matter.

Installation planning

The installation plan (Fig. 1) was developed in cooperation with the leaders of the eight most important work packages, during six one-hour meetings prepared, moderated and post-processed by members of the RF System group.

At the first meeting, the current state of the installation process was analysed. All installation steps were listed by the work

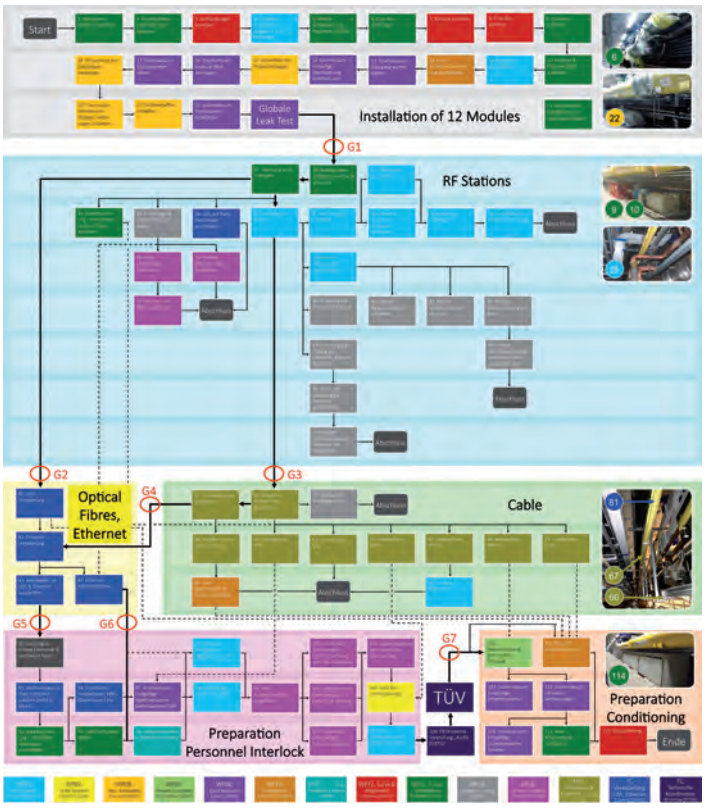

Figure 1

Description of the installation process in the cold accelerator section by means of a process map. Each box represents one installation step. The sequence of installation steps is fixed in the process map.

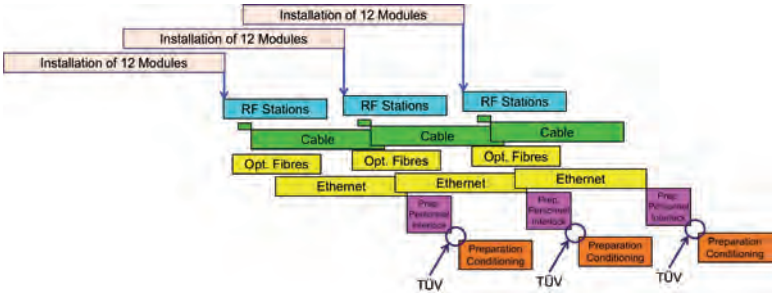

Figure 2

Installation sequence of several accelerator sections (so-called cryostrings, each including 12 modules) in time flow representation

package leaders, noted down on cards and arranged on a magnet board exactly in the sequence of previous installations. Furthermore, first ideas were collected on how to optimise the installation sequence. These ideas were taken up at the second meeting, and installation steps that could be done in parallel were identified. Before the third meeting, the work package leaders were interviewed about how long each step would take and which boundary conditions would have to be fulfilled (or which other steps would have to be finished) so that these steps could start. With this information, a reasonable parallelisation of steps was figured out, presented in the meeting and accepted by the work package leaders. At the fourth meeting, the global installation process was defined, describing how the time flow of several cryostrings was to be realised (Fig. 2).

Before the fifth meeting, the installation plan was visualised, presented to and approved by the work package leaders. At the sixth meeting, the plan was presented to the European XFEL linear accelerator project management (DESY) and technical coordination (TC), who accepted it. The installation plan is optimised after each cryostring installation based on the newly gained experience.

Controlling the installation process

To translate the installation plan into action, a weekly tunnel meeting was established (Fig. 3). At these tunnel meetings, the status is checked to determine which installation steps are ongoing or finished. The status of each cryostring is visualised on a poster and sent to the project management. Next, the forthcoming work for the week is discussed and planned. At the end of the meeting, starting dates for the installation steps beyond the current week are set, so the work package leaders can plan their resources.

Typically, on-site inspections take place after the tunnel meeting to tackle arising problems and optimise the ongoing installation work. As one important measure to speed up the installation process, the so-called territory management proved to be most effective. Territory management means that installation positions (for klystrons, racks, etc.) and working areas are marked with special tape on the ground, preventing time-consuming “collisions” between different work packages in the tunnel.

Results

The described methods have proven valuable tools for planning and controlling the installation of the European XFEL main linear accelerator. Thanks to the permanent optimisation, the actual installation process for cryostring number 3 after adoption of the new plan in August 2015 proceeded two weeks faster than scheduled (Fig. 4). Instead of the 15 weeks foreseen from starting the RF station installation to finishing the preparation of the personnel interlock, only 13 weeks were needed. The experience gained was used to improve the plan for the next cryostring installation.

Thanks to the application of the described planning and controlling methods in August 2015, the installation rate in the cold accelerator sections was significantly increased.

Figure 3

Weekly tunnel meeting at the installation front next to the cold accelerator. The installation status poster can be seen on the right.

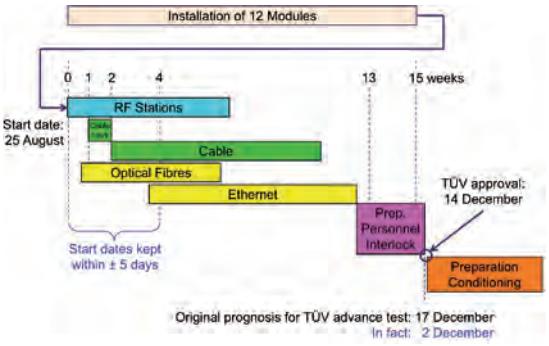

Figure 3

The first installation run with the newly developed plan ended two weeks earlier than scheduled.

Contact: Michael Bousonville, michael.bousonville@desy.de,
Frank Eints, frank.eints@desy.de,
Stefan Choroba, stefan.choroba@desy.de

Production of superconducting 1.3 GHz cavities for the European XFEL.

Completion of series production of 800 superconducting niobium cavities

The production of 800 series cavities for the European XFEL X-ray laser, the largest in the history of superconducting radio frequency (RF) cavity production, was realised by the companies Research Instruments GmbH (RI), Germany, and Ettore Zanon S.p.A. (EZ), Italy, on the principle "build to print". DESY provided high-purity niobium and niobium–titanium alloy for the cavities. The conformity of production principles with the European Pressure Equipment Directive (PED) was developed together with the contracted notified body, TUEV NORD. New or upgraded infrastructure was established at both companies. Delivery of series cavities, fully equipped and ready for cold RF testing, began in January 2013 and finished in December 2015. The performance of "as received" cavities fulfils the European XFEL specifications on average; further improvement was reached by retreatments at DESY or at the companies.

The production of 800 superconducting cavities for the European XFEL was a real challenge, especially because a large amount of know-how had to be transferred to industry. The experience gained is very important for subsequent large projects, such as the upgrade of the LCLS X-ray laser (LCLS-II) in the USA or the European Spallation Source (ESS) in Sweden. The International Linear Collider (ILC) project especially could consider the European XFEL cavity production as a feasibility check and benefit from it.

The cavity production was prepared from 2006 to 2010. The setup of facilities and the production itself continued for about five years from 2010 to 2015. Serial cavities were delivered from January 2013 until December 2015.

After several negotiation steps, a "basic order" of 560 serial cavities was contracted in equal amount in September 2010 to RI and EZ on the principle "build to print". Each company had to deliver 280 serial, 12 high-grade, four dummy (DCV) and four reference (RCV) cavities. The ILC HiGrade cavities, planned to be produced without helium tanks (HT), were foreseen as a tool for QC. The "cavity option" (the remaining 240 serial cavities) was allocated at the beginning of 2013 to both companies in equal amounts (120 to EZ and 120 to RI).

Procurement of material for the cavities (semi-finished products (SFPs)), QC, PED adaption, documentation and shipment to the cavity producers were taken over by DESY. Four companies produced about 25 000 SFPs of high-purity niobium and niobium–titanium alloy in three years.

The term "build to print" means that a performance guarantee is not obligatory for the companies. Therefore, the main principle for production supervision was that the cavities had to be built strictly according to the European XFEL specifications. This required very precise specifications and a lot of effort in production monitoring.

Technology transfer to industry and supervision of the vendors' infrastructure and work were executed by teams of DESY and INFN/LASA, Italy. Frequent visits of experts proved to be more fruitful than instating inspectors permanently at the companies. For that, several teams of experts responsible for general coordination, material, cavity mechanical fabrication, HT issues, treatment, RF, vacuum and documentation were established.

The cavities, when integrated in the HT, are pressure-loaded parts (subject to the danger of implosion) that have to fulfil the European Pressure Equipment Directive (PED, 97/23/EC). In cooperation with the contracted notified body, TUEV NORD, the certification of industrially manufactured resonators with HT was done.

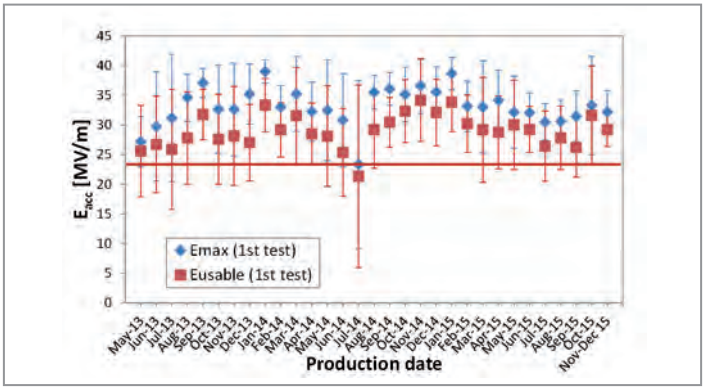

Figure 1

Average value of the accelerating gradient E_{acc} for "as received" European XFEL cavities produced at company RI, sorted by test date

To ensure the “build to print” production, DESY/INFN executed an external QC procedure in addition to the processes that the cavity manufacturers implemented internally. The acceptance for delivery of fully equipped cavities was split according to specification into three acceptance levels (AL1–AL3) that defined the contractual hold points:

- AL1: Release cavity for surface treatment after mechanical fabrication without HT
- AL2: Release cavity after dressing it with HT for further treatment
- AL3: European XFEL expert team releases cavity for shipment to DESY for the vertical RF test

An engineering data management system (EDMS) was used as a central repository of all engineering information. Timely uploaded documents allowed DESY/INFN to perform QC and access data in the early stages of the production process. Because of the large number of reports that had to be handed over, an automated and completely paperless transfer of the quality management documents for cavities was developed and implemented.

A major part of the work was dedicated to upgrading the existing infrastructure and creating a new infrastructure for cavity production at both companies. This comprised several techniques and equipment mostly made available by DESY/INFN and transferred to industry. The DCV and RCV cavities were used to debug and qualify the infrastructure. The DCVs were applied at the companies for operator training, mechanical test of devices, process parameter adaptation, infrastructure setup and ramp-up, final treatment tests, tuning tests, etc. After treatment at DESY, the RCVs reached RF accelerating gradients of E_{acc} = 30–35 MV/m and exceeded the European XFEL requirements before hand-over to the two companies. The RCVs were then used for stepwise qualification of the new infrastructure after setup using the DCVs was done.

Five steps were defined for qualification of the surface treatment infrastructure. After each step, the respective RCV was sent to DESY for cold RF testing. Each qualification step was repeated in case of failure.

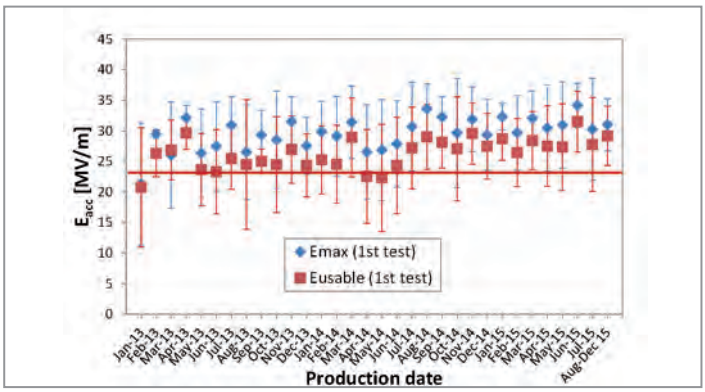

Figure 2

Average value of the accelerating gradient E_{acc} for “as received” European XFEL cavities produced at company EZ, sorted per by test date

The serial production was ramped up using the first eight serial cavities fabricated by each company (pre-series cavities (PCVs)). These cavities passed the complete cavity preparation process equipped with all accessories at the first attempt. After successful test of the PCVs, the serial production was released and ramped up to the contracted delivery rates. A production rate of 3–4 cavities per week per company was maintained for the entire period of production.

Adjustment of the main parameters – length, frequency and homogeneity of RF field distribution over the cavity’s nine cells (field flatness) – was successfully done for the complete production. The length adjustment procedure basically contained the following sequences: frequency measurement on dumb-bell, trimming of dumb-bell at equator and positioning of dumb-bell for cavity completion. To carry out the frequency measurements for a large number of cavity parts, semi-automatic RF measurement machines (HAZEMEMA) were designed, built at DESY and handed over to industry. Automatic tuning machines (CTM) for nine-cell TESLA-type cavities were designed, fabricated, installed at RI and EZ and successfully operated throughout the whole production period.

The only available diagnostic method was the optical inspection of the cavity’s internal surface using a high-resolution camera (OBACHT) in combination with the replica technique, in which the surface is studied non-destructively by imprinting the surface details onto a hardened rubber.

The typical surface flaws observed in the OBACHT camera can be differentiated into the following types: electron beam welding errors, etching irregularities (pits and “cat eyes”, rough polishing, etching corrosion), foreign material inclusions, scratches and dirt (dust). The flaws were mainly repaired by the companies. Accelerating gradients up to 35 MV/m could be reached after proper repair.

Figures 1 and 2 show the average values of maximal and usable accelerating gradient E_{acc} (with unloaded quality factor $Q_o = 1x10^{10}$ at maximum E_{acc} and X-ray level lower than $1x10^{-2}$ mGy/min) per month for cavities produced by RI and EZ, respectively. As can be seen, the majority of the “as received” cavities exceeded the specification requirement (red line) immediately.

Nonetheless, further performance improvement through additional treatment was still obtainable for a lot of cavities. After retreatement, the usable E_{acc} finally reached E_{usable} = 29.9 ± 5.1 MV/m on average for both companies (E_{usable} = 31.2 ± 5.0 MV/m for RI and E_{usable} = 28.6 ± 4.8 MV/m for EZ). This is about 25% higher than the specification requirements.

Contact: Waldemar Singer, waldemar.singer@desy.de,
Axel Matheisen, axel.matheisen@desy.de,
Jens Iversen, jens.iversen@desy.de

Digital accelerator facility.

Configuration management for the European XFEL

In parallel with the construction of the European XFEL X-ray free-electron laser, a digital accelerator facility is being built. It provides a visual model of the accelerator, its tunnels and buildings and all their infrastructure, together with a hierarchical breakdown structure of systems, subsystems and components. A central configuration database collects design models and drawings, work instructions and checklists, test records and maintenance manuals. It helps to standardise and thereby optimise procedures. The information is collected during production and installation and accessible anywhere and at any time. It improves communication, saves time and costs by helping to prevent design mismatches and maintains knowledge and history throughout and beyond the project.

Configuration management

Building complete and consistent documentation, which is easily accessible and maintainable, is one of the many fundamentals for managing complex projects. Configuration management collects documents in a central configuration database, including for example 3D models and design drawings, work instructions and checklists for quality control, inspection records and test certificates, as well as maintenance documentation. It provides a foundation for quality management, ensures compliance with legal requirements and enables progress monitoring from in-time data records.

Configuration management was started in the European XFEL project already in the very early design phase. Since then, it has been a continuous activity, which will last throughout the entire project and beyond. The documentation needs to be kept available and up-to-date for the whole lifetime of the facility, ready to serve as a basis for maintenance and upgrades for several decades. DESY has therefore implemented the European XFEL configuration database in an engineering data management system (EDMS). Figure 1 shows the digital accelerator facility next to its physical counterpart and illustrates the content of the configuration database.

Design integration

The accelerator facility can be described as a hierarchy of systems, subsystems and components, which serves as structure for organising and navigating the design documentation. Component and subsystem designs are optimised both at an individual level and as an integrated whole, and the 3D models are integrated to visualise the entire facility.

The first design documents were created in the early planning stages, gaining increasing level of detail as the project progressed. The configuration database makes the up-to-date design information available within the entire project. It helps the teams to develop interfaces and to identify and control the impact of design changes and improvements.

Parts tracking during fabrication

All the components and subsystems are provided to the European XFEL facility as in-kind contributions from the project collaboration partners. Numerous research laboratories from all over the world have taken responsibility for contributing certain parts. Most of the labs have subcontracted the series production of the parts to industrial vendors, while assembly,

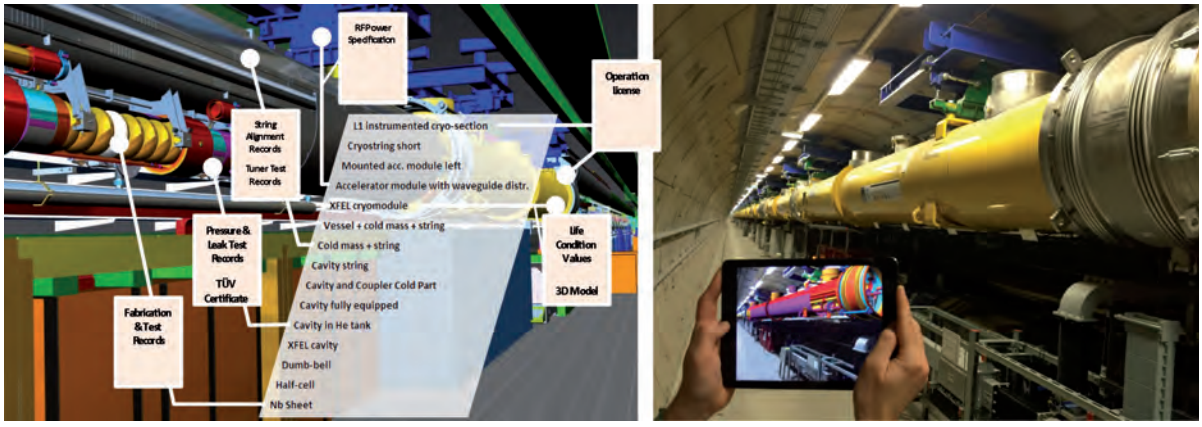

Figure 1
Digital and physical accelerator facility together with examples of the content of the configuration database

testing and installation are performed by the collaboration partners, both at the their home laboratories and at the European XFEL facility.

Every important physical part of the facility is uniquely identified. All those parts and all their related documentation are registered in the EDMS, which is used to manage the inventory of the accelerator. Documents and acceptance test records have to be delivered at the latest when the components are installed in the facility. But often, the information is already provided during production. Many partner labs and subcontractors are connected to the EDMS and upload their documentation along as they work. This in-process documentation enables fabrication progress tracking and allows for monitoring which parts and supplies are available at which locations. Furthermore, it helps to involve experts from several collaboration partners in reviewing quality documents and taking decisions. As shipping and assembly of physical parts are tracked as well, the EDMS can also provide detailed reports of the configuration of components and the whereabouts of parts.

Figure 2 shows a tuner, a component of the accelerator modules, with an engraved EDMS-ID for identification, and the configuration of the particular accelerator module that contains this tuner.

Installation progress monitoring

The documentation mechanisms used in fabrication can be extended to installation activities. Incoming components are identified with labels, and work records, test and inspection certificates are added to the EDMS, which can in turn provide installation progress reports and capture the configuration of the beamline sections.

Benefits

Configuration management with an EDMS is something the project teams first had to get used to, but once adopted, its benefits were manifold. Most prominently, the digital facility enables vision sharing, thus making sure everybody had the same picture in mind long before the first components were produced. The virtual integration prior to production and installation also saves time and costs by preventing design mismatches.

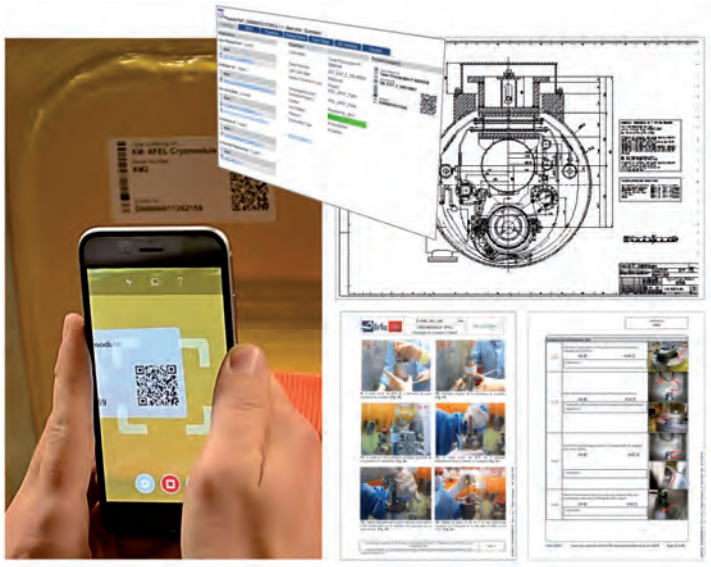

Figure 3

In-situ access to technical documentation, work instructions and checklists for inspection

The EDMS enables efficient processing of huge amounts of quality control documents. It contains several hundreds of thousands of work and inspection certificates, many of which are required by legal regulations and will be relevant for years to come for maintenance and upgrade activities. The EDMS improves the communication and exchange of information across subsystems, when communicating the status of work or following up on changes, for example. It makes the documentation available anywhere at any time. The same information can be accessed in design offices and in workshops, in the tunnel and in meetings, at subcontractors and at collaboration partners around the world. As an example, Fig. 3 shows the in-situ access to technical documentation and work instructions.

Configuration management helps to standardise and thereby optimise procedures, and to maintain knowledge and history when staff changes after the end of the project and during long-term operation. The effort required for keeping information up-to-date is relatively small, as capturing information is well integrated into the processes and to a large extent automated based on the EDMS.

Contact: Lars Hagge, lars.hagge@desy.de

Figure 2

Tuner with engraved part identification number (left) and configuration of the module in which it is used (right)

First operation of European XFEL electron beam diagnostics.

Using diagnostics to find the beam – and not the beam to get diagnostics working

As foreseen in the planning of the European XFEL X-ray laser, the injector was completed as the first functional unit; start-up of this important part of the facility should be about one year before the entire facility. The about 50-m-long injector comprises not only the electron source, but also almost all key components used in the main accelerator and the warm beamlines. The demands for the commissioning of the injector are therefore similar to or even the same, but on a smaller scale, as those for the whole facility. Concerning the diagnostic devices, almost all systems are installed in the injector and have been commissioned and used for putting the injector into operation with the first beam just in time for Christmas 2015.

Figure 1

Overview of the European XFEL injector. Left: warm beamline. Right: electron gun and accelerator modules.

The injector of the European XFEL accelerator complex is located in a separate vault allowing for independent operation of other parts of the facility. A lot of effort was put into reaching the goal to get the injector into operation about one year before the start-up of the entire facility. This advance year of operation allows for commissioning and gaining operational experience with key systems as well as for preparing settings covering the wide operation space of the European XFEL.

The injector consists of the electron gun section, two cold acceleration structures, one operated at 1.3 GHz and the other at 3.9 GHz, used as a phase space lineariser, followed

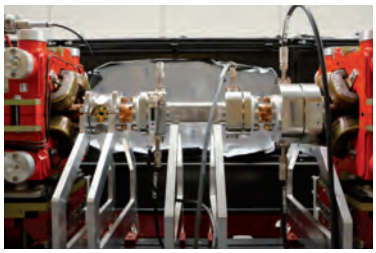

Figure 2

From left to right: beam arrival monitor, 40.5 mm aperture cavity BPM and dark-current monitor

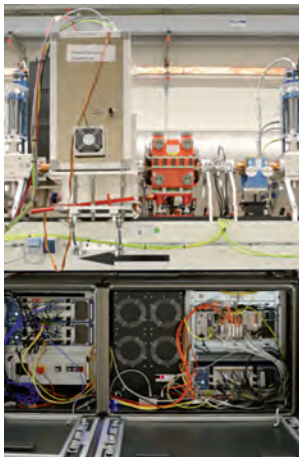

Figure 3

Electronic rack for the diagnostics below the beam pipe. This rack contains an MTCA crate (toroids, dark-current monitoring and beam loss monitors) and three crates with BPM electronics. The arrow on the support indicates the beam direction.

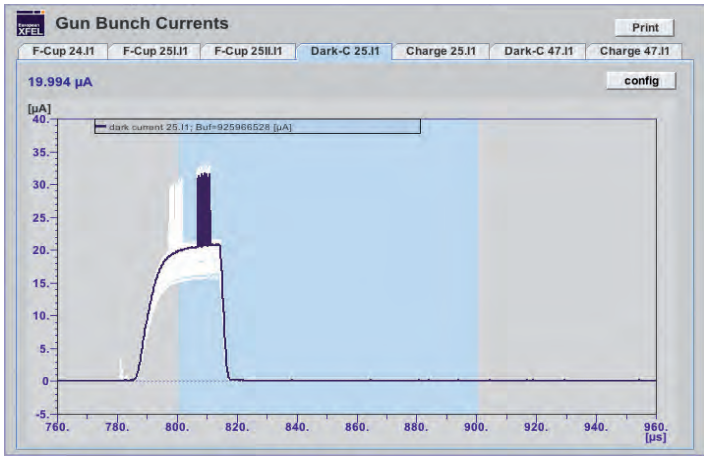

Figure 4

First electron beam from the European XFEL gun. The laser-driven bunches can be seen on top of the continuum of dark-current signal from the gun. The white trace shows some previous shots and the attempt to adjust the timing.

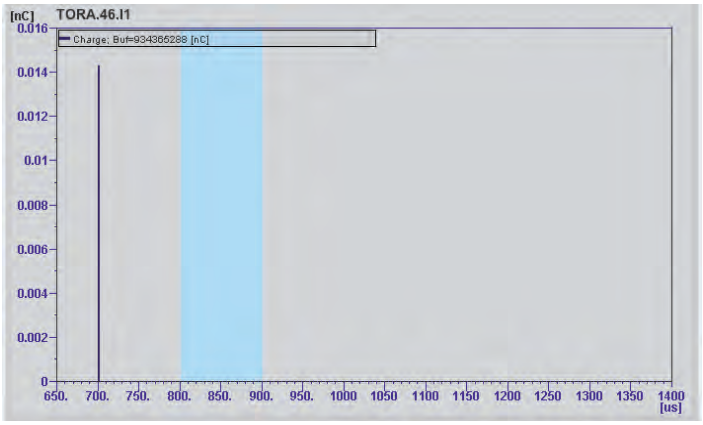

Figure 5

First beam behind the accelerator module. The self-triggered signal appears at position 700; switching to machine trigger moves the signal to the standard position for the first bunch, located at position 800.

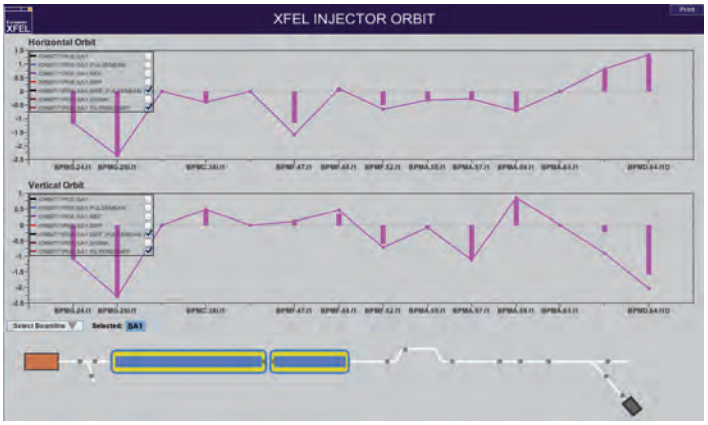

Figure 7

Picture showing the BPM readings in the European XFEL injector, taken during the first shift

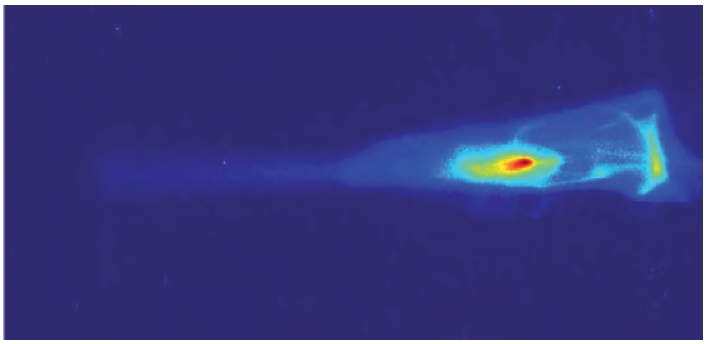

Figure 6

Picture of the beam on the screen in front of the beam dump

by a warm beamline with a laser heater and a diagnostic section foreseen for longitudinal and phase space diagnostics. An overview of the injector accelerator is shown in Fig. 1.

All standard electron beam diagnostic systems except wire scanners are required on the first 50 m of the facility and have been installed. Four toroids, two dark-current monitors and three Faraday cups are used for charge measurements. In total, 14 beam position monitors (BPMs) with their readout electronics developed as an in-kind contribution by PSI in Switzerland are available, including two module and three high-precision cavity BPMs. Eleven screens are installed, five of them including off-axis screens for phase space tomography even with long bunch trains. Sixteen beam loss monitors and one beam halo monitor detect losses along the beamline. The electronics of all systems are installed below the injector beam pipe, as in the rest of the facility (Fig. 3).

The commissioning of the diagnostics started in spring 2015 with the first operation of the gun section. At that time, three Faraday cups, three screens, one toroid, one dark-current monitor and three BPMs were put into operation. After completion of the full injector installation, beam operation started on 8 December with the first electron beam from the gun. It was possible to detect charge on a level below 1 pC during synchronisation of the gun and the injector laser (Fig. 4).

Shortly after these first signals, the toroid and three BPMs were also operational with a charge of about 2 pC. Even with these low signals, which were due to the still not optimised laser spot on the photocathode and lay well below the charge range specified for the European XFEL, the diagnostics could be used from scratch to support the further conditioning work. After cool-down and tuning of the superconducting cavities, the accelerator modules became available for beam operation on 18 December. Immediately after the first attempt, beam was detected by a toroid located after the modules and running in self-triggered mode (Fig. 5). Within one shift, it was possible to steer the electron beam to the dump (Fig. 6). All diagnostic devices were available during start-up. After some basic adjustments, mainly of the timing parameters, the information from the diagnostics was also available from middle-layer servers of the control system, enabling more advanced display and beam steering options (Fig. 7).

Summarising the results of the injector commissioning from the diagnostics point of view, it should be emphasised that all the devices worked from start-up. Even at sub-pC charge levels, the devices operated in self-triggered and timing-system-driven modes, and provided the necessary information for beam steering with a minimum of commissioning actions. The devices are well integrated in the control system, so that even more advanced tasks were possible from the beginning. Following the work for the first beam, further commissioning steps will bring all the systems to the performance required to support the full bandwidth of the European XFEL parameter space. Some improvement potential has been figured out that will allow an even more effective use of the diagnostics during the start-up of the entire facility.

Contact: Dirk Noelle, dirk.noelle@desy.de,
Dirk Lipka, dirk.lipka@desy.de

Cryomodule installation in the European XFEL tunnel.

Installation of cryogenic components in the European XFEL linear accelerator

The linear accelerator of the European XFEL X-ray laser uses superconducting technology and thus needs to be cryogenically cooled. The cold accelerator consists of 100 assembled cryomodules, six cryogenic feed and end boxes and six string connection boxes, which have to be connected together at their final position in the tunnel after cold testing, transport, final positioning and alignment. Installation activities in the European XFEL main tunnel started at the end of 2014 and passed the 40th connection at the end of 2015. The installation process includes welding, non-destructive testing and assembly under cleanroom conditions. In addition, as a pressure equipment, the cold accelerator is subject to the requirements of the European Pressure Equipment Directive (PED).

European XFEL accelerator layout

The cold linear accelerator of the European XFEL consists of 100 1.3 GHz accelerator cryomodules divided into three sections (L1, L2 and L3); between the sections are two warm bunch compressors (BC1 and BC2), where the continuity of the cryogenic distribution is made possible by two transfer lines (Fig. 1). Each section is composed of several cryomodules and one feed and one end cap; the L3 section is divided into seven cryostrings (CS3–CS9, with 12 modules each) separated by string connection boxes, where a vacuum barrier is installed to separate the insulation vacuum, allowing for independent pumping.

The cryogenic circuits at 2.2 K, 5–8 K and 50–80 K flow along the whole accelerator without interruptions, while the two-phase circuit and the warm-up and cool-down line are filled with helium from the 2.2 K circuit at the beginning of each cryostring. The gas return pipe is connected to the two-phase pipe at each module connection and runs through the whole linear accelerator without interruption, making the 2 K circuit too a unique cryocircuit for the whole European XFEL cold accelerator.

Component connection

All the cryogenic pipes contained in the cryomodules, feed and end caps and string connection boxes are connected together by welding to reduce the risk of leaks introduced by flanged connections (Fig. 2). At each connection, a bellows is installed between the two pipe ends protruding from the modules, caps and boxes, and a beamline absorber is mounted on the beamline with flanged connections using a portable cleanroom to avoid contamination. Since there are eight different lines in total, this amounts to 16 or 17 welds per connection, i.e. ~2000 welds in the whole linear accelerator.

The welding and beam connection are performed one cryostring at the time, starting from the end of the string (farthest component along the beamline) and moving toward the electron source. The whole process takes about three months per cryostring in ideal conditions. During this period, no other activity is allowed on the whole cryostring. The components are all automatically welded, either with a tractor machine (Fig. 3) or with a commercial orbital machine. The welding heads of the tractor machines had to be developed in-house by the DESY welding team since commercial parts would not fit into the tight space available.

Since the cryopiping is part of a pressure equipment, the pipes in the modules and the bellows welded in the connection area are supplied by PED-certified producers with an EN10204 3.1 certificate. Moreover, the welding procedure specifications and qualification records are approved by a notified body, and the welders are certified from the notified body for each type of welding machine (tractor or orbital) and

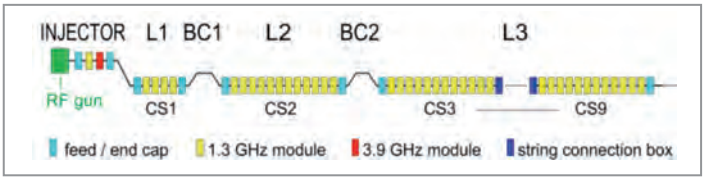

Figure 1

Layout of the European XFEL injector and cold linear accelerator

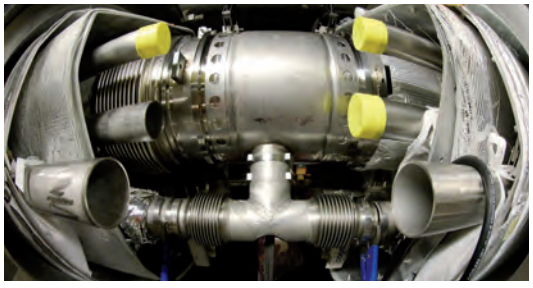

Figure 2

Typical module–module connection

for the hand welds. The welding procedures require filling the weld region with pure argon gas with a maximum concentration of impurities below 50 ppm during the whole welding operation. The insertion of the shielding gas is a long and delicate process.

Welding qualification

To complete the qualification of the welds (also as part of a pressure equipment), they have to undergo a series of non-destructive tests. The “standard” pressure test could not be enforced in the European XFEL case, since the test could have caused damage to the delicate tuning mechanism of the accelerating cavities installed inside the cryomodules, with the potential consequence of precluding the operation of the linear accelerator. The pressure test was therefore replaced with a radiography test.

The following non-destructive tests are thus foreseen for each weld: 100% visual test, 100% radiography test and 100% leak test.

- The visual test is performed just after the welding and is done on both the inner and outer surface of the weld. The inner surface is reached using an endoscope with an 18-m-long arm.
- The standard radiography test for pipes with a thickness of around 2 mm is an X-ray test; unfortunately, the X-ray equipment is big and does not allow the 100% requirement to be met. It was therefore agreed to use a selenium (Se75) source of gamma rays.
- The leak test is performed for a whole cryostring at a time, since the pipes to be tested are actually one long pipe. Special tools were developed to perform the helium leak test of the single welds. Helium is inserted in one circuit at a time while the special tool/sleeve is assembled on the outside of the pipe, pumped and attached to the leak detector. So far, only one leaky connection was found among the first four completed cryostrings.

If a weld does not pass one of the tests, it has to be repaired. All the repair welds are performed manually, after grinding the area around the defect.

Assembly of the beamline absorbers

The connection of the electron beamline is done in most cases by inserting a beamline absorber (BLA). In a few exceptional cases, simple copper-coated steel bellows are used. The most important requirement for the beamline vacuum is to avoid contamination of the superconducting cavities during installation. As both particulates and gas layers can deteriorate the cavities’ accelerating gradient, all installation work on the beam pipe needs to be done in a cleanroom environment.

Figure 3

Tractor welding machine

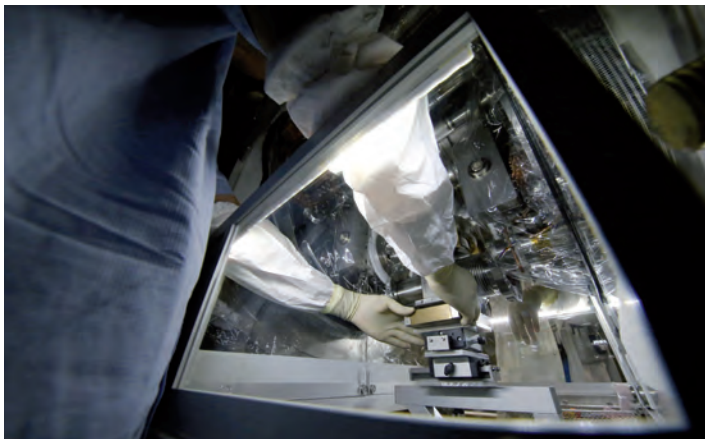

Figure 4

Assembly of a beamline absorber

A custom-made dedicated cleanroom has been developed for the installation of the BLAs (Fig. 4), in which clean air is streamed from the bottom towards the top, since the space above the installation site is crowded with cryogenic pipes. A support lever arm system is integrated to facilitate an easy and thus reliable and reproducible mechanical installation of the BLAs. For the pump-down, the mass flow is limited to avoid particle transport.

To avoid carbohydrate contaminants, vigorous cleaning and proper handling of ultrahigh-vacuum components is foreseen. Typical measures are ultrasonic cleaning, thermal treatments and backfilling with (particle-filtered) dry nitrogen directly from the liquid phase. As a quality control procedure, residual-gas analysis and a helium leak check are done. If these are successful, the manual gate valves on the adjacent modules are opened and the cleanroom is moved to the next position.

Final steps

After welding and BLA assembly, a few components are mounted at each connection: a BLA support, bellows covers, two thermal shields and multilayer insulation; then the big DN1100 bellows is closed and the cryostring is pumped to perform the final leak check of the isolation vacuum. If the leak check is successful, the connection is finished.

In 2015, the cryostrings in the injector as well as CS1, CS3 and CS4 were completed; the welding of CS5 was almost concluded, with the full completion of the cryostring foreseen for January 2016.

Contact: Serena Barbanotti, serena.barbanotti@desy.de

Quality assurance for 800 European XFEL cavities.

RF measurements as a tool for quality assurance during series production

The linear accelerator of the European XFEL X-ray laser will comprise 800 superconducting (SC) cavities. Severe requirements for the cavity characteristics and the need to provide quick and accurate quality control during series production incited DESY to set up a semi-automatic quality assurance system based on radio frequency (RF) measurements. From investigations of the niobium sheets to the accelerator modules being ready for installation, many critical RF measurements have to be performed, which enable the cavities to be accurately characterised throughout the various fabrication and assembly steps. Further important aspects to ensure high cavity quality are data collection, automatic analysis and quality information feedback between DESY and the cavity manufacturers.

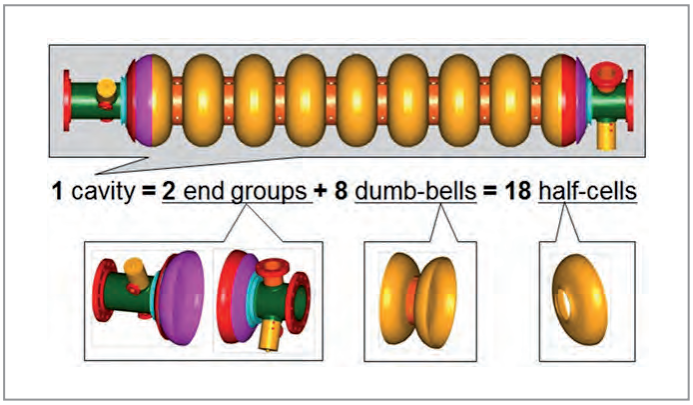

Figure 1

Superconducting European XFEL cavity and its parts

Besides the accelerating gradient and quality factor [1], one of the main goals for the fabrication of SC cavities is the accuracy of the mechanical length and eccentricity. In addition, for the operation of the SC cavities in an accelerator, the electric RF frequency and flatness of the accelerating field as well as the damping of the higher-order mode (HOM) fields must stay within tight tolerance limits after welding of the whole structure [2]. To reach these very high quality goals, detailed RF measurements were chosen to characterise the cavity during its different fabrication steps. RF measurements are very sensitive to mechanical deviations and at the same time more flexible and easier to perform than mechanical measurements. In addition, less contact with the delicate superconducting surface is needed.

The main purpose of the quality assurance (QA) based on RF measurements is to achieve both the RF and mechanical specification of the European XFEL SC cavities:

1. Fundamental-mode frequency at 2 K before tuning to 1.3 GHz: F(TM010, pi) = 1299.7 ± 0.1 MHz
2. Flatness of accelerating electric field: > 90%
3. Cavity straightness: cell and flange eccentricity < 0.4 mm

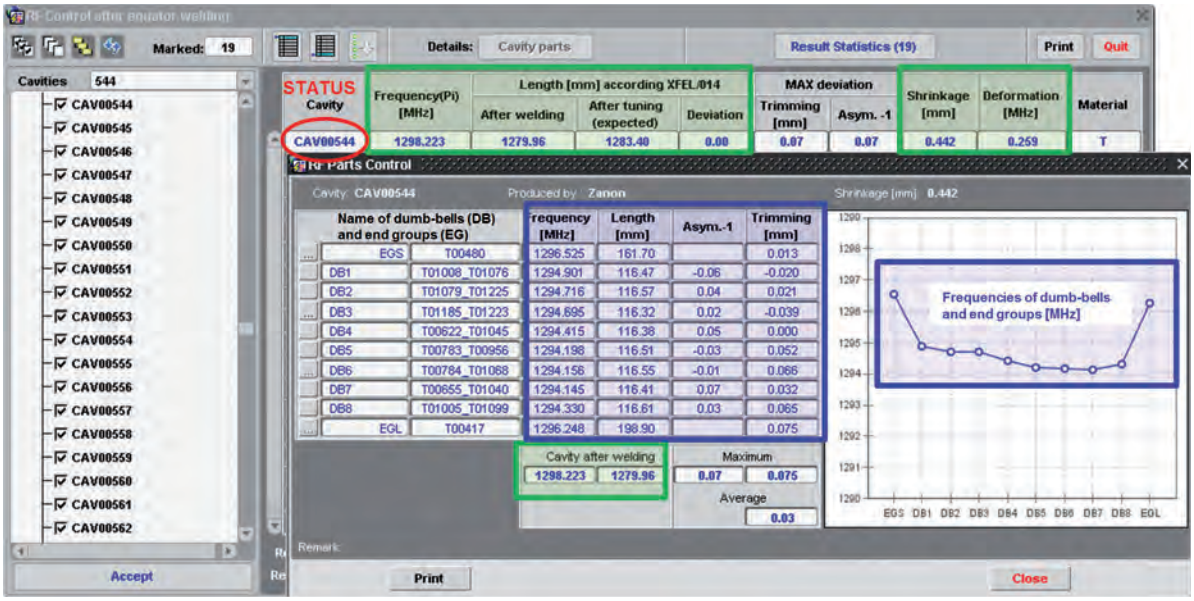

Figure 2

Cavity and parts parameters in the European XFEL cavity database (in blue boxes: before cavity welding, in green boxes: after welding)

4. Final cavity length at the target frequency: 1059 ± 3 mm
5. Cell shape accuracy of the inner SC surface: ± 0.2 mm

Different process steps that influence these parameters have to be taken into account, e.g. welding shrinkage, chemical treatment, frequency tuning and frequency shift during cool-down.

The cavity welding cycle can be divided into three major phases (Fig. 1):

1. Cavity half-cell fabrication
2. Welding of 18 half-cells into eight dumb-bells and two end groups
3. Final welding of end groups and dumb-bells into cavity

During mechanical fabrication, the cavity half-cells, dumb-bells and end groups are RF-measured and trimmed to the right length and frequency. Sorting the components in order to get an optimal RF result after welding allows the cavity length to be predicted with a mean accuracy of ± 0.4 mm. Transverse deviations of the cavity cell diameter can be determined with an accuracy of about 0.1 µm/kHz. The relation of the fundamental-mode frequency to longitudinal cavity deformations is 300 kHz/mm, which is sensitive enough to identify fabrication changes.

After welding, all cavities have to be tuned and measured several times before they can be welded into the helium vessel. The goal of cavity tuning is to achieve at once the nominal RF (spectrum and field flatness) and geometry (length and eccentricity) characteristics. Mechanical and RF measurements are needed to calculate an effective tuning model. The flatness of the accelerating field on the cavity axis (ratio of minimum electric field amplitude and maximum electric field) must be greater than 0.98 at a given length tolerance of ± 3 mm. At the same time, the eccentricity of the nine-cell cavity has to be less than 0.4 mm. Two or three iterations might be necessary to reach this ambitious goal. On the welded cavity, the fundamental-mode spectrum and the field distributions are measured and mechanically tuned together with the straightness.

Both European XFEL cavity manufacturers (RI Research Instruments GmbH in Germany and Ettore Zanon S.p.A. in

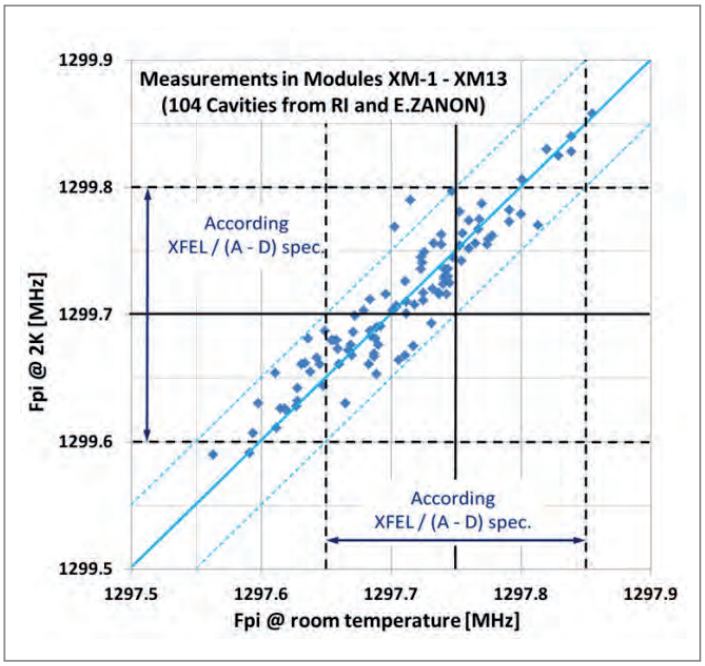

Figure 3

Comparison of the pi-mode frequency (Fpi) at room temperature and at 2 K

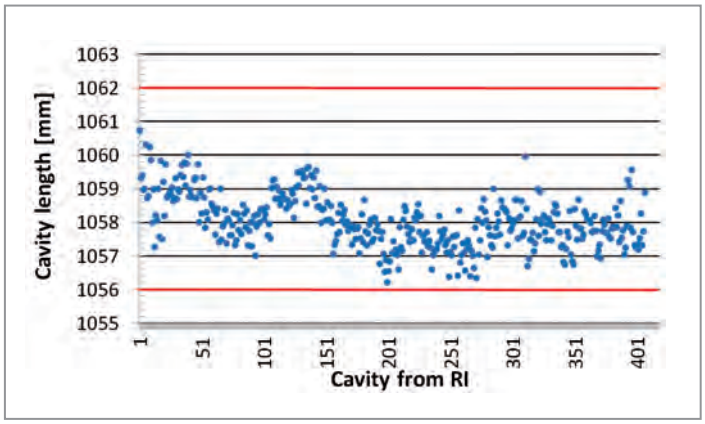

Figure 4

Final cavity length throughout series production

Italy) were provided with machines developed within a collaboration of DESY, Fermilab in the USA and KEK in Japan. These machines, dubbed cavity tuning machine (CTM) and half-cell measurement machine (HAZEMEMA), allowed the companies to perform the RF measurements in a very precise and fast semi-automatic way [3]. The semi-automatic operation decreased the cavity tuning time considerably – down to four hours compared with two days for manual operation – and provided automatic data handling.

After welding into the helium tank, cavity tuning is no longer possible. It is also not possible to do a field flatness measurement after the cavity has been fully prepared for the vertical RF test at cryogenic temperature. One of the main RF characteristics in this cavity configuration is the cavity fundamental-mode spectrum, which correlates with the RF field distribution. During the next steps in cavity testing, transportation and assembly, the fundamental-mode spectrum is measured, and the mean deviation is calculated and used to monitor the field flatness in the cavity. A mean spectrum deviation value of 10 kHz indicates a cavity deformation, which can cause strong fundamental-mode field distribution changes up to 20%.

The results of the final measurements for all subcomponents and cavities after welding are saved in the European XFEL cavity database (Fig. 2). In case any parameter is out of tolerance, the measured or calculated value will be marked on the graphical user interface with a red background along with the cavity status and name.

Statistical data are very important and provide a very good tool to detect trends during series production. Moreover, the data give the possibility to correct unwanted developments.

Figure 3 shows the comparison between the pi-mode frequency at room temperature and at 2 K for the first 104 cavities. The average frequency shift during cool-down from room temperature to 2 K is 2.00 MHz. The fluctuation of about ± 0.05 MHz can be explained by seasonal changes in room temperature of ± 5°C.

The very high accuracy of the cavity length is a result of accurate trimming of the subcomponents, efficient dumb-bell composition and stable infrastructure parameters for chemical treatment and electron beam welding. It allowed the average value of the cavity length to be shifted towards lower values

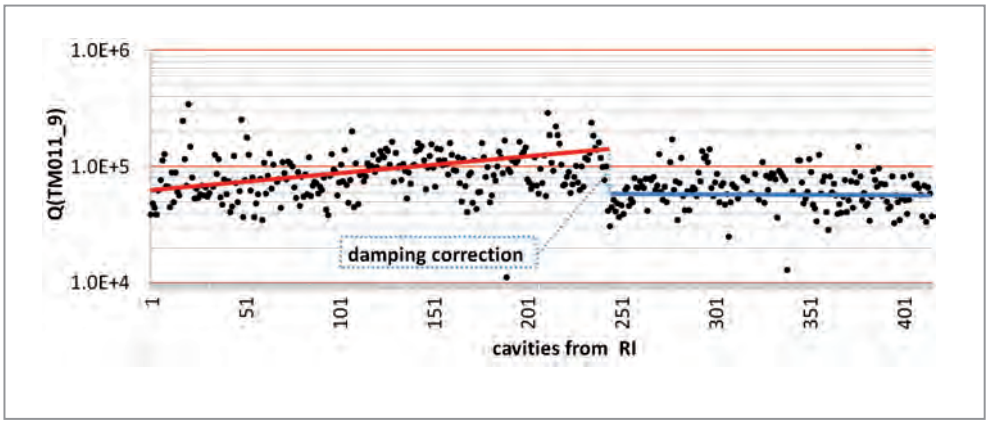

Figure 5

Measured quality factor of the TM011 mode during series production. A lower quality factor corresponds to a higher suppression of the TM011 mode.

during cavity production. This was necessary to compensate helium tank tolerances and optimise the cavity position inside the accelerator modules (Fig. 4).

Another very good example of the use of statistical data is the correction of HOM suppression during the ongoing cavity series production. The first two dipole modes, TE111 and TM110, are well coupled to the HOM couplers because they have their maximum field in the cavity end cells. The second monopole mode, TM011, requires an additional asymmetry of the cavity geometry; its field distribution is very sensitive to inaccuracies of the cavity shape. Unfortunately, the original European XFEL tolerance for the cavity inner shape was not satisfied for many cavity parts. Up to 10% of the surface had shape deviations between ± (0.2–0.3) mm. Based on the high sensitivity of the TM011 field distribution to the accuracy of the cavity shape, the impact of mechanical form deviations on HOM suppression efficiency was determined. In close collaboration with RI, the suppression of TM011 was improved (Fig. 5).

The fabrication of more than 800 SC cavities lasted about 100 weeks and was finished in December 2015. During this time, about 560 000 RF values were measured (about 700 per cavity), stored in a database and evaluated in a semi-automatic system. In several cases, corrections of fabrication parameters were necessary and successfully executed in close collaboration with the cavity manufacturers.

The high quality of the SC cavities achieved thanks to the well elaborated and effective quality assurance system based on RF measurements will ensure the success of the European XFEL in the future.

Contact: Wolf-Dietrich Möller, wolf-dietrich.moeller@desy.de, Alexey Sulimov, alexey.sulimov@desy.de

References:

D. Reschke, “Recent Progress with EU-XFEL”, SRF2015, Whistler, BC, Canada, 2015
A. Sulimov, “RF Measurements for quality assurance during cavity mass production”, SRF2015, Whistler, BC, Canada, 2015
W.-D. Möller, “European XFEL Cavities, Automated RF measurements for SC cavity mass production”, Accelerators 2010, Highlights and annual report, Deutsches Elektronen Synchrotron, 2010

Technical interlock for the European XFEL.

Electronic design to protect RF power couplers and cavities

In the European XFEL X-ray laser, the safe operation of 28 radio frequency (RF) systems for 808 superconducting cavities (1.3 GHz), eight third-harmonic superconducting cavities (3.9 GHz) and the RF electron gun will be secured by a new technical interlock (TIL) system. Several key parameters are measured to protect the main RF couplers and cavities against malfunctions and destructively high power levels. The new system is based on the MTCA.4 crate standard, which offers a very good crate management. In addition, the interlock itself uses many internal diagnostics, which ensure correct operation and enable most of the maintenance work to be carried out without any physical access. To reduce space costs, a very high channel density is used.

Self-sufficient working board pair

The MTCA.4 crate standard allows two boards per slot, one from the rear and one from the front side. The rear transition module of the technical interlock (RTM TIL) contains all electronic parts for sensor and alarm input/output (I/O). On the front side, the universal DESY standard field programmable gate array (FPGA) board (DAMC2) is used for the logical part. The DAMC2 was initiated by the DESY MCS4 group (Control Systems) and developed by the DESY FEA group for several applications such as the machine protection system, beam position monitors, beam loss monitors, laser controller, experiment clock controller and the TIL system (Fig. 1).

Each board pair is a self-sufficient working interlock, independent of the CPU, that is able to access the FPGA via a PCIe (4x) bus system for parameter initialisation and monitoring of the sensor data. The machine trigger for the monitoring traces and the redundant alarm and reset signals are distributed through the standard backplane of the crate (via an M-LVDS bus system).

Four couplers on one board

As the idea was to build only one type of interlock electronics for many different signals, the design mainly refers to the channel needs for one standard main RF coupler in the European XFEL linear accelerator. Usually, it uses three sensors for free electrons (e-) in the vacuum of the coaxial part of the coupler, one spark (light) sensor on the waveguide air side and two temperature sensors outside of the ceramic windows at $T = 70$ K and $T = 300$ K. Except for the temperatures, the input signals are measured with up to 50 MS/s (14 bit).

In addition to the bias voltage supply for the electron sensors and the power supply for the spark (light) detector, four test signal outputs are available, which will trigger a light source in the light detector or, in parallel, a current load to the electron antenna to provide an overall signal test. The temperature sensors can be checked by measuring and adjusting their (normally constant) currents.

A big effort was made to realise all sensor needs of four couplers on one RTM TIL board. Furthermore, we produced a second variant of the same board without the electron bias voltage unit to handle all other signals from the cryogenic and vacuum systems. A system overview is shown in Fig. 2.

The alarm I/O port offers three RS422 channels for each direction and two potential free contacts. The contacts and the first RS422 alarm output are driven additionally by a hardware watchdog, which secures correct operation of the FPGA board. To permit a simpler master–slave system and handle

Figure 1
MTCA.4 RTM TIL (left) and DAMC2 (right) boards, developed for the technical interlock of the European XFEL

Figure 3

Overview of system parts (from left to right: TIL coupler interface box, rack interfaces, create rear side and crate front side)

watchdog alarms without complex ticket messaging between the boards, an extra alarm interface is used to build the alarm sum of a complete RF station. The alarm outputs use redundant ways to switch off the same RF in different stages (TIL → klystron pre-amplifier, TIL → MPS → LLRF …). These outputs can be individually triggered to test the behaviour of the subsequent systems independently.

Count	Signal	Remark
96	e- sensor	Current measurement with bias voltage
32	Spark	Main coupler air side (waveguide)
64	PT1000	Ceramic RF window (T = 70 K, T = 300 K)
12	Analogue	Ion getter pump vacuum and high voltage
2	Analogue	Cryo signals (He level, He pressure)
1	Contact	Vacuum system status
1	RS422	Cryogenic system status

Table 1: Interlock signals for one RF station (32 cavities)

The TIL system is managed by a DOOCS server, which runs on a Linux OS inside the crate. The DOOCS server is responsible for the correct start-up of the boards, the configuration of all parameters (power, thresholds etc.) and the reception and distribution of the monitoring trace data during operation (Fig. 4).

Already in operation

In June 2015, the first set of cavities and devices was operated in the European XFEL linear accelerator during warm coupler conditioning. The start-up of the TIL system worked very smoothly. Just after completion of the cable

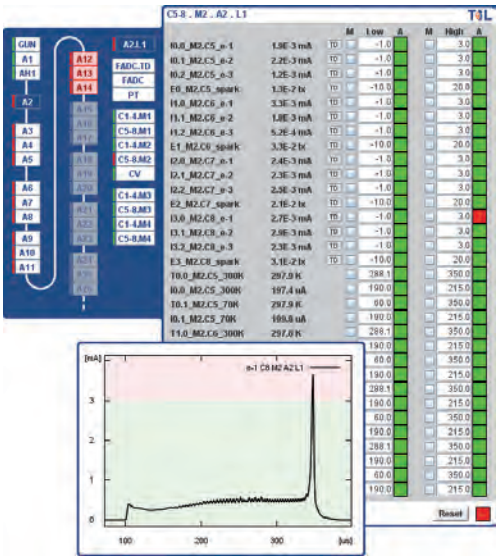

Figure 4

TIL control overview showing the status of channels and a signal trace for a single pulse

work and connection of the coupler signals, the script for testing all the sensors ran through. Some problems, such as broken temperature sensors or a bent connector pin, were found and solved very quickly.

At the end of 2015, the injector stations (one 1.3 GHz module and one 3.9 GHz module) were operated also at cryogenic temperature – the first time that the cryogenic sensors (Cernox temperature sensors and RF diodes) were operated too.

The excellent start-up and operation of the first RF stations in the European XFEL show that a robust, electromagnetically compatible (EMC) design has been achieved, running with a rock-stable firmware and DOOCS server. The testing of parts, completion of crates and installation into the European XFEL tunnel are ongoing.

MTCA (Micro Telecommunications Computing Architecture) is a standard defined by the PCI Industrial Computer Manufacturers Group (PICMG, www.picmg.org).

Contact: Dimitri Tischhauser, dimitri.tischhauser@desy.de, Manuel Mommertz, manuel.mommertz@desy.de, André Gössel, andre.goessel@desy.de

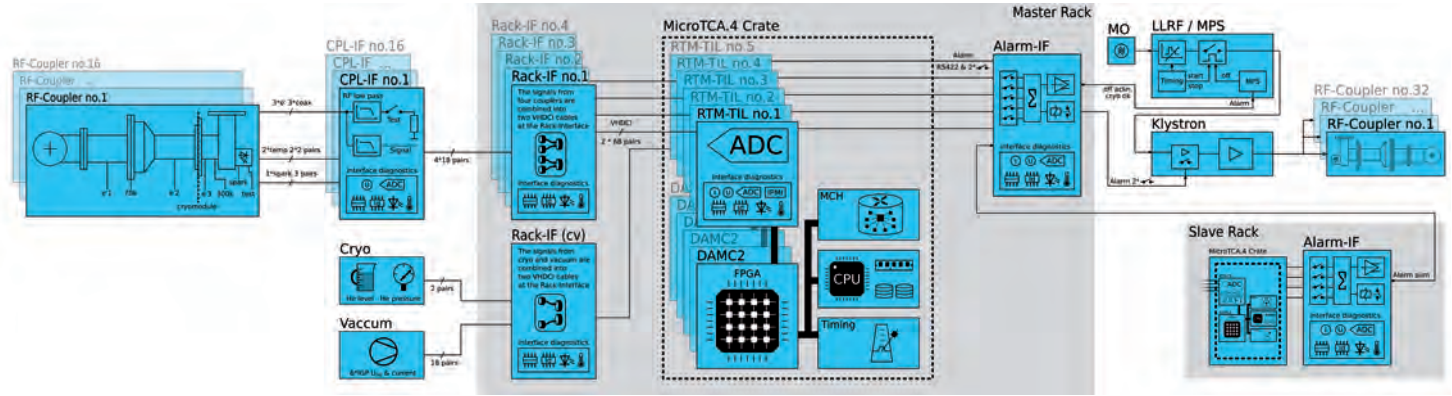

Figure 2

Overview of the technical interlock system

RF waveguide distributions for the European XFEL.

Series production of waveguide distributions

The European XFEL X-ray laser requires 100 accelerator modules, each comprising eight superconducting nine-cell cavities. To achieve the nominal accelerating gradient of 23.4 MV/m, a radio frequency (RF) input power of 120 kW per cavity is required. The power for four cryogenic modules with 32 cavities is provided by a high-power klystron capable of delivering 10 MW of RF power at 1.4 ms pulse duration and 10 Hz repetition rate. This allows even higher RF power of up to 320 kW for each cavity. All components of the RF distribution system are capable of this higher power demand. Starting from the initial design, which foresaw the provision of equal power per cavity and, in an advanced version, equal power for a pair of cavities, it became necessary to modify the layout even further to allow for individual power delivery to each cavity. This modification was required because, during module production, a wide spread of maximum achievable gradients showed up in the cavities. In order not to be limited by the weakest cavity in the modules connected to one RF power source, individual power distribution was developed. Despite the more complicated layout, the production process could be optimised and the production rate increased.

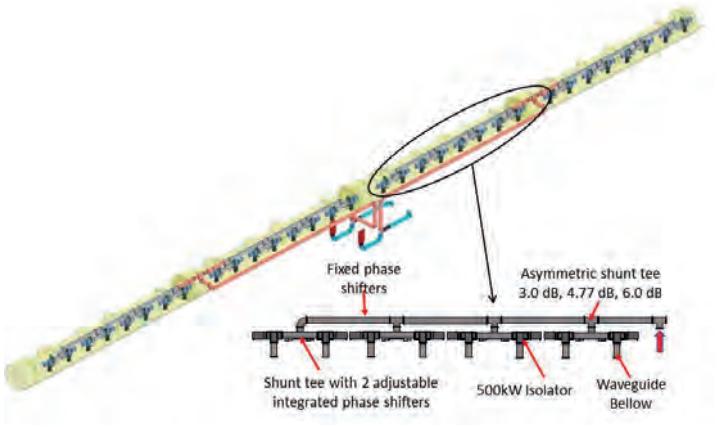

Figure 1

RF waveguide distribution layout for one RF station

RF system layout

Figure 1 shows the RF waveguide distribution of one RF station for four cryogenic accelerator modules. The klystron has two output waveguides (blue) and generates up to 10 MW of RF power, two times 5 MW, at 1.4 ms pulse duration and 10 Hz repetition rate. The output power can be absorbed in RF loads (red) during tests of the RF station or transmitted by waveguides (orange) to the accelerator modules (yellow) during accelerator operation. The output power of each arm is split again into two module waveguide distributions (grey).

The module waveguide distribution is shown magnified. In the linear part, the RF power is branched off by asymmetric shunt tees for a pair of cavities and then split again. In front of each cavity, an isolator is installed, which protects the klystron from reflected power. Within the module waveguide distribution, the phase is adjusted by fixed phase shifters and controlled for each individual cavity by adjustable phase shifters. The phase between the modules can be adjusted by additional adjustable phase shifters if required.

In the first layout, the shunt tees between modules and for a pair of cavities were assumed to be 3 dB shunt tees, whereas the asymmetric shunt tees in the linear part of the distribution were 3 dB, 4.77 dB and 6 bB. With this design, all cavities would be supplied by the same RF power. The advantage of this layout was that it used the same type of components for all waveguide distributions and allowed for pre-production of the distributions independently of the accelerator module production status. The disadvantage was that the weakest cavity with lowest achievable gradient would determine the input power for all cavities connected to this power station and thus limit the stronger and better cavities.

Therefore, it was assumed that, during production of the cavities, pre-sorting them with respect to maximum achievable gradient and grouping them appropriately in modules would be possible. It was further assumed that two cavities with the same maximum achievable gradient could be grouped into a pair. By changing the coupling ratios of the asymmetric shunt tees, it would be possible to provide the appropriate power for a pair of cavities. The advantage of this intermediate layout was that there would be no limitation by the weakest cavity and that production of the module waveguide distribution could already start after selection of the cavities for a specific cryogenic module. All components of the distributions would be of the same type with the exception of the asymmetric shunt tees between a pair of cavities.

Figure 2

Example: Layout and tailoring of module waveguide distribution WD55 for accelerator module XM64 at the waveguide assembly and test facility (WATF). The table shows the desired maximum achievable gradients of the cavities, actual achievable gradients and the required RF input power. In addition, the relative phases of the cavities were measured. The columns show the input power to the cavities (zero suppressed) and the relative phases. Measurements were done at the WATF high-power test stand. Through individual tailoring, an additional beam energy gain of 78 MeV (about 50% more) was possible for this module compared with a module with equal power distribution. WD55 was preliminarily phase-tuned for beam acceleration with ±3° between cavities.

Series production

During production of the accelerator modules, it turned out that many cavities degrade when installed in the accelerator modules. It was therefore necessary to change the layout of the RF waveguide distribution further in order to allow for individual power delivery to each cavity. To this end, all the shunt tees between two cavities and between modules have to be asymmetric with individual coupling ratio. Since the adjustment of the coupling ratios changes the phase advance too, some fixed phase shifters have to be modified and the adjustable phase shifters have to be tuned near to the edges of their tuning range in order to compensate for this phase change. The advantage of this solution is that it allows for maximum achievable gradient in a module (Fig. 2).

Figure 3

Five assembled module waveguide distributions at the WATF

The disadvantage is that most of the waveguide components are now individual components, which makes the entire production and tuning process much more complicated, time-consuming and expensive. In addition, production of the module waveguide distributions is only possible after a full test of the accelerator modules. The adjustment and tuning of all the components between the klystron and the module distribution are more difficult and time-consuming too.

Status

Although the task is now more complex and difficult, it was possible to achieve all milestones in 2015 thanks to a common effort of the collaboration of TU Sofia (Bulgaria), SINP Moscow (Russia), IHEP Protvino (Russia) and DESY. In 2015, 58 individual module waveguide distributions were designed, assembled, tuned, measured, tested at full power and installed on the accelerator modules at the waveguide assembly and test facility (WATF) (Fig. 3). The average production rate was 1.1 module distributions per week. This rate was increased during the second half of the year to 1.5 module distributions per week. This was only possible by refining and optimising all single steps during the production of a distribution and by increasing the personnel working on the tasks. Figure 4 shows one module waveguide distribution connected to a cryogenic module.

In addition, installation, tuning and measurement of waveguide components between the klystrons and the module distributions started in the European XFEL tunnel. Besides two RF stations in the European XFEL injector, four RF stations are already installed and being commissioned in the main linear accelerator. Waveguides are almost fully installed for three additional stations and partially installed for eight more stations.

Figure 4

Module waveguide distribution connected to one accelerator module

Contact: Valery Katalev, valery.katalev@desy.de,
Stefan Choroba, stefan.choroba@desy.de

References.

Committees.

DESY Board of Directors

R. Brinkmann
(Accelerator division)

H. Dosch
(Chairman of the DESY Board of Directors)

J. Mnich
(High-energy physics and astroparticle physics)

C. Scherf
(Administrative division)

E. Weckert
(Photon science division)

C. Stegmann
(Representative of the directorate in Zeuthen)

Machine Advisory Committee (MAC)

Michael Borland (ANL, USA)
Hans Braun (PSI, CH)
Massimo Ferraio (INFN, I)
Zhirong Huang (SLAC, USA)
Andreas Jankowiak (HZB, Chair)
Katsunobu Oide (KEK, JP)
Pantaleo Raimondi (ESRF, F)
Rüdiger Schmidt (CERN, CH)

DESY Scientific Board

R. Aßmann (DESY)
F. Beckmann (HZG)
T. Behnke (DESY)
M. Bieler (DESY)
I. Bloch (DESY)
I. Brock (KET)
W. Buchmüller (DESY)
K. Büsser (DESY)
H. Chapman (DESY)
M. Diehl (DESY)
R. Döhrmann (DESY)
W. Drube (DESY)
G. Eckerlin (DESY)
H.-J. Eckoldt (DESY)
A. Ehnes (DESY)
E. Elsen (DESY)
S. Fiedler (EMBL)
T. Finnern (DESY)
B. Foster (DESY)
E. Gallo (DESY)
H. Graafsma (DESY)
I. M. Gregor (DESY)
C. Grojean (DESY)
G. Grübel (DESY)
W. Gülzow (DESY)
J. Haller (Univ. Hamburg)
M. Hempel (DESY)
K. Honkavaara (DESY)
K. Jansen (DESY)
F. Kärtner (DESY)
M. Kasemann (DESY)
C. Kluth (DESY)
M. Kowalski (DESY)
T. Laarmann (DESY)
A. Maier (KfB)
N. Meyners (DESY)
W.-D. Möller (DESY)
K. Mönig (DESY)
B. Murphy (KfS)
A. Mußgiller (DESY)
T. Naumann (DESY)
C. Niebuhr (DESY)
D. Nölle (DESY)
B. Petersen (DESY)
E. Plönjes-Palm (DESY)
M. Pohl (DESY)
B. Racky (DESY)
A. Ringwald (DESY)
R. Röhlsberger (DESY)
W. Sandner (DESY)
R. Santra (DESY)
V. Schomerus (DESY)
T. Schörner-Sadenius (DESY)
S. Schreiber (DESY)
C. Schroer (DESY)
H. Schulte-Schrepping (DESY)
C. Schwanenberger (DESY)
U. Schwanke (HU Berlin)
A. Schwarz (DESY)
O. Seek (DESY)
G. Servant (DESY)
J. Spengler (DESY)
A. Stierle (DESY)
K. Tackmann (DESY)
S. Techert (DESY)
M. Tischer (DESY)
T. Tschentscher (European XFEL)
J. Viefhaus (DESY)
M. Vogt (DESY)
P. Wegner (DESY)
G. Weiglein (DESY)
H. Weise (DESY)
M. v. Zimmermann (DESY)

Memberships.

ANKA Machine Advisory Committee
Klaus Balewski

APAC ESRF
Reinhard Brinkmann

AREAL Project, Armenia, International Technical Advisory Committee
Klaus Flöttmann

Apollon/CILEX Technical Advisory Committee
Ralph Aßmann

Accelerator Test Facility (ATF) Program Advisory Committee
Ralph Aßmann

ACHIP (International Collaboration for an Accelerator on a chip) Executive Board
Ralph Aßmann

AWAKE Experiment CERN Collaboration Board
Ralph Aßmann

BerlinPro Machine Advisory Committee
Holger Schlarb, Siegfried Schreiber

BESSY Machine Advisory Committee
Winfried Decking

CERN Accelerator School Advisory Committee
Winfried Decking

CERN Accelerator School on FELs and ERLs (CAS 2016) Program Committee and Local Chair
Kay Wittenburg

CERN Accelerator School Introductory (2016) and Advanced Level (2017) Program Committee
Kay Wittenburg

CERN Accelerator School on Vacuum Systems and Technologies Program Committee
Lutz Lilje

CERN Machine Advisory Committee
Reinhard Brinkmann

DEELS Workshop 2016 Local Chair
Gero Kube

European Advanced Accelerator Concepts Workshop (EAAC2015) Organizing Committee
Ralph Aßmann

European Advanced Accelerator Concepts Workshop (EAAC2015) Co-Chairman
Ralph Aßmann

European Physical Society Accelerator Group (EPS-AG)
Ralph Aßmann, Kay Wittenburg

ESRF Machine Advisory Committee
Ralph Aßmann

European Spallation Source (ESS) Technical Advisory Committee
Hans Weise

ESS Vacuum and System Cost Review
Lutz Lilje

European Coordination for Accelerator R&D (EuCARD2) Deputy Coordinator
Ralph Aßmann

European Coordination for Accelerator R&D (EuCARD2) Steering Board
Ralph Aßmann

European Coordination for Accelerator R&D (EuCARD2) Governing Board
Ralph Aßmann

European Coordination for Accelerator R&D (EuCARD2) Coordinator
Ralph Aßmann

European Coordination for Accelerator R&D (EuCARD2) Deputy Coordinator WP12
Nicoleta Baboi

European Physical Society Accelerator Group (EPS AG) Elected Member
Ralph Aßmann

FAIR Machine Advisory Committee
Kay Wittenburg

FEL 2015 Scientific Program Committee
Frank Stephan, Siegfried Schreiber

FLAC, Machine Advisory Committee SwissFEL
Holger Schlarb

Future Circular Collider (FCC) Collaboration Board
Ralph Aßmann

Helmholtz Virtual Institute 2012 "Plasma Wakefield Acceleration of Highly Relativistic Electrons with FLASH"
Brian Foster (Coordinator)

High Lumi LHC Collaboration Board
Rainer Wanzenberg

ICALEPCS International Scientific Advisory Committee (ISAC)
Reinhard Bacher

IBIC International Program Committee (IBIC 2015, IBIC 2016)
Kay Wittenburg

ICFA Beam Dynamics Panel
Rainer Wanzenberg

ILC Accelerator Advisory Panel (AAP) and International Detector Advisory Group (IDAG)
Eckhard Elsen

ILC and High-Gradient Superconducting RF Cavities (ILC-HiGrade)
Eckhard Elsen (Project Coordinator)

ILC Program Advisory Committee
Hans Weise

ILC Technical Board
Nicholas Walker

International Conference on RF Superconductivity International Program Committee
Wolf-Dietrich Möller

IPAC 2016 + 2017 Organizing Committee
Ralph Aßmann

IPAC 2017 Scientific Advisory Board
Lutz Lilje

Joint University Accelerator School Advisory Board
Winfried Decking

Komitee für Beschleunigerphysik
Hans Weise

LINAC 2016 International Organizing Committee
Hans Weise

LINAC 2016 Conference Scientific Program Committee
Stefan Choroba, Hans Weise

LCLS-II Directors Review
Winfried Decking, Lutz Lilje

LCLS-II Facility Advisory Committee
Jacek Sekutowicz

LCLS-II Vacuum System PDR
Lutz Lilje

MAX IV Machine Advisory Committee
Klaus Balewski

PCaPAC Program Committee
Philip Duval, Reinhard Bacher

PHIL Scientific Committee
Frank Stephan

PIP-II Fermilab Machine Advisory Committee
Hans Weise

OLAV-V (Operation of Large Vacuum Systems) Organizing Committee
Lutz Lilje, Sven Lederer

QRC-KAERI World Class Institute, International Advisory Committee
Klaus Flöttmann

RadSynch 2015 Scientific Committee
Albrecht Leuschner, Norbert Tesch

Real Time Conference Scientific Advisory Committee
Kay Rehlich

RREPS - 15 (Radiation from Relativistic Electrons in Periodic Structures) Program Committeee
Gero Kube

Scientific Program Committee SPIE Advances in X-ray Free-Electron Lasers Instrumentation
Siegfried Schreiber

STFC Accelerator Strategy Board
Reinhard Brinkmann

Super KEKB Machine Advisory Committee
Ralph Aßmann

TIARA Council DESY Deputy
Ralph Aßmann

TIARA Governing Board
Reinhard Brinkmann

TTC Executive Committee
Hans Weise

TTC Technical Board
Wolf-Dietrich Möller, Detlef Reschke

US LHC Accelerator Research Program Advisory Committee
Kay Wittenburg

XFEL Detector Advisory Committee
Kay Rehlich

XFEL Council Appointed Member - Advisor to the German Delegation
Reinhard Brinkmann

Publications.

Publications

A. Angelovski et al.
Evaluation of the Cone-Shaped Pickup Performance for low Charge Sub-10 fs Arrival-Time Measurements at Free Electron Laser Facilities.
Physical review / Special topics / Accelerators and beams, 18(1):012801, and PUBDB-2015-01443.
doi: 10.1103/PhysRevSTAB.18.012801.

A. Aschikhin et al.
The FLASHForward facility at DESY.
Nuclear instruments & methods in physics research / A, 806:175, and PUBDB-2015-04861, DESY-15-143, arXiv:1508.03192.
doi: 10.1016/j.nima.2015.10.005.

K. Ayyer et al.
Perspectives for imaging single protein molecules with the present design of the European XFEL.
Structural dynamics, 2(4):041702, and PUBDB-2015-04293.
doi: 10.1063/1.4919301.

M. Beckmann and V. Ziemann.
How well do we know the circumference of a storage ring?
Nuclear instruments & methods in physics research / A, 771:115, and PUBDB-2016-00242.
doi: 10.1016/j.nima.2014.10.044.

M. Bieler et al.
Radiation Damage of Insertion Devices at PETRA III – A Perspective View from Optics and Tracking Studies.
ICFA beam dynamics newsletters, 66:45, and PUBDB-2015-02832.

R. Bruce, S. Redaelli and R. Assmann.
Calculations of safe collimator settings and β * at the CERN Large Hadron Collider.
Physical review / Special topics / Accelerators and beams, 18(6):061001, and PUBDB-2016-00234.
doi: 10.1103/PhysRevSTAB.18.061001.

M. Cauchi et al.
Thermomechanical response of Large Hadron Collider collimators to proton and ion beam impacts.
Physical review / Special topics / Accelerators and beams, 18(4):041002, and PUBDB-2016-00235.
doi: 10.1103/PhysRevSTAB.18.041002.

G. Ciovati et al.
Mechanical properties of niobium radio-frequency cavities.
Materials science and engineering / A, 642:117, and PUBDB-2016-00288.
doi: 10.1016/j.msea.2015.06.095.

Y. Ding et al.
Generating femtosecond X-ray pulses using an emittance-spoiling foil in free-electron lasers.
Applied physics letters, 107(19):191104, and PUBDB-2016-00305.
doi: 10.1063/1.4935429.

I. Dornmair, K. Floettmann and A. Maier.
Emittance Conservation by Tailored Focusing Profiles in a Plasma Accelerator.
Physical review / Special topics / Accelerators and beams, 18(4):041302, and PUBDB-2015-04875.
doi: 10.1103/PhysRevSTAB.18.041302.

Z. Duan et al.
A Monte-Carlo Simulation of the Equilibrium Beam Polarization in Ultra-High Energy Electron (Positron) Storage Rings.
Nuclear instruments & methods in physics research / A, 793:81, and PUBDB-2015-03686, arXiv:1505.02392; DESY-15-072.
doi: 10.1016/j.nima.2015.04.063.

M. Fenner et al.
Standardized Solution for Management Controller for MTCA.4.
IEEE transactions on nuclear science, 62(3):932, and PUBDB-2015-03434.
doi: 10.1109/TNS.2015.2408452.

K. Floettmann.
rf-induced beam dynamics in rf guns and accelerating cavities.
Physical review / Special topics / Accelerators and beams, 18(6):064801, and PUBDB-2016-00093.
doi: 10.1103/PhysRevSTAB.18.064801.

E. I. Gacheva et al.
Disk Yb:KGW amplifier of profiled pulses of laser driver for electron photoinjector.
Optics express, 23(8):9627, and PUBDB-2015-05403.
doi: 10.1364/OE.23.009627.

K. Hacker et al.
Measurements and simulations of seeded electron microbunches with collective effects.
Physical review / Special topics / Accelerators and beams, 18(9):090704, and PUBDB-2016-00389.
doi: 10.1103/PhysRevSTAB.18.090704.

F. Ludwig et al.
2π Low Drift Phase Detector for High-Precision Measurements.
IEEE transactions on nuclear science, 62(3):1142, and PUBDB-2016-00315.
doi: 10.1109/TNS.2015.2425733.

B. Marchetti et al.
Novel Schemes for the Optimization of the SPARC Narrow Band THz Source.
Review of scientific instruments, 86:073301, and PUBDB-2015-04857.
doi: 10.1063/1.4922882.

A. Marinelli et al.
High-intensity double-pulse X-ray free-electron laser.
Nature Communications, 6:6369, and PUBDB-2016-00394.
doi: 10.1038/ncomms7369.

A. Marinelli et al.
Time-resolved imaging of the microbunching instability and energy spread at the Linac Coherent Light Source.
Physical review / Special topics / Accelerators and beams, 18(3):030704, and PUBDB-2016-00378.
doi: 10.1103/PhysRevSTAB.18.030704.

A. Mielczarek et al.
High-Speed Data Processing Module for LLRF.
IEEE transactions on nuclear science, 62(3):1083, and PUBDB-2015-04706.
doi: 10.1109/TNS.2015.2416120.

A. Navitski et al.
Review of $R\&D$ at DESY on ingot niobium for accelerators.
JLab Ingot Niobium CRADA Workshop, Newport News (Virginia, USA), 4 Dec 2015 - 4 Dec 2015.
Inst., Melville, NY, 4th Dec. 2015.
doi: 10.1063/1.4935324.

Y. Nie.
Wakefields in THz Cylindrical Dielectric Lined Waveguides Driven by Femtosecond Electron Bunches.
Radiation physics and chemistry, 106:140, and PUBDB-2014-03885.
doi: 10.1016/j.radphyschem.2014.07.007.

M. Omet et al.
FPGA-based klystron linearization implementations in scope of ILC.
Nuclear instruments & methods in physics research / A, 780:1, and PUBDB-2016-00335.
doi: 10.1016/j.nima.2015.01.056.

P. Predki et al.
Rapid-X - An FPGA Development Toolset Using a Custom Simulink Library for MTCA.4 Modules.
IEEE transactions on nuclear science, 62(3):940, and PUBDB-2016-00376.
doi: 10.1109/TNS.2015.2413673.

D. Ratner et al.
Experimental Demonstration of a Soft X-Ray Self-Seeded Free-Electron Laser.
Physical review letters, 114(5):054801, and PUBDB-2016-00587.
doi: 10.1103/PhysRevLett.114.054801.

J. Schaffran et al.
Test Sequence for Superconducting XFEL Cavities in the Accelerator Module Test Facility (AMTF) at DESY.
Physics procedia, 67:874, and PUBDB-2015-06172.
doi: 10.1016/j.phpro.2015.06.147.

E. A. Schneidmiller and M. V. Yurkov.
Coherence Properties of the Radiation from FLASH.
Journal of modern optics, 62:1, and PUBDB-2016-00079.
doi: 10.1080/09500340.2015.1066456.

E. A. Schneidmiller and M. V. Yurkov.
Statistical properties of the radiation from SASE FEL operating in a post-saturation regime with and without undulator tapering.
Journal of modern optics, 63:1, and PUBDB-2016-00083.
doi: 10.1080/09500340.2015.1035349.

E. A. Schneidmiller and M. Yurkov.
Optimization of a High Efficiency Free Electron Laser Amplifier.
Physical review / Special topics / Accelerators and beams, 18(3):030705, and PUBDB-2015-02026.
doi: 10.1103/PhysRevSTAB.18.030705.

S. Schreiber and B. Faatz.
The free-electron laser FLASH.
High power laser science and engineering, 3:e20, and PUBDB-2015-06256.
doi: 10.1017/hpl.2015.16.

S. Schulz et al.
Femtosecond all-optical synchronization of an X-ray free-electron laser.
Nature Communications, 6:5938, and PUBDB-2015-01441.
doi: 10.1038/ncomms6938.

J. Sekutowicz et al.
Research and development towards duty factor upgrade of the European X-Ray Free Electron Laser linac.
Physical review / Special topics / Accelerators and beams, 18(5):050701, and PUBDB-2016-00380.
doi: 10.1103/PhysRevSTAB.18.050701.

W. Singer et al.
Hydroforming of Elliptical Cavities.
Physical review / Special topics / Accelerators and beams, 18(2):022001, and PUBDB-2015-02191.
doi: 10.1103/PhysRevSTAB.18.022001.

W. Singer et al.
Superconducting cavity material for the European XFEL.
Superconductor science and technology, 28(8):085014, and PUBDB-2015-06018.
doi: 10.1088/0953-2048/28/8/085014.

E. Syresin et al.
THz wiggler applied for measurements of electron bunch longitudinal structure in FEL.
Physics of particles and nuclei letters, 12(1):118, and PUBDB-2015-00199, BMBF 05K10CHE; HRJRG-400.
doi: 10.1134/S1547477115010203.

R. Wanzenberg.
Radiation damage of accelerator components – Detection, measurements and simulations.
ICFA beam dynamics newsletters, 66:10, and PUBDB-2015-06202.

R. Wanzenberg et al.
Radiation Damage of Insertion Devices at PETRA III - A perspective View from Optics and Tracking Studies,
ICFA beam dynamics newsletters, 66:45, and PUBDB-2015-06200.

I. Zagorodnov, K. L. F. Bane and G. Stupakov.
Calculation of Wakefields in 2D Rectangular Structures.
Physical review / Special topics / Accelerators and beams, 18(10):104401, and PUBDB-2015-04801, DESY-15-134.
doi: 10.1103/PhysRevSTAB.18.104401.

B. Zeitler, K. Floettmann and F. Grüner.
Linearization of the Longitudinal Phase Space without Higher Harmonic Field.
Physical review / Special topics / Accelerators and beams, 18(12):120102, and PUBDB-2016-00036.
doi: 10.1103/PhysRevSTAB.18.120102.

Preprints and Internal Reports

D. T. Abell et al.
Accurate and Efficient Spin Integration for Particle Accelerators.
PUBDB-2015-01232, arXiv:1501.03450; DESY-15-009.

W. Ackermann et al.
Eigenmode Calculations for the TESLA Cavity Considering Wave-Propagation Losses through Fundamental and Higher-Order Mode Couplers.
PUBDB-2015-05269.

A. Aschikhin et al.
The FLASHForward Facility at DESY.
PUBDB-2015-03071, DESY-15-143; arXiv:1508.03192.

D. P. Barber and K. Heinemann.
Spin Decoherence in Electron Storage Rings - More from a Simple Model.
PUBDB-2015-03389, DESY-15-142; arXiv:1508.05318.

D. P. Barber, M. Vogt and A. Kling.
The Uniqueness of the Invariant Polarisation-Tensor Field for Spin-1 Particles in Storage Rings.
PUBDB-2015-04461, DESY-15-192; arXiv:1510.07963.

D. P. Barber.
The invariant polarisation-tensor field for deuterons in storage rings and the Bloch equation for the polarisation-tensor density.
PUBDB-2015-04462, DESY-15-181; arXiv:1510.04936.

W. Decking, A. Sargsyan and V. Sahakyan.
Parallel Operation of SASE1 and SASE3.
PUBDB-2016-00219, TESLA-FEL 2015-01.

M. Dohlus and C. Henning.
Periodic Poisson Solver for Particle Tracking.
PUBDB-2015-02072, DESY-15-071; arXiv:1505.01330.

G. Geloni, V. Kocharyan and E. Saldin.
Modulated Electron Bunch with Amplitude Front Tilt in an Undulator.
PUBDB-2015-05371, DESY 15-236; arXiv:1512.01056.

G. Geloni, V. Kocharyan and E. Saldin.
Scheme to increase the output average spectral flux of the European XFEL at 14.4 keV.
PUBDB-2015-03387, DESY-15-141; arXiv:1508.04339.

V. Gharibyan.
Probing Positron Gravitation at HERA.
PUBDB-2015-02697, DESY-15-109; arXiv:1507.02589.

E. Gschwendtner et al.
AWAKE, The Advanced Proton Driven Plasma Wakefield Acceleration Experiment at CERN.
PUBDB-2016-00230.

K. Heinemann et al.
A Detailed and Unified Treatment of Spin-Orbit Systems Using Tools Distilled from the Theory of Bundles.
PUBDB-2015-02311, arXiv:1501.02747; DESY-15-010.

E. A. Schneidmiller and M. Yurkov.
Coherence Properties of the Radiation from FLASH.
PUBDB-2016-00086, DESY 15-023; arXiv:1502.04486.

I. Zagorodnov, K. L. F. Bane and G. Stupakov.
Calculation of Wakefields in 2D Rectangular Structures.
PUBDB-2015-03065, DESY-15-134; SLAC-PUB-16353; arXiv:1508.00066.

Contributions to a book

F. Stephan and M. Krasilnikov.
High Brightness Photo Injectors for Brilliant Light Sources.
Synchrotron Light Sources and Free-Electron Lasers.
Springer International Publishing, Cham, 2015.
doi: 10.1007/978-3-319-04507-8_15-1.

Conference Contributions

ICALEPCS 2015

A. Aghababyan et al.
The Large Scale European XFEL Control System: Overview and Status of the Commissioning.
15th International Conference on Accelerator and Large Experimental Physics Control Systems, Melbourne (Australia), 17 Oct 2015 - 23 Oct 2015.
17th Oct. 2015.

V. Ayvazyan et al.
Low Level RF Control Implementation and Simultaneous Operation of Two FEL Undulator Beamlines at FLASH.
15th International Conference on Accelerator and Large Experimental Physics Control Systems, Melbourne (Australia), 17 Oct 2015 - 23 Oct 2015.
17th Oct. 2015.

R. Bacher et al.
The Large Scale European XFEL Control System: Overview and Status of the Commissioning.
15th International Conference on Accelerator and Large Experimental Physics Control Systems, Melbourne (Australia), 17 Oct 2015 - 23 Oct 2015.
17th Oct. 2015.

L. Butkowski et al.
FPGA Firmware Framework for MTCA.4 AMC Modules.
15th International Conference on Accelerator and Large Experimental Physics Control Systems, Melbourne (Australia), 17 Oct 2015 - 23 Oct 2015.
17th Oct. 2015.

L. Froehlich, P. Bartkiewicz and M. Walla.
Magnet Server and Control System Database Infrastructure for the European XFEL.
15th International Conference on Accelerator and Large Experimental Physics Control Systems, Melbourne (Australia), 17 Oct 2015 - 23 Oct 2015.
17th Oct. 2015.

L. Froehlich et al.
High Level Controls for the European XFEL.
15th International Conference on Accelerator and Large Experimental Physics Control Systems, Melbourne (Australia), 17 Oct 2015 - 23 Oct 2015.
17th Oct. 2015.

R. Kammering et al.
The Virtual European XFEL Accelerator.
15th International Conference on Accelerator and Large Experimental Physics Control Systems, Melbourne (Australia), 17 Oct 2015 - 23 Oct 2015.
17th Oct. 2015.

M. Killenberg et al.
Drivers and Software for MicroTCA.4.
15th International Conference on Accelerator and Large Experimental Physics Control Systems, Melbourne (Australia), 17 Oct 2015 - 23 Oct 2015.
17th Oct. 2015.

M. Killenberg et al.
Integrating Control Applications into Different Control Systems.
15th International Conference on Accelerator and Large Experimental Physics Control Systems, Melbourne (Australia), 17 Oct 2015 - 23 Oct 2015.
17th Oct. 2015.

S. Meykopff.
Advanced MATLAB GUI Development with the DATAGUI LIBRARY.
15th International Conference on Accelerator and Large Experimental Physics Control Systems, Melbourne (Australia), 17 Oct 2015 - 23 Oct 2015.
17th Oct. 2015.

A. Napieralski et al.
European XFEL Cavities Piezoelectric Tuners Control Range Optimization.
15th International Conference on Accelerator and Large Experimental Physics Control Systems, Melbourne (Australia), 17 Oct 2015 - 23 Oct 2015.
17th Oct. 2015.

I. Rutkowski et al.
Real-time Beam Loading Compensation for Single SRF Cavity LLRF Regulation.
15th International Conference on Accelerator and Large Experimental Physics Control Systems, Melbourne (Australia), 17 Oct 2015 - 23 Oct 2015.
17th Oct. 2015.

C. Schmidt et al.
High Level Software Structure for the European XFEL LLRF System.
15th International Conference on Accelerator and Large Experimental Physics Control Systems, Melbourne (Australia), 17 Oct 2015 - 23 Oct 2015.
17th Oct. 2015.

SRF2015

S. Aderhold et al.
Analysis of Degraded Cavities in Prototype Modules for the European XFEL.
17th International Conference on RF Superconductivity, Whistler (Canada), 13 Sep 2015 - 18 Sep 2015.
13th Sept. 2015.

S. Barbanotti et al.
Connection of EU-XFEL Cryomodules, Caps and Boxes in the EU-XFEL Main LINAC And Injector: Welding of Cryo-Pipes and Assembly of Beamline Absorbers under the Requirements of the PED Regulation.
17th International Conference on RF Superconductivity, Whistler (Canada), 13 Sep 2015 - 18 Sep 2015.
13th Sept. 2015.

M. Bertucci et al.
Development of an X-Ray Fluorescence Probe for Inner Cavity Inspection.
17th International Conference on RF Superconductivity, Whistler (Canada), 13 Sep 2015 - 18 Sep 2015.
13th Sept. 2015.

C. G. Maiano et al.
Horizontal RF Test of a Fully Equipped 3.9 GHz Cavity for the European XFEL in the DESY AMTF.
17th International Conference on RF Superconductivity, Whistler (Canada), 13 Sep 2015 - 18 Sep 2015.
13th Sept. 2015.

G. Massaro et al.
Inspection and repair techniques for the EXFEL superconducting 1.3 GHz cavities at Ettore Zanon S.p.A.
17th International Conference on RF Superconductivity, Whistler (Canada), 13 Sep 2015 - 18 Sep 2015.
13th Sept. 2015.

L. Monaco et al.
Study of the evolution of artificial defects on the surface of niobium during electrochemical and chemical polishing.
17th International Conference on RF Superconductivity, Whistler (Canada), 13 Sep 2015 - 18 Sep 2015.
13th Sept. 2015.

P. Pierini et al.
Preparation of the 3.9 GHz System for the European XFEL Injector Commissioning.
17th International Conference on RF Superconductivity, Whistler (Canada), 13 Sep 2015 - 18 Sep 2015.
13th Sept. 2015.

M. Wiencek et al.
Update and Status of Test Results of the XFEL Series Accelerator Modules.
17th International Conference on RF Superconductivity, Whistler (Canada), 13 Sep 2015 - 18 Sep 2015.
13th Sept. 2015.

FEL 2015

M. Bakr et al.
Beam Dynamics Simulation for the Upgraded Pitz Photo Injector Applying Various Photocathode Laser Pulses.
37th International Free Electron Laser Conference, Daejeon (South Korea), 23 Aug 2015 - 28 Aug 2015.
23rd Aug. 2015.

B. Beutner, H. Dinter and M. Dohlus.
RFTweak 5 - An Efficient Longitudinal Beam Dynamics Code.
37th International Free Electron Laser Conference, Daejeon (South Korea), 23 Aug 2015 - 28 Aug 2015.
23rd Aug. 2015.

P. Boonpornprasert et al.
Numerical Simulations of a Sub-THz Coherent Transition Radiation Source at PITZ.
37th International Free Electron Laser Conference, Daejeon (South Korea), 23 Aug 2015 - 28 Aug 2015.
23rd Aug. 2015.

H. Dinter et al.
Prototype of the Improved Electro-Optical Unit for the Bunch Arrival Time Monitors at FLASH and the European XFEL.
37th International Free Electron Laser Conference, Daejeon (South Korea), 23 Aug 2015 - 28 Aug 2015.
23rd Aug. 2015.

M. Felber et al.
Implementation of MTCA.4-based Controls for the Pulsed Optical Synchronization Systems at DESY.
37th International Free Electron Laser Conference, Daejeon (South Korea), 23 Aug 2015 - 28 Aug 2015.
23rd Aug. 2015.

G. Geloni, V. Kocharyan and E. Saldin.
Scheme to increase the output average spectral flux of the European XFEL at 14.4 keV.
37th International Free Electron Laser Conference, Daejeon (South Korea), 23 Aug 2015 - 28 Aug 2015.
23rd Aug. 2015.

J. Good et al.
New Ellipsoidal Laser at the upgraded PITZ Facility.
37th International Free Electron Laser Conference, Daejeon (South Korea), 23 Aug 2015 - 28 Aug 2015.
23rd Aug. 2015.

K. Honkavaara et al.
Status of the soft X-ray User Facility FLASH.
37th International Free Electron Laser Conference, Daejeon (South Korea), 23 Aug 2015 - 28 Aug 2015.
23rd Aug. 2015.

H. Huck et al.
First Results of Commissioning of the PITZ Transverse Deflecting Structure.
37th International Free Electron Laser Conference, Daejeon (South Korea), 23 Aug 2015 - 28 Aug 2015.
23rd Aug. 2015.

E. Janas et al.
MTCA.4 Phase Detector for Femtosecond-Precision Laser Synchronization.
37th International Free Electron Laser Conference, Daejeon (South Korea), 23 Aug 2015 - 28 Aug 2015.
23rd Aug. 2015.

C. Lechner et al.
Suppression of FEL Lasing by a Seeded Microbunching Instability.
37th International Free Electron Laser Conference, Daejeon (South Korea), 23 Aug 2015 - 28 Aug 2015.
23rd Aug. 2015.

E. A. Schneidmiller and M. Yurkov.
Fundamental Limitations of the SASE FEL Photon Beam Pointing Stability.
37th International Free Electron Laser Conference, Daejeon (South Korea), 23 Aug 2015 - 28 Aug 2015.
23rd Aug. 2015.

E. A. Schneidmiller and M. Yurkov.
Optimization of a High Efficiency Free Electron Laser Amplifier.
37th International Free Electron Laser Conference, Daejeon (South Korea), 23 Aug 2015 - 28 Aug 2015.
23rd Aug. 2015.

M. Scholz and B. Beutner.
Electron Beam Phase Space Tomographie at the European XFEL Injector.
37th International Free Electron Laser Conference, Daejeon (South Korea), 23 Aug 2015 - 28 Aug 2015.
23rd Aug. 2015.

M. Scholz et al.
First Simultaneous Operation of Two SASE Beamlines in FLASH.
37th International Free Electron Laser Conference, Daejeon (South Korea), 23 Aug 2015 - 28 Aug 2015.
23rd Aug. 2015.

S. Schreiber and S. Lederer.
Lifetime of Cs2Te Cathodes Operated at the FLASH Facility.
37th International Free Electron Laser Conference, Daejeon (South Korea), 23 Aug 2015 - 28 Aug 2015.
23rd Aug. 2015.

S. Schreiber et al.
Simultaneous Operation of Three Laser Systems at the FLASH Photoinjector.
37th International Free Electron Laser Conference, Daejeon (South Korea), 23 Aug 2015 - 28 Aug 2015.
23rd Aug. 2015.

C. Sydlo et al.
Femtosecond Timing Distribution at the European XFEL.
37th International Free Electron Laser Conference, Daejeon (South Korea), 23 Aug 2015 - 28 Aug 2015.
23rd Aug. 2015.

G. Vashchenko et al.
Emittance Measurements of the Electron Beam at PITZ for the Commissioning Phase of the European XFEL.
37th International Free Electron Laser Conference, Daejeon (South Korea), 23 Aug 2015 - 28 Aug 2015.
23rd Aug. 2015.

4th MicroTCA workshop for Industry and Research

M. Fenner.
Production and in-system programming of MicroTCA boards.
4th MicroTCA workshop for Industry and Research, Hamburg (Germany), 9 Dec 2015 - 10 Dec 2015.
9th Dec. 2015.

M. Grzegrzolka et al.
AMC and RTM Boards Intended for Performance Evaluation of MTCA.4 Based Modules.
4th MicroTCA workshop for Industry and Research, Hamburg (Germany), 9 Dec 2015 - 10 Dec 2015.
9th Dec. 2015.

M. Hierholzer et al.
MTCA4U – The DESY MicroTCA.4 User Tool Kit.
4th MicroTCA workshop for Industry and Research, Hamburg (Germany), 9 Dec 2015 - 10 Dec 2015.
9th Dec. 2015.

F. Ludwig and U. Mavric.
High Precision Analog Measurements in High Speed Modular Standards.
4th MicroTCA workshop for Industry and Research, Hamburg (Germany), 9 Dec 2015 - 10 Dec 2015.
9th Dec. 2015.

P. Perek, L. Butkowski and D. Makowski.
Firmware Upgrade Framework for MTCA.4.
4th MicroTCA workshop for Industry and Research, Hamburg (Germany), 9 Dec 2015 - 10 Dec 2015.
9th Dec. 2015.

K. Przygoda, R. Rybaniec and P. Echevarria.
MicroTCA.4 based Single Cavity Regulation.
4th MicroTCA workshop for Industry and Research, Hamburg (Germany), 9 Dec 2015 - 10 Dec 2015.
9th Dec. 2015.

IPAC 2015

I. Agapov, G. Geloni and I. Zagorodnov.
Statistical Optimization of FEL Performance.
6th International Particle Accelerator Conference, Richmond, VA (USA), 3 May 2015 - 8 May 2015.
3rd May 2015.

I. Agapov et al.
FEL Simulations with OCELOT.
6th International Particle Accelerator Conference, Richmond, VA (USA), 3 May 2015 - 8 May 2015.
3rd May 2015.

D. Alesini et al.
Study of a A C-BAND Harmonic RF System to Optimize the RF Bunch Compressin Process of the SPARC Beam.
6th International Particle Accelerator Conference, Richmond, VA (USA), 3 May 2015 - 8 May 2015.
3rd May 2015.

P. Amstutz et al.
Optics Compensation for Variable-gap Undulator Systems at FLASH.
6th International Particle Accelerator Conference, Richmond, VA (USA), 3 May 2015 - 8 May 2015.
3rd May 2015.

V. Balandin, W. Decking and N. Golubeva.
Mirror Symmetric Chicane-type Emittance Exchange Beamline with two Deflecting Cavities.
6th International Particle Accelerator Conference, Richmond, VA (USA), 3 May 2015 - 8 May 2015.
3rd May 2015.

V. Balandin, W. Decking and N. Golubeva.
Sensitivity of Linac Optics to Focusing and Energy Errors.
6th International Particle Accelerator Conference, Richmond, VA (USA), 3 May 2015 - 8 May 2015.
3rd May 2015.

V. Balandin et al.
Emittance Reduction Possibilities in the PETRA III Magnet Lattice.
6th International Particle Accelerator Conference, Richmond, VA (USA), 3 May 2015 - 8 May 2015.
3rd May 2015.

J. Boedewadt and N. Ekanayake.
Simulation of Optical Transport Beamlines for High-quality Optical Beams for Accelerator Applications.
6th International Particle Accelerator Conference, Richmond, VA (USA), 3 May 2015 - 8 May 2015.
3rd May 2015.

J. Branlard et al.
LLRF Commissioning of the European XFEL RF Gun and Its First Linac RF Station.
6th International Particle Accelerator Conference, Richmond, VA (USA), 3 May 2015 - 8 May 2015.
3rd May 2015.

Y. Chen et al.
Investigations of the Space-Charge-Limited Emission in the L-Band E-XFEL Photoinjector at PITZ.
6th International Particle Accelerator Conference, Richmond, VA (USA), 3 May 2015 - 8 May 2015.
3rd May 2015.

U. Dorda et al.
Simulation Results of the Beam Transport of Ultra-Short Electron Bunches in Existing Beam Transfer Lines to SINBAD.
6th International Particle Accelerator Conference, Richmond, VA (USA), 3 May 2015 - 8 May 2015.
3rd May 2015.

U. Dorda et al.
Simulations of Electron-Proton Beam Interaction before Plasma in the AWAKE Experiment.
6th International Particle Accelerator Conference, Richmond, VA (USA), 3 May 2015 - 8 May 2015.
3rd May 2015.

M. Fakhari et al.
Design of a Normal Conducting Cavity for Arrival Time Stabilization at FLASH.
6th International Particle Accelerator Conference, Richmond, VA (USA), 3 May 2015 - 8 May 2015.
3rd May 2015.

M. Hachmann and K. Floettmann.
Transverse Emittance Measurement at REGAE.
6th International Particle Accelerator Conference, Richmond, VA (USA), 3 May 2015 - 8 May 2015.
3rd May 2015.

M. Hachmann et al.
Design and Characterization of Permanent Magnetic Solenoids for REGAE.
6th International Particle Accelerator Conference, Richmond, VA (USA), 3 May 2015 - 8 May 2015.
3rd May 2015.

M. Hoffmann et al.
Operation of Normal Conducting RF Guns with MicroTCA.4.
6th International Particle Accelerator Conference, Richmond, VA (USA), 3 May 2015 - 8 May 2015.
3rd May 2015.

K. Kasprzak et al.
Automated Quench Limit Test Procedure for Serial Production of XFEL RF Cavities.
6th International Particle Accelerator Conference, Richmond, VA (USA), 3 May 2015 - 8 May 2015.
3rd May 2015.

B. Marchetti et al.
Compression of an Electron-Bunch by Means of Velocity Bunching at ARES.
6th International Particle Accelerator Conference, Richmond, VA (USA), 3 May 2015 - 8 May 2015.
3rd May 2015.

B. Marchetti et al.
Compression of Train of Bunches with Ramped Intensity Profile at $SPARC_{LAB}$.
6th International Particle Accelerator Conference, Richmond, VA (USA), 3 May 2015 - 8 May 2015.
3rd May 2015.

B. Marchetti et al.
ARES: Accelerator Research Experiment at SINBAD.
6th International Particle Accelerator Conference, Richmond, VA (USA), 3 May 2015 - 8 May 2015.
3rd May 2015.

U. Mavrič et al.
Commissioning of the Low-Noise MTCA.4-based Local Oscillator and Clock Generation Module.
6th International Particle Accelerator Conference, Richmond, VA (USA), 3 May 2015 - 8 May 2015.
3rd May 2015.

F. Mayet et al.
Implementation of a Diagnostic Pulse for Beam Optics Stability Measurements at FLASH.
6th International Particle Accelerator Conference, Richmond, VA (USA), 3 May 2015 - 8 May 2015.
3rd May 2015.

J. Mueller et al.
All-Optical Synchronization of Pulsed Laser Systems at FLASH and XFEL.
6th International Particle Accelerator Conference, Richmond, VA (USA), 3 May 2015 - 8 May 2015.
3rd May 2015.

M. J. Nasse et al.
Status of the Accelerator Physics Test Facility FLUTE.
6th International Particle Accelerator Conference, Richmond, VA (USA), 3 May 2015 - 8 May 2015.
3rd May 2015.

A. Nawaz et al.
Physical Parameter Identification of Cross-Coupled Gun and Buncher Cavity at REGAE.
6th International Particle Accelerator Conference, Richmond, VA (USA), 3 May 2015 - 8 May 2015.
3rd May 2015.

Y. Nie et al.
Progress in the Injector Upgrade of the LINAC II at DESY.
6th International Particle Accelerator Conference, Richmond, VA (USA), 3 May 2015 - 9 May 2015.
3rd May 2015.

M. Omet et al.
Operation Experiences with the MICROTCA.4-based LLRF Control System at FLASH.
6th International Particle Accelerator Conference, Richmond, VA (USA), 3 May 2015 - 8 May 2015.
3rd May 2015.

A. Oppelt et al.
Facility Upgrade at PITZ and First Operation Results.
6th International Particle Accelerator Conference, Richmond, VA (USA), 3 May 2015 - 8 May 2015.
3rd May 2015.

G. Pathak et al.
Simulations Study for Self-Modulation Experiment at PITZ.
6th International Particle Accelerator Conference, Richmond, VA (USA), 3 May 2015 - 8 May 2015.
3rd May 2015.

S. Pfeiffer et al.
Virtual Cavity Probe Generation using Calibrated Forward and Reflected Signals.
6th International Particle Accelerator Conference, Richmond, VA (USA), 3 May 2015 - 8 May 2015.
3rd May 2015.

K. Przygoda et al.
High Voltage RTM Piezo Driver for XFEL Special Diagnostics.
6th International Particle Accelerator Conference, Richmond, VA (USA), 3 May 2015 - 8 May 2015.
3rd May 2015.

K. Przygoda et al.
Testing Procedures for Fast Frequency Tuners of XFEL Cavities.
6th International Particle Accelerator Conference, Richmond, VA (USA), 3 May 2015 - 8 May 2015.
3rd May 2015.

T. Rublack et al.
First Results Attained With the Quasi 3-D Ellipsoidal Photo Cathode Laser Pulse System at the High Brightness Photo Injector PITZ.
6th International Particle Accelerator Conference, Richmond, VA (USA), 3 May 2015 - 8 May 2015.
3rd May 2015.

R. Rybaniec et al.
Microphonic Disturbances Prediction and Compensation in Pulsed Superconducting Accelerators.
6th International Particle Accelerator Conference, Richmond, VA (USA), 3 May 2015 - 8 May 2015.
3rd May 2015.

G. K. Sahoo et al.
Investigation of Radiation Damage of Insertion Devices at PETRA III due to Particle Losses using Tracking Results with SixTrack.
6th International Particle Accelerator Conference, Richmond, VA (USA), 3 May 2015 - 8 May 2015.
JACOW, CERN, 3rd May 2015.

M. Titberidze et al.
Present and Future Optical-to-Microwave Synchronization Systems at REGAE Facility for Electron Diffraction and Plasma Acceleration Experiments.
6th International Particle Accelerator Conference, Richmond, VA (USA), 3 May 2015 - 8 May 2015.
3rd May 2015.

A. Tsakanian et al.
A New Approach for Resistive Wakefield Calculations in Time Domain.
6th International Particle Accelerator Conference, Richmond, VA (USA), 3 May 2015 - 8 May 2015.
3rd May 2015.

M. Vogt et al.
Status of the Soft X-ray Free Electron Laser FLASH.
6th International Particle Accelerator Conference, Richmond, VA (USA), 3 May 2015 - 8 May 2015.
3rd May 2015.

R. Wanzenberg et al.
Status of the Recommissioning of the Synchrotron Light Source PETRA III.
6th International Particle Accelerator Conference, Richmond, VA (USA), 3 May 2015 - 8 May 2015.
Jacow, CERN, 3rd May 2015.

J. Zhu et al.
Sub-fs Electron Bunch Generation Using Magnetic Compressor at SINBAD.
6th International Particle Accelerator Conference, Richmond, VA (USA), 3 May 2015 - 8 May 2015.
3rd May 2015.

J. Zhu et al.
Timing Jitter Studies for Sub-FS Electron Bunch Generation at SINBAD.
6th International Particle Accelerator Conference, Richmond, VA (USA), 3 May 2015 - 8 May 2015.
3rd May 2015.

IBIC 2015

S. Jablonski, H. Schlarb and C. Sydlo.
CW Laser Based Phase Reference Distribution for Particle Accelerators.
International Beam Instrumentation Conference 2015, Melbourne (Australia), 13 Sep 2015 - 17 Sep 2015.
13th Sept. 2015.

F. Schmidt-Föhre et al.
Commissioning of the New Online-Radiation-Monitoring-System at the New European XFEL Injector with First Tests of the High-Sensitivity-Mode for Intra-Tunnel Rack Surveillance.
International Beam Instrumentation Conference 2015, Melbourne (Australia), 13 Sep 2015 - 17 Sep 2015.
Jacow, CERN, 13th Sept. 2015.

LLRF15

V. Ayvazyan et al.
Low Level RF Control Implementation and Simultaneous Operation of Two FEL Undulator Beamlines at FLASH.
Low Level Radio Frequency Workshop 2015, Shanghai (China), 3 Nov 2015 - 6 Nov 2015.
3rd Nov. 2015.

J. Branlard.
LLRF Installation and Commissioning at the European XFEL.
Low Level Radio Frequency Workshop 2015, Shanghai (China), 3 Nov 2015 - 6 Nov 2015.
3rd Nov. 2015.

M. Grecki.
Rapid Recovery after RF Breakdown of High Average Power RF Gun.
Low Level Radio Frequency Workshop 2015, Shanghai (China), 3 Nov 2015 - 6 Nov 2015.
3rd Nov. 2015.

M. Hoffmann.
Sub-10 fs RF Regulation at REGAE.
Low Level Radio Frequency Workshop 2015, Shanghai (China), 3 Nov 2015 - 6 Nov 2015.
3rd Nov. 2015.

P. Jatczak et al.
RF Phase Reference Distribution for the European XFEL.
Low Level Radio Frequency Workshop 2015, Shanghai (China), 3 Nov 2015 - 6 Nov 2015.
3rd Nov. 2015.

F. Ludwig and U. Mavric.
Field Detection and Drift Calibration for the European XFEL.
Low Level Radio Frequency Workshop 2015, Shanghai (China), 3 Nov 2015 - 6 Nov 2015.
3rd Nov. 2015.

F. Makowski et al.
Software Design and Implementation for LLRF Modules in the European XFEL.
Low Level Radio Frequency Workshop 2015, Shanghai (China), 3 Nov 2015 - 6 Nov 2015.
3rd Nov. 2015.

U. Mavric and C. Schmidt.
Operational Experience with the MicroTCA Based LLRF System at FLASH.
Low Level Radio Frequency Workshop 2015, Shanghai (China), 3 Nov 2015 - 6 Nov 2015.
3rd Nov. 2015.

U. Mavric et al.
Drift Compensation Module for Pulsed or CW Machines at 1.3GHz, 3.0 GHz and 3.9 GHz.
Low Level Radio Frequency Workshop 2015, Shanghai (China), 3 Nov 2015 - 6 Nov 2015.
3rd Nov. 2015.

A. Napieralski et al.
XFEL Cryomodule under CW Operation.
Low Level Radio Frequency Workshop 2015, Shanghai (China), 3 Nov 2015 - 6 Nov 2015.
3rd Nov. 2015.

M. Omet et al.
Automatic Testing of Cryomodules in Scope of the European XFEL.
Low Level Radio Frequency Workshop 2015, Shanghai (China), 3 Nov 2015 - 6 Nov 2015.
3rd Nov. 2015.

S. Pfeiffer.
Frequency Control through Pulse Width Modulation for NRF Cavities.
Low Level Radio Frequency Workshop 2015, Shanghai (China), 3 Nov 2015 - 6 Nov 2015.
3rd Nov. 2015.

H. Schlarb.
Status of LLRF Developments at DESY.
Low Level Radio Frequency Workshop 2015, Shanghai (China), 3 Nov 2015 - 6 Nov 2015.
3rd Nov. 2015.

RREPS-15

G. Kube, L. Sukhikh and A. Potylitsyn.
Simulation of 2D Point Spread Function Dominated Beam Profile Images Based on Backward Transition Radiation from the Tilted Target.
Radiation from Relativistic Electrons in Periodic Structures, St. Petersburg (Russia), 6 Sep 2015 - 12 Sep 2015.
6th Sept. 2015.

L. Sukhikh et al.
Micron-Scale Vertical Beam Size Measurements Based on Transition Radiation Imaging with a Schwarzschild Objective.
Radiation from Relativistic Electrons in Periodic Structures, St. Petersburg (Russia), 6 Sep 2015 - 12 Sep 2015.
6th Sept. 2015.

I. Vnukov et al.
Spatial distribution of PXR generated by 855 MeV electrons. Comparison of simulation results with experimental data.
Radiation from Relativistic Electrons in Periodic Structures, St. Petersburg (Russia), 6 Sep 2015 - 12 Sep 2015.
6th Sept. 2015.

SPIE Optics + Optoelectronics: Advances in X-ray Free-Electron Laser Instrumentation

E. A. Schneidmiller and M. V. Yurkov.
The Universal Method for Optimization of Undulator Tapering in FEL Amplifiers.
SPIE Optics + Optoelectronics: Advances in X-ray Free-Electron Laser Instrumentation, Prague (Czech Republic), 13 Apr 2015 - 16 Apr 2015.
13th Apr. 2015.
doi: 10.1117/12.2181230.

E. A. Schneidmiller and M. V. Yurkov.
Polarization Control in X-ray FELs by Reverse Undulator Tapering.
SPIE Optics + Optoelectronics: Advances in X-ray Free-Electron Laser Instrumentation, Prague (Czech Republic), 13 Apr 2015 - 16 Apr 2015.
13th Apr. 2015.
doi: 10.1117/12.2181224.

Other Conference Contributions

K. Heinemann et al.
An Informal Summary of a New Formalism for Classifying Spin-Orbit Systems Using Tools Distilled from the Theory of Bundles; Conference Series.
21st International Symposium on Spin Physics, Beijing (China), 20 Oct 2014 - 24 Oct 2014.
International Journal of Modern Physics, 20th Oct. 2014.

K. Kruppa et al.
High Precision Temperature Control of Normal-Conducting RF GUN for a High Duty Cycle Free-Electron Laser.
5th International Conference on Simulation, Modeling Methodologies, Technologies and Applications, Colmar (France), 21 Jul 2015 - 23 Jul 2015.
21st July 2015.

M. Rehders et al.
Beam Dynamic Simulations for Single Spike Radiation with Short-Pulse Injector Laser at FLASH.
36th International Free Electron Laser Conference, Basel (Switzerland), 25 Aug 2014 - 29 Aug 2014.
CERN, Genf, 25th Aug. 2014.

Conference Presentations

ICALEPCS 2015

R. Bacher.
A Multi-Modal Human-Machine-Interface for Accelerator Operation and Maintenance Applications.
15th International Conference on Accelerator and Large Experimental Physics Control Systems, Melbourne (Australia), 17 Oct 2015 - 23 Oct 2015.
17th Oct. 2015.

R. Bacher et al.
The Large Scale European XFEL Control System: Overview and Status of the Commissioning.
15th International Conference on Accelerator and Large Experimental Physics Control Systems, Melbourne (Australia), 17 Oct 2015 - 23 Oct 2015.
17th Oct. 2015.

P. Duval, M. Lomperski and J. Bobnar.
TINE Studio, Making Life Easy for Administrators, Operators and Developers.
15th International Conference on Accelerator and Large Experimental Physics Control Systems, Melbourne (Australia), 17 Oct 2015 - 23 Oct 2015.
17th Oct. 2015.

R. Kammering et al.
The Virtual European XFEL Accelerator.
15th International Conference on Accelerator and Large Experimental Physics Control Systems, Melbourne (Australia), 17 Oct 2015 - 23 Oct 2015.
17th Oct. 2015.

V. Rybnikov and V. Petrosyan.
A Self-Configurable Server for Controlling Devices Over the Simple Network Management Protocol.
15th International Conference on Accelerator and Large Experimental Physics Control Systems, Melbourne (Australia), 17 Oct 2015 - 23 Oct 2015.
17th Oct. 2015.

E. Sombrowski.
A HTML5 Web Interface for JAVA DOOCS Data Display.
15th International Conference on Accelerator and Large Experimental Physics Control Systems, Melbourne (Australia), 17 Oct 2015 - 23 Oct 2015.
17th Oct. 2015.

SRF2015

A. Goessel, M. Mommertz and D. Tischhauser.
Next Generation Cavity and Coupler Interlock for the European XFEL.
17th International Conference on RF Superconductivity, Whistler (Canada), 13 Sep 2015 - 18 Sep 2015.
13th Sept. 2015.

D. Kostin et al.
SRF Gun Cavity $R\&D$ at DESY.
17th International Conference on RF Superconductivity, Whistler (Canada), 13 Sep 2015 - 18 Sep 2015.
13th Sept. 2015.

A. Matheisen et al.
Exchange and Repair of Titanium Service Pipes for the EXFEL Series Cavities.
17th International Conference on RF Superconductivity, Whilster (Canada), 13 Sep 2015 - 18 Sep 2015.
13th Sept. 2015.

A. Matheisen et al.
Experiences on Retreatment of EU-XFEL Series Cavities at DESY.
17th International Conference on RF Superconductivity, Whistler (Canada), 13 Sep 2015 - 18 Sep 2015.
13th Sept. 2015.

A. Matheisen et al.
Series Production of BQU at DESY for the EU-XFEL Module Assembly at CEA Saclay.
17th International Conference on RF Superconductivity, Whistler (Candad), 13 Sep 2015 - 18 Sep 2015.
13th Sept. 2015.

A. Matheisen et al.
String Assembly for the EU-XFEL 3.9 GHz Module at DESY.
17th International Conference on RF Superconductivity, Whistler (Canada), 13 Sep 2015 - 18 Sep 2015.
13th Sept. 2015.

A. Matheisen et al.
Vertical Electro-Polishing at DESY of a 1.3 GHz Gun Cavity for CW Application.
17th International Conference on RF Superconductivity, Whistler (Canada), 13 Sep 2015 - 18 Sep 2015.
13th Sept. 2015.

D. Reschke.
Recent Progress with EU-XFEL.
17th International Conference on RF Superconductivity, Whistler (Canada), 13 Sep 2015 - 18 Sep 2015.
13th Sept. 2015.

J. Schaffran et al.
Analysis of the Test Rate for European XFEL Series Cavities.
17th International Conference on RF Superconductivity, Whistler (Canada), 13 Sep 2015 - 18 Sep 2015.
13th Sept. 2015.

A. Sulimov.
HOM Coupler Notch Filter Tuning for the European XFEL Cavities.
17th International Conference on RF Superconductivity, Whistler (Canada), 13 Sep 2015 - 18 Sep 2015.
13th Sept. 2015.

A. Sulimov.
RF Analysis of Equator Welding Stability for the European XFEL Cavities.
17th International Conference on RF Superconductivity, Whistler (Canada), 13 Sep 2015 - 18 Sep 2015.
13th Sept. 2015.

A. Sulimov.
RF Measurements for Quality Assurance during SC Cavity Mass Production.
17th International Conference on RF Superconductivity, Whistler (Canada), 13 Sep 2015 - 18 Sep 2015.
13th Sept. 2015.

A. Sulimov et al.
Practical Aspects of HOM Suppression Improvement for TM011.
17th International Conference on RF Superconductivity, Whistler (Canada), 13 Sep 2015 - 18 Sep 2015.
13th Sept. 2015.

EAAC 2015

J. Dale et al.
FLASH pulse stacker for FLASHForward double electron bunch generation.
2nd European Advanced Accelerator Concepts Workshop, La Biodola (Italy), 12 Sep 2015 - 19 Sep 2015.
12th Sept. 2015.

U. Dorda et al.
SINBAD the accelerator $R\&D$ facility under construction at DESY.
2nd European Advanced Accelerator Concepts Workshop, La Biodola (Italy), 14 Sep 2015 - 19 Sep 2015.
14th Sept. 2015.

M. Gross et al.
First plasma acceleration experiments at PITZ.
2nd European Advanced Accelerator Concepts Workshop, La Biodola (Italy), 13 Sep 2015 - 19 Sep 2015.
13th Sept. 2015.

O. Lishilin et al.
First results of the plasma wakefield acceleration experiment at PITZ.
2nd European Advanced Accelerator Concepts Workshop, La Biodola (Italy), 13 Sep 2015 - 19 Sep 2015.
13th Sept. 2015.

O. Lishilin et al.
Status of the preparations for a plasma wakefield acceleration experiment at PITZ.
2nd European Advanced Accelerator Concepts Workshop, La Biodola (Italy), 13 Sep 2015 - 19 Sep 2015.
13th Sept. 2015.

B. Marchetti et al.
Electron-Beam Manipulation Techniques in the SINBAD Linac for External Injection in Plasma Wake-Field Acceleration.
2nd European Advanced Accelerator Concepts Workshop, La Biodola (Italy), 13 Sep 2015 - 19 Sep 2015.
13th Sept. 2015.

Y. Nie et al.
Potential Applications of the Dielectric Wakefield Accelerators in the SINBAD Facility at DESY.
2nd European Advanced Accelerator Concepts Workshop, La Biodola (Italy), 12 Sep 2015 - 19 Sep 2015.
12th Sept. 2015.

T. Rublack et al.
Production of quasi ellipsoidal laser pulses for next generation high brightness photoinjectors.
2nd European Advanced Accelerator Concepts Workshop, La Biodola (Italy), 13 Sep 2015 - 19 Sep 2015.
13th Sept. 2015.

B. Zeitler, K. Floettmann and F. Gruener.
Advanced Bunching Scheme at REGAE.
2nd European Advanced Accelerator Concepts Workshop, La Biodola (Italy), 13 Sep 2015 - 19 Sep 2015.
13th Sept. 2015.

FEL 2015

W. Decking.
European XFEL Construction Status.
37th International Free Electron Laser Conference, DAEJEON (South Korea), 24 Aug 2015 - 28 Aug 2015.
24th Aug. 2015.

K. Honkavaara et al.
Status of the FLASH Facility.
37th International Free Electron Laser Conference, Daejeon (South Korea), 23 Aug 2015 - 28 Aug 2015.
23rd Aug. 2015.

S. Schreiber and S. Lederer.
Lifetime of Cs2Te Cathodes Operated at the FLASH Facility.
37th International Free Electron Laser Conference, Daejeon (South Korea), 23 Aug 2015 - 28 Aug 2015.
23rd Aug. 2015.

S. Schreiber et al.
Simultaneous Operation of Three Laser Systems at the FLASH Photoinjector.
37th International Free Electron Laser Conference, Daejeon (South Korea), 23 Aug 2015 - 28 Aug 2015.
23rd Aug. 2015.

3rd ARD Workshop: ST3 - ps-fs Electron and Photon Beams

P. Boonpornprasert et al.
Simulations of the IR/THz Options at PITZ (High-gain FEL and CTR).
3rd ARD Workshop: ST3 - ps-fs Electron and Photon Beams, Karlsruhe (Germany), 15 Jul 2015 - 17 Jul 2015.
15th July 2015.

M. Krasilnikov.
Improved beam-based method for RF photo gun stability measurements.
3rd ARD Workshop: ST3 - ps-fs Electron and Photon Beams, Karlsruhe (Germany), 15 Jul 2015 - 17 Jul 2015.
15th July 2015.

M. Krasilnikov.
Status of PITZ.
3rd ARD Workshop: ST3 - ps-fs Electron and Photon Beams, Karlsruhe (Germany), 15 Jul 2015 - 17 Jul 2015.
15th July 2015.

B. Marchetti.
SINBAD and ATHENA$_e$.
3rd ARD Workshop: ST3 - ps-fs Electron and Photon Beams, Karlsruhe (Germany), 15 Jul 2015 - 17 Jul 2015.
15th July 2015.

A. Mielczarek et al.
High-Speed Linear Camera for Electro-Optic Experiment.
3rd ARD Workshop: ST3 - ps-fs Electron and Photon Beams, Karlsruhe (Germany), 15 Jul 2015 - 17 Jul 2015.
15th July 2015.

B. Zeitler, K. Floettmann and F. Gruener.
Linearization of the Longitudinal Phase Space Without Higher Harmonic Field.
3rd ARD Workshop: ST3 - ps-fs Electron and Photon Beams, Karlsruhe (Germany), 15 Jul 2015 - 17 Jul 2015.
15th July 2015.

LA3NET

G. Kube.
Beam Diagnostics at Free Electron Lasers.
5th Topical Workshop on Beam Diagnostics, Mallorca (Spain), 25 Mar 2015 - 27 Mar 2015.
25th Mar. 2015.

L. Shi et al.
HOM Based Beam Diagnostics Study at FLASH.
5th Topical Workshop on Beam Diagnostics, Mallorca (Spain), 23 Mar 2015 - 24 Mar 2015.
23rd Mar. 2015.

IPAC 2015

I. Agapov, S. Tomin and R. Wanzenberg.
Possibility of Longitudinal Bunch Compression in Petra III.
6th International Particle Accelerator Conference, Richmond, VA (USA), 3 May 2015 - 8 May 2015.
3rd May 2015.

M. Bieler et al.
Investigation of Radiation Damage of Insertion Devices at PETRA III due to Particle Losses using Tracking Results with SixTrack.
6th International Particle Accelerator Conference, Richmond, VA (USA), 3 May 2015 - 8 May 2015.
3rd May 2015.

M. Bieler et al.
Status of the Recommissioning of the Synchrotron Light Source PETRA III.
6th International Particle Accelerator Conference, Richmond, VA (USA), 3 May 2015 - 8 May 2015.
3rd May 2015.

J. Boedewadt et al.
Recent Results from FEL Seeding at FLASH.
6th International Particle Accelerator Conference, Richmond, VA (USA), 3 May 2015 - 8 May 2015.
3rd May 2015.

N. Golubeva et al.
Emittance Reduction Possibilities in the PETRA III Magnet Lattice.
6th International Particle Accelerator Conference, Richmond, VA (USA), 3 May 2015 - 8 May 2015.
3rd May 2015.

F. Mayet et al.
Implementation of a Diagnostic Pulse for Beam Optics Stability Measurements at FLASH.
6th International Particle Accelerator Conference, Richmond, VA (USA), 3 May 2015 - 8 May 2015.
3rd May 2015.

DPG 2015

P. Boonpornprasert et al.
Start-to-End Simulations for a 100 μm SASE FEL at PITZ.
DPG 2015, Wuppertal (Germany), 9 Mar 2015 - 13 Mar 2015.
9th Mar. 2015.

J. Good et al.
Preliminary Results from the Laser System generating Quasi 3-D Ellipsoidal Photocathode Laser Pulses at PITZ.
DPG 2015, Wuppertal (Germany), 9 Mar 2015 - 13 Mar 2015.
9th Mar. 2015.

I. Isaev and M. Krasilnikov.
RF field asymmetry simulations for the PITZ RF Photo Gun.
DPG 2015, Wuppertal (Germany), 9 Mar 2015 - 13 Mar 2015.
9th Mar. 2015.

G. Kourkafas.
Space-charge matching of the transverse phase space at PITZ.
DPG 2015, Wuppertal (Germany), 9 Mar 2015 - 13 Mar 2015.
9th Mar. 2015.

F. Mueller, M. Vogt and J. Zemella.
Compensation of Steerer Crosstalk between FLASH1 and FLASH2.
DPG 2015, Wuppertal (Germany), 9 Mar 2015 - 13 Mar 2015.
9th Mar. 2015.

A. Navitski et al.
ILC-HiGrade cavities as a tool of quality control for the EXFEL and further SRF $R\&D$.
DPG 2015, Wuppertal (Germany), 9 Mar 2015 - 13 Mar 2015.
9th Mar. 2015.

G. Pathak, M. Gross and F. Stephan.
Gas density measurement for self-modulation experiments at PITZ.
DPG 2015, Wuppertal (Germany), 9 Mar 2015 - 13 Mar 2015.
9th Mar. 2015.

B. Zeitler, K. Floettmann and F. Gruener.
Advanced Bunching Scheme at REGAE.
DPG 2015, Wuppertal (Germany), 9 Mar 2015 - 13 Mar 2015.
9th Mar. 2015.

IBIC 2015

V. Gharibyan et al.
Vector Polarimeter for Photons in keV-MeV Energy Range.
International Beam Instrumentation Conference 2015, Melbourne (Australia), 13 Sep 2015 - 17 Sep 2015.
13th Sept. 2015.

G. Kube et al.
Micron-Scale Vertical Beam Size Measurements Based on Transition Radiation Imaging With a Schwarzschild Objective.
International Beam Instrumentation Conference 2015, Melbourne (Australia), 13 Sep 2015 - 17 Sep 2015.
13th Sept. 2015.

G. Kube et al.
Transverse Beam Profile Imaging of Few-Micrometer Beam Sizes Based on a Scintillator Screen.
International Beam Instrumentation Conference 2015, Melbourne (Australia), 13 Sep 2015 - 17 Sep 2015.
13th Sept. 2015.

B. Lorbeer et al.
Development Status and Performance Studies of the New MicroTCA Based Button and Strip-line BPM Electronics at FLASH 2.
International Beam Instrumentation Conference 2015, Melbourne (Australia), 13 Sep 2015 - 17 Sep 2015.
13th Sept. 2015.

LAOLA Workshop

M. Gross.
The PITZ Plasma Source.
LAOLA Workshop, Wismar (Germany), 23 Jun 2015 - 24 Jun 2015.
23rd June 2015.

O. Lishilin et al.
Status of the Self-Modulation Experiment at PITZ.
LAOLA Workshop, Wismar (Germany), 23 Jun 2015 - 24 Jun 2015.
23rd June 2015.

G. Pathak et al.
Simulations Study for Self-Modulation Experiment at PITZ.
LAOLA Workshop, Wismar (Germany), 23 Jun 2015 - 24 Jun 2015.
23rd June 2015.

D. Richter.
Investigations of foils for the termination of the plasma cell.
LAOLA Workshop, Wismar (Germany), 23 Jun 2015 - 24 Jun 2015.
23rd June 2015.

LPAW 2015

M. Gross et al.
Towards a Self-Modulation Experiment with long Electron Beams at PITZ.
Laser Plasma Acceleration Workshop 2015, Guadeloupe (France), 10 May 2015 - 15 May 2015.
10th May 2015.

L. Schaper et al.
Beam driven plasma wakefield acceleration at FLASHForward.
Laser Plasma Acceleration Workshop 2015, Guadeloupe (France), 10 May 2015 - 15 May 2015.
10th May 2015.

F. Stephan et al.
Photo Cathode Laser Pulse Shaping for Generating Ultimate Electron Beam Quality.
Laser Plasma Acceleration Workshop 2015, Guadeloupe (France), 10 May 2015 - 15 May 2015.
10th May 2015.

Mini-Workshop on THz option at PITZ

P. Boonpornprasert.
Simulations of the IR/THz Source at PITZ (SASE FEL and CTR).
Mini-Workshop on THz option at PITZ, Zeuthen (Germany), 22 Sep 2015 - 22 Sep 2015.
22nd Sept. 2015.

M. Krasilnikov.
PITZ: facility overview.
Mini-Workshop on THz option at PITZ, Zeuthen (Germany), 22 Sep 2015 - 22 Sep 2015.
22nd Sept. 2015.

PITZ Collaboration Meeting

O. Anton.
Simulation model of a Solc fan pulse shaper.
PITZ Collaboration Meeting, Hamburg (Germany), 2 Jun 2015 - 3 Jun 2015.
2nd June 2015.

P. Boonpornprasert.
First experimental characterization of electron beam for THz options at PITZ.
PITZ Collaboration Meeting, Zeuthen (Germany), 24 Nov 2015 - 25 Nov 2015.
24th Nov. 2015.

Y. Chen.
Current Status of the Bunch Emission Modelling for PITZ.
PITZ Collaboration Meeting, Hamburg (Germany), 2 Jun 2015 - 3 Jun 2015.
2nd June 2015.

Y. Chen.
Modeling and simulation of dynamic photoemission including Schottky-like effect for the Cs_2Te cathode.
PITZ Collaboration Meeting, Zeuthen (Germany), 24 Nov 2015 - 25 Nov 2015.
24th Nov. 2015.

J. D. Good.
Laser System for Generation of Quasi Ellipsoidal Pulses – Status Report.
PITZ Collaboration Meeting, Zeuthen (Germany), 24 Nov 2015 - 25 Nov 2015.
24th Nov. 2015.

M. Gross.
Status of plasma acceleration experiment.
PITZ Collaboration Meeting, Hamburg (Germany), 2 Jun 2015 - 3 Jun 2015.
2nd June 2015.

I. Hartl.
News from laser systems at Hamburg.
PITZ Collaboration Meeting, Zeuthen (Germany), 24 Nov 2015 - 25 Nov 2015.
24th Nov. 2015.

C. Hernandez-Garcia.
Photoemission studies at PITZ: Analysis of extracted bunch charge vs laser pulse energy from CS_2 Te photocathodes under high RF field strengths.
PITZ Collaboration Meeting, Hamburg (Germany), 2 Jun 2015 - 3 Jun 2015.
2nd June 2015.

M. C. Hoffmann.
Activities and Laboratory Reports – Gun/Water Stability.
PITZ Collaboration Meeting, Zeuthen (Germany), 24 Nov 2015 - 25 Nov 2015.
24th Nov. 2015.

H. Huck.
First measurements with the PITZ TDS.
PITZ Collaboration Meeting, Zeuthen (Germany), 24 Nov 2015 - 25 Nov 2015.
24th Nov. 2015.

H. Huck.
Status of the PITZ TDS.
PITZ Collaboration Meeting, Hamburg (Germany), 2 Jun 2015 - 3 Jun 2015.
2nd June 2015.

I. Isaev.
Electron beam asymmetry studies at PITZ.
PITZ Collaboration Meeting, Zeuthen (Germany), 24 Nov 2015 - 25 Nov 2015.
24th Nov. 2015.

E. Khazanov.
Review of Photocathode laser driver activity in IAP.
PITZ Collaboration Meeting, Hamburg (Germany), 2 Jun 2015 - 3 Jun 2015.
2nd June 2015.

G. Kourkafas.
Measurements of space-charge matching at PITZ.
PITZ Collaboration Meeting, Hamburg (Germany), 2 Jun 2015 - 3 Jun 2015.
2nd June 2015.

M. Krasilnikov.
Mini-workshop on THz option at PITZ.
PITZ Collaboration Meeting, Zeuthen (Germany), 24 Nov 2015 - 25 Nov 2015.
24th Nov. 2015.

M. Krasilnikov.
PITZ RF-gun stability measurements.
PITZ Collaboration Meeting, Hamburg (Germany), 2 Jun 2015 - 3 Jun 2015.
2nd June 2015.

P. Lepercq.
LAL: PHIL status and perspectives.
PITZ Collaboration Meeting, Zeuthen (Germany), 24 Nov 2015 - 25 Nov 2015.
24th Nov. 2015.

T. Limberg.
European XFEL Status.
PITZ Collaboration Meeting, Hamburg (Germany), 2 Jun 2015 - 3 Jun 2015.
2nd June 2015.

O. Lishilin.
Status of plasma acceleration experiments.
PITZ Collaboration Meeting, Zeuthen (Germany), 24 Nov 2015 - 25 Nov 2015.
24th Nov. 2015.

O. Lishilin.
Status of plasma cell preparations.
PITZ Collaboration Meeting, Hamburg (Germany), 2 Jun 2015 - 3 Jun 2015.
2nd June 2015.

G. Loisch.
Argon Gas Discharge Plasma for PITZ Wakefield Experiments – Technical Design Proposal.
PITZ Collaboration Meeting, Zeuthen (Germany), 24 Nov 2015 - 25 Nov 2015.
24th Nov. 2015.

P. Lu.
Status of the SRF gun at HZDR & LSC experiments at PITZ.
PITZ Collaboration Meeting, Zeuthen (Germany), 24 Nov 2015 - 25 Nov 2015.
24th Nov. 2015.

J. McKenzie.
Bunch length measurements using a transverse deflecting cavity on VELA.
PITZ Collaboration Meeting, Zeuthen (Germany), 24 Nov 2015 - 25 Nov 2015.
24th Nov. 2015.

S. Mironov, M. Krasilnikov and F. Stephan.
3D ellipsoidal laser beams in IAP RAS.
PITZ Collaboration Meeting, Zeuthen (Germany), 24 Nov 2015 - 25 Nov 2015.
24th Nov. 2015.

S. Mistry.
Investigating Polycrystalline and Thin Film Metal Photocathodes for use in NCRF guns.
PITZ Collaboration Meeting, Hamburg (Germany), 2 Jun 2015 - 3 Jun 2015.
2nd June 2015.

T. C. Q. Noakes.
Photoinjectors and Photocathode Activity at Daresbury Laboratory.
PITZ Collaboration Meeting, Zeuthen (Germany), 24 Nov 2015 - 25 Nov 2015.
24th Nov. 2015.

M. Nozdrin.
Joint Institute for Nuclear Research and its activity in FEL.
PITZ Collaboration Meeting, Hamburg (Germany), 2 Jun 2015 - 3 Jun 2015.
2nd June 2015.

V. Paramonov.
Current INR activity in PITZ $R\&D$ collaboration.
PITZ Collaboration Meeting, Hamburg (Germany), 2 Jun 2015 - 3 Jun 2015.
2nd June 2015.

G. Pathak.
Results from gas density measurements for plasma cell.
PITZ Collaboration Meeting, Zeuthen (Germany), 24 Nov 2015 - 25 Nov 2015.
24th Nov. 2015.

Y. Renier.
Interlock statistics at PITZ.
PITZ Collaboration Meeting, Hamburg (Germany), 2 Jun 2015 - 3 Jun 2015.
2nd June 2015.

Y. Renier.
Interlock Statistics of Gun 4.2.
PITZ Collaboration Meeting, Zeuthen (Germany), 24 Nov 2015 - 25 Nov 2015.
24th Nov. 2015.

T. Rublack.
Laser System for Generation of Quasi Ellipsoidal Pulses – Status Report.
PITZ Collaboration Meeting, Hamburg (Germany), 2 Jun 2015 - 3 Jun 2015.
2nd June 2015.

S. Schreiber.
News from FLASH - the First Soft X-ray FEL Operating Two Undulator Beamlines Simultaneously.
PITZ Collaboration Meeting, Hamburg (Germany), 2 Jun 2015 - 3 Jun 2015.
2nd June 2015.

S. Schreiber.
News from FLASH - the first soft X-ray FEL operating two undulator beamlines simultaneously.
PITZ Collaboration Meeting, Zeuthen (Germany), 24 Nov 2015 - 25 Nov 2015.
24th Nov. 2015.

G. Shirkov.
JINR: Basic Facilities and New Projects at JINR.
PITZ Collaboration Meeting, Zeuthen (Germany), 24 Nov 2015 - 25 Nov 2015.
24th Nov. 2015.

C. Stegmann.
Report from the Collaboration Board Meeting.
PITZ Collaboration Meeting, Hamburg (Germany), 2 Jun 2015 - 3 Jun 2015.
2nd June 2015.

C. Stegmann.
Report from the Collaboration Board Meeting.
PITZ Collaboration Meeting, Zeuthen (Germany), 24 Nov 2015 - 25 Nov 2015.
24th Nov. 2015.

F. Stephan.
PITZ Status in November 2015.
PITZ Collaboration Meeting, Zeuthen (Germany), 24 Nov 2015 - 25 Nov 2015.
24th Nov. 2015.

F. Stephan.
Status of the accelerator $R\&D$ at PITZ.
PITZ Collaboration Meeting, Hamburg (Germany), 2 Jun 2015 - 3 Jun 2015.
2nd June 2015.

C. Topping.
Emittance measurements with coupling and linear space-charge approximations on the Versatile Electron Linear Accelerator.
PITZ Collaboration Meeting, Hamburg (Germany), 2 Jun 2015 - 3 Jun 2015.
2nd June 2015.

R. Valizadeh.
Metal thin films for photocathode applications.
PITZ Collaboration Meeting, Zeuthen (Germany), 24 Nov 2015 - 25 Nov 2015.
24th Nov. 2015.

G. Vashchenko.
Emittance measurements with the gun and laser operated close to E-XFEL startup conditions.
PITZ Collaboration Meeting, Hamburg (Germany), 2 Jun 2015 - 3 Jun 2015.
2nd June 2015.

I. Will.
XFEL Photocathode Laser: (Phase I: Gaussian pulses).
PITZ Collaboration Meeting, Hamburg (Germany), 2 Jun 2015 - 3 Jun 2015.
2nd June 2015.

L. Winkelmann.
European XFEL photocathode laser installation and commissioning.
PITZ Collaboration Meeting, Hamburg (Germany), 2 Jun 2015 - 3 Jun 2015.
2nd June 2015.

Q. Zhao.
Beam dynamics simulation study with core + halo laser beam distribution for emittance measurement experiment.
PITZ Collaboration Meeting, Hamburg (Germany), 2 Jun 2015 - 3 Jun 2015.
2nd June 2015.

SPIE Optics + Optoelectronics: Advances in X-ray Free-Electron Laser Instrumentation

K. Honkavaara.
FLASH at DESY - The first soft X-ray FEL operating two undulator beamlines simultaneously.
SPIE Optics + Optoelectronics: Advances in X-ray Free-Electron Laser Instrumentation, Prague (Czech Republic), 13 Apr 2015 - 16 Apr 2015.
13th Apr. 2015.

S. Schreiber.
Operation of FLASH.
SPIE Optics + Optoelectronics: Advances in X-ray Free-Electron Laser Instrumentation, Prague (Czech Republic), 13 Apr 2015 - 16 Apr 2015.
13th Apr. 2015.

Other Conference Presentations

R. Assmann.
Accelerator $R\&D$ towards a New Generation of Accelerators.
ATS Seminar, Geneva (Switzerland), 12 Mar 2015 - 12 Mar 2015.
12th Mar. 2015.

R. Assmann.
Advanced Accelerator $R\&D$ Leading the Way?
Universities meet Laboratories, Frankfurt (Germany), 1 Oct 2014 - 1 Oct 2014.
1st Oct. 2014.

R. Assmann.
Pathway from Particles to Light.
Lasers and Accelerators for Science & Society, Liverpool (England), 26 Jun 2015 - 26 Jun 2015.
26th June 2015.

R. Assmann.
The EuPRAXIA Project- a european plasma accelerator.
Annual meeting IZEST, Palaiseau Cedex (France), 15 Oct 2015 - 16 Oct 2015.
15th Oct. 2015.

A. Bonucci.
European XFEL In-Kind Contributions: A Look Into the Main Features of the Designed Vacuum Systems.
Associazione Italiana del Vuoto, Genova (Italy), 20 Apr 2015 - 22 Apr 2015.
20th Apr. 2015.

W. Decking.
Commissioning Plans & Parameters 1st User Run.
European XFEL Users Meeting, Hamburg (Germany), 28 Jan 2015 - 29 Jan 2015.
28th Jan. 2015.

U. Dorda et al.
SINBAD and it's Experiments.
CoAXSA Compact Attosecond X - ray Sources and their Applications, Hamburg (Germany), 19 Jul 2015 - 22 Jul 2015.
19th July 2015.

M. Heuer et al.
Plant Modeling for Observer-Based Control of the Link Stabilizing Units at the European X-ray Free-Electron Laser.
2015 American Control Conference (ACC), Chicago (IL, USA), 1 Jul 2015 - 3 Jul 2015.
1st July 2015.
doi: 10.1109/ACC.2015.7172197.

J. Keil.
PETRA III Upgrade.
Low Emittance Rings 2015 Workshop, Grenoble (France), 15 Sep 2015 - 17 Sep 2015.
15th Sept. 2015.

M. Krasilnikov.
PITZ – Photo Injector Test Facility at DESY, Zeuthen Site.
DESY Scientific Council, Zeuthen (Germany), 28 May 2015 - 28 May 2015.
28th May 2015.

K. Kruppa et al.
High Precision Temperature Control of Normal-Conducting RF GUN for a High Duty Cycle Free-Electron Laser.
5th International Conference on Simulation, Modeling Methodologies, Technologies and Applications, Colmar (France), 21 Jul 2015 - 23 Jul 2015.
21st July 2015.

G. Kube.
Radiation Sources and their Applications for Beam Profile Diagnostics.
Radiation from Relativistic Electrons in Periodic Structures, St. Petersburg (Russia), 6 Sep 2015 - 12 Sep 2015.
6th Sept. 2015.

G. Kube.
Status of Beam Loss Detector Tests and Developments at Petra III & ESRF.
Diagnostics Experts of European Light Sources, ALBA (Spain), 15 Jun 2015 - 16 Jun 2015.
15th June 2015.

G. Kube and K. Wittenburg.
Characterization of Instrumentation for Transverse and Longitudinal Beam Diagnostics; Introduction to Beam Diagnostics and Instrumentation.
Excellence in Detectors and Instrumentation Technologies, Laboratori Nazionali di Frascati (Italy), 20 Oct 2015 - 29 Oct 2015.
20th Oct. 2015.

D. Lipka.
Experience on Design, Prototyping and Testing of Cavity BPM for the European-XFEL.
1st PACMAN Workshop, Geneve, CERN (Switzerland), 2 Feb 2015 - 4 Feb 2015.
2nd Feb. 2015.

B. Marchetti.
ATHENA$_c$ infrastructure.
Matter and Technologies Kickoff Meeting, Hamburg (Germany), 23 Feb 2015 - 26 Feb 2015.
23rd Feb. 2015.

C. Schmidt.
Status and Experience with MicroTCA.4 LLRF systems at DESY.
4th MicroTCA workshop for Industry and Research, Hamburg (Germany), 9 Dec 2015 - 10 Dec 2015.
9th Dec. 2015.

Thesis

Ph.D. Thesis

G. Kourkafas.
Incorporating space charge in the transverse phase-space matching and tomography at PITZ.
Universität Hamburg, Hamburg, 2015.

S. Serkez.
Design and Optimization of the Grating Monochromator for Soft X-Ray Self-Seeding FELs.
Universität Hamburg, Hamburg, 2015.

Master Thesis

O. Anton.
Erstellung eines Programms zur Simulation einer zeitlichen Strahlformung mittels doppelbrechender Kristalle ausgehend von gaußförmigen Laserimpulsen.
BTU Cottbus, Cottbus, 2015.

M. Schinkel.
Aufbau und Optimierung einer Laser-Beamline für den Ionisationslaser des Plasmabeschleunigungsexperiments bei PITZ.
TH Wildau, Wildau, 2015.

Photographs and graphics

Lars Berg/DESY
DESY
European XFEL
Sebastian Schulz/MPSD
Jörg Harms/MPSD
Dirk Nölle/DESY
Heiner Müller-Elsner/DESY
SLAC National Accelerator Laboratory

The figures were reproduced by permission of authors or journals.

Acknowledgement

We would like to thank all authors and everyone who helped in the creation of this annual report.

Imprint

Publishing and contact
Deutsches Elektronen-Synchrotron DESY
A Research Centre of the Helmholtz Association

Hamburg location:
Notkestr. 85, 22607 Hamburg, Germany
Tel.: +49 40 8998-0, Fax: +49 40 8998-3282
desyinfo@desy.de

Zeuthen location:
Platanenallee 6, 15738 Zeuthen, Germany
Tel.: +49 33762 7-70, Fax: +49 33762 7-7413
desyinfo.zeuthen@desy.de

www.desy.de
ISBN 978-3-945931-03-5

Editing
Klaus Balewski,
Ilka Flegel, Kapellendorf

Layout
Sabine Kuhls-Dawideit

Production
Britta Liebaug

Printing
ehs druck gmbh, Schenefeld

Editorial deadline
1 March 2016

Editorial note
The authors of the individual scientific contributions published in this report are fully responsible for the contents.

HELMHOLTZ ASSOCIATION

Deutsches Elektronen-Synchrotron
A Research Centre of the Helmholtz Association

The Helmholtz Association is a community of 18 scientific-technical and biological-medical research centres. These centres have been commissioned with pursuing long-term research goals on behalf of the state and society. The Association strives to gain insights and knowledge so that it can help to preserve and improve the foundations of human life. It does this by identifying and working on the grand challenges faced by society, science and industry. Helmholtz Centres perform top-class research in strategic programmes in six core fields: Energy, Earth and Environment, Health, Key Technologies, Structure of Matter, Aeronautics, Space and Transport.

www.helmholtz.de